International Conference on Molecular Imaging and Clinical PET-CT in the Era of Theranostics

IPET - 2020 *goes virtual*

BOOK OF ABSTRACTS

IAEA
International Atomic Energy Agency
Atoms for Peace and Development

International Conference on Clinical PET-CT and Molecular Imaging in the Era of Theranostics (IPET-2020)

24 – 26 November 2020

IAEA Headquarters, Vienna, Austria

Organized by the IAEA

In Cooperation with:

Latin American Association of Societies of Biology and Nuclear Medicine

Asia Oceania Federation of Nuclear Medicine and Biology

Asian Regional Cooperative Council for Nuclear Medicine

Arab Society of Nuclear Medicine

European Association of Nuclear Medicine

European Association of Radiology

International Society of Radiology

Society of Nuclear Medicine and Molecular Imaging

World Association of Radiopharmaceutical and Molecular Therapy

The World Federation of Nuclear Medicine and Biology

BOOK OF ABSTRACTS

IAEA-CN-285

IAEA-CN-285/2

The Use of Three-Phase Bone Scintigraphy in the Differentiated Selection of the Components of Endoprosthesis In Patients with Septic and Aseptic Osteoarthrosis of the Hip Joint

P. Korol

Clinical City Hospital, Ukraine

Corresponding Author: p.korol@online.ua

Background
To determine the diagnostic value of three-phase bone scintigraphy in the differentiated selection of endoprosthesis components ("friction units") in patients with septic and aseptic osteoarthrosis (OA) of the hip joints.

Methodology
255 patients with septic and aseptic OA (161 women and 94 men) aged 30 to 75 years were imaged by bone scintigraphy: I stage - angiographic stage, II stage - early stage, 3 stage - delayed static phase. 3 hours after the intravenous administration of 740 MBq 99mTc MDP.

Results
According to the results of microbiological analysis of diagnostic puncture of the hip joints, the patients were divided into two cohorts. The first cohort included 146 patients with aseptic OA of the hip joint, the second - 109 patients with septic OA (in 71 cases was detected S. aureus, in 38 cases – St. haemolyticus). A significant increase in arterial inflow ($t = 2.48$; $p < 0.05$) and integral perfusion ($t = 2.65$; $p < 0.05$) in the angiographic phase of patients with septic OA was determined due to intensification osteoblastic activity and angiogenesis, compared with patients with aseptic OA. In patients with septic OA, there was a significant predominance of retention ($t = 3.29$; $p < 0.05$) and specific accumulation of the radiopharmaceutical in the early ($t = 2.23$; $p < 0.05$) and delayed static phase of three-phase bone scintigraphy ($t = 2.36$; $p < 0.05$) as compared with indicators for aseptic OA. When endoprosthetics of patients with aseptic OA using the component of endoprosthesis – «ceramics-ceramics» in the postoperative period, no implant-associated complications were detected. In patients with septic OA, paraprosthetic complications were not recorded when using the «metal-ceramic» component.

Conclusion
The parameters of the distribution kinetics of the radiopharmaceutical of three-phase bone scintigraphy have diagnostic value in patients with aseptic and septic OA of the hip joint when choosing the components of the endoprosthesis, especially when it is impossible to perform a diagnostic puncture of the hip joint.

IAEA-CN-285/3

The Value of Isolated and Integrated Brain PET and MRI Imaging Findings to Predict Treatment Response in Patients with Alzheimer's Disease

T. Thietunyakit[1], N. Wannasoupol[1], C. Sethanandha[1], W. Muangpaisan[1], J. Gelovani[2]

[1] Siriraj Hospital, Thailand
[2] Wayne State University, United States

Corresponding Author: stanyalu@hotmail.com

Background
Alzheimer's disease (AD) is the major cause of dementia in elderly. Currently, the goals of treatment are to stabilize or slow progression, reduce behavioral and psychological symptoms, and improve quality of life. Due to cost, potential side effects and low efficacy of current medications for AD, factors which can be used for predicting treatment response might be of value for selecting patients with high likelihood to respond and for considering alternative or additional treatment for those with low likelihood to respond. We investigate the predictive value of treatment response in AD patients using MRI and PET findings including morphological change, amyloid load and glucose hypometabolism.

Methodology
33 AD patients who received AD medication(s) were included in the study. The treatment responses were categorized into 2 groups based on the changes of neurocognitive test scores at 1 year. Treatment responder (TR) was defined by stable test scores including 1) no change of Thai Mental State Examination (TMSE) score, 2) no change of clinical dementia rating-sum of boxes (CDR-SB) score and 3) <4 scores increase of Alzheimer's Disease Assessment Cognitive Sub-scale (ADAS-Cog) score. Baseline brain MRI, 18F-Florbetapir (AMY) and 18F-FDG brain PET were performed within 6 weeks from neurocognitive assessments. Visual analysis of MRI using medial temporal atrophy (MTA) scale and both PET studies were done in consensus by 2 experienced radiologists. Morphological volumetry and cerebellar normalized SUVR of AMY and FDG were analyzed using FreeSurfer image analysis suite version 6.0.0 (https://surfer.nmr.mgh.harvard.edu/) and PETSurfer. The AMY/FDG/Vol index was also calculated. Patient characteristics, baseline and change of neurocognitive test scores as well as MRI and PET imaging findings were compared using Chi-square and t statistical tests.

Results
Nine patients were excluded from the study due to loss to follow up and/or death. The remaining 26 AD patients were categorized into 2 groups as treatment responder (TR, n = 6) and non-responder (NR, n = 20) based on changes of neurocognitive scores. There was neither significant difference in baseline characteristics (age, gender, APOE4 carrier, education, onset of symptom) nor baseline neurocognitive score between 2 groups. Using visual analysis, higher likelihood of TR was found in AD patients with negative MTA (RR 6.67, 95%CI 1.59-27.90, p = 0.009) and integrated visual score index less than 3 (RR 8.00, 95%CI 1.08-58.89, p = 0.041). Neither visual results from amyloid (p = 0.133) nor FDG (p = 0.548) PET were significant predictor of treatment response using overall neurocognitive scores. Using quantitative analysis, significantly lower amyloid-load in most areas (p 0.021-0.048) except temporal and hippocampus, and

significantly lower AMY/FDG/Vol index at parietal, posterior cingulate and precuneus (p 0.027-0.046) were found in AD patients with TR. No significant difference between groups was detected using quantitative data from FDG or MRI volume alone.

Conclusion

This study demonstrated that qualitative MTA scale and integrated visual score index as well as quantitative data of cerebral amyloid load and integrated AMY/FDG/Vol index are potentially predictive of treatment response in AD patients but not glucose hypometabolism or quantitative MRI volume alone.

IAEA-CN-285/8

Clinical Impact of 68Ga-PSMA Imaging on Primary Staging of High-Risk Patients, Localization of Biochemical Recurrence Sites and Therapy Response Evaluation

B. Gunalp

Gulhane Medical Faculty, Department of Nuclear Medicine, Turkey

Corresponding Author: bgunalp@yahoo.com

Background
After primary treatment, approximately 30%-40% of patients develop recurrent or metastatic disease. Some of them are due to unrecognized metastatic sites initially with conventional imaging modalities (CIM) and not receiving appropriate treatment. When biochemical recurrence (BCR) developed correct restaging is also very important for therapy planning and management of patients. Therapy response evaluation is another key role for continuing or changing the therapy regimen. The aim of this study is to assess the additional value of 68Ga-PSMA to conventional imaging modalities for primary staging of high-risk patients, the restaging of biochemically recurrent patients and therapy response evaluation for providing the most effective therapy regimen.

Methodology
Patients: This is a retrospective study which include 157 high risk patients with Gleason Score >7 for initial staging. 275 BCR patients with PSA >0.5 ng/ml and/or recurrence suspected with other imaging modalities and 85 patients for therapy response evaluation. 68Ga-PSMA-11 was used as an imaging agent. Images were taken by GE Discovery PET-CT. Results were evaluated with pathology reports and follow-up scans.

Results
68Ga-PSMA for primary staging: 68Ga-PSMA PET-CT detected distant metastases in 15 patients (10%), abdominal lymph node metastases in 13 patients (8%) and pelvic lymph node metastases in 22 (14%) of patients which were not identified before by CIM. Therapy planning was changed in 48 patients (31%) with additional 68Ga-PSMA scan findings.
68Ga-PSMA PET-CT detected recurrence sites in 228 of 275 (83%) BCR patients, even in very low PSA levels (>1 ng/ml) especially in pelvic lymph nodes with normal size and abdominal lymph node and distant metastases which are usually outside of imaging area of CIM. Treatment strate- gies (salvage surgery/radiotherapy or systemic therapy) changed in 109 of 228 (48%) patients.
68Ga-PSMA PET-CT was found superior to CIMs for treatment response evaluation especially differentiation of viable- non-viable tumor masses, determining activity of involved sites and detection of new metastatic foci if progression occurs.

Conclusion

It is concluded that 68Ga-PSMA PET-CT is superior to CIM for the detection of metastases in pelvic lymph nodes with normal size and abdominal lymph nodes and distant metastases which are usually outside of the scan area of CIMs. 68Ga-PSMA PET-CT can be used solely for primary staging of intermediate/high-risk patients and detection of metastatic sites in BCR patients. Treatment response evaluation with 68Ga-PSMA PET-CT is also very useful for selection of effective treatment regimen.

IAEA-CN-285/13

Immuno-SPECT with 99mTc-Nimotuzumab for Planning Immunotherapy in Patients with Non- Small Cell Lung Cancer

Y. Peña Quián[1], T. Crombet Ramos[2], A. Perera Pintado[1], L. Torres Aroche[1], R. Menéndez Perez[3], A. Prats Capote[1], R. Leyva Montaña[1]

[1] Isotope Center, Cuba
[2] Center of Molecular Immunology, Cuba
[3] Ameijeiras Brothers Hospital, Cuba

Corresponding Author: yamicuba2014@gmail.com

Background
Targeted drugs, as well as immunotherapies, are beginning to change the treatment prognosis for people with non-small cell lung cancer (NSCLC). Research efforts are currently focusing on tailoring such therapies according to predictive clinical and molecular markers. Nimotuzumab is a humanized IgG1 monoclonal antibody directed against the epidermal growth factor receptor (EGFr), overexpressed in the surface of some tumors. The selection of patients by immuno-SPECT with 99mTc-nimotuzumab could be crucial to maximize the clinical benefit of the immunotherapy with this MAb. The aim of this study was to determine the utility of the immuno-SPECT with 99mTc-nimotuzumab for planning the immunotherapy in patients with non-small cell lung carcinoma.

Methodology
108 patients (98 with diagnosis of NSCLC and 10 with benign solitary pulmonary nodules, confirmed by biopsy) were included. Average age of the patients was 67 ± 7 years. All were evaluated by both immune-SPECT with 99mTc-nimotuzumab and computed axial tomography before of "cold therapy" with nimotuzumab. Whole body and SPECT images at 4 and 24 hours after intravenous administration of 99mTc-nimotuzumab (6 mg of MAb labeled with 1480 MBq of 99mTc) were acquired, to assess in vivo the expression of EGFr in the malignant lesions. Conventional bone scintigraphy 99mTc-MDP (methyl diphosphonate) was performed on all patients before and after immunotherapy. The therapeutic dose of nimotuzumab, administered to the patients with NSCLC, was 200 mg every 14 days for a year. The result of the immuno-SPECT was compared with the clinical response to immunotherapy. The correlation between the Results of the immuno-SPECT and the Results of clinical parameters was calculated.

Results
The immuno-SPECT with 99mTc-nimotuzumab showed values of sensitivity, specificity, positive predictive value, negative predictive value and accuracy for NSCLC of 73.4%, 100%, 100%, 55.5%, and 75.9% respectively. Allowed the correct location of the lesions, the assessment of their extent, the establishment of the prognosis and the selection of patients, who would be benefited from immunotherapy. Taking the bone scan as a gold standard, the values of sensitivity and specificity of the immune- SPECT for the detection of bone metastases were 37.7% and 100%, respectively.

Patients with positive immuno-SPECT showed a better response to immunotherapy, better quality of life and longer survival time ($r = 0.885$).

Conclusion

The immuno-SPECT with 99mTc-nimotuzumab proved to be a useful tool for planning of immunotherapy in patients with NSCLC. This procedure showed satisfactory values of sensitivity, specificity and diagnostic accuracy. Poor sensitivity, but high specificity for the detection of bone metastases was observed. The experience acquired served as the basis for starting the production of diagnostic and therapeutic kit with these monoclonal antibodies.

IAEA-CN-285/14

Image Quality Evaluation and Quantification of Positron Emitters Using PET-CT GE Discovery ST

M. A. Said[1], M. Musarudin[2], N. F. Zulkaffli[2]

[1] National Cancer Institute, Malaysia
[2] Science University, Malaysia

Corresponding Author: aminhpj@gmail.com

Background
18F is the most extensively used radioisotope in current clinical practices of PET imaging. This selection is based on the several criteria of pure PET radioisotopes with optimum half-life, low positron energy contributes to smaller positron range. In addition to 18F, other radioisotopes such as 68Ga and 124I have gained much attention with the increase of interest in new PET tracers entering clinical trials.
The main goal of this study was to evaluate the PET-CT image quality of 18F, 68Ga and 124I ra- dioisotopes by using the NEMA body phantom.

Methodology
The European Association of Nuclear Medicine procedure guidelines version 2.0 for FDG-PET tumor imaging has been adhered for the purpose of evaluate PET-CT image quality of 18F, 68Ga and 124I radioisotopes by using the NEMA body phantom. This phantom was filled with tumor to background ratio of 10:1 with the activity concentration of 30 kBq/ml ± 10% and 3 kBq/ml ± 10% for each radioisotope. The phantom was scanned using different acquisition times per bed position (1, 5, 7, 10 and 15 minutes) to determine the minimal scan time per bed position (Tmin). Definition of Tmin was performed by using an image coefficient of variance (COV) of 15%.

Results
Tmins obtained for 18F, 68Ga and 124I were 3.08 minutes, 3.24 minutes and 32.93 minutes respectively. Quantitative analyses of 18F, 68Ga and 124I images were performed. Signal to noise ratio (SNR), contrast recovery coefficients (CRC) and visibility (VH) are the image quality parameters analyzed in this study.
Generally, 68Ga and 18F gave better image quality as compared to 124I for all the parameters studied. Meanwhile, a comparison shows that significant difference was observed between 68Ga and 18F at different sphere volume. However, imaging with 68Ga will require a 10 second longer acquisition time compares to 18F.

Conclusion
With the longer scanning time suggested by the Tmin, improvement in the image quality is acquired especially for 124I.

IAEA-CN-285/16

Practical Aspects on Radiolabelling of 177Lu-DOTA-TATE: Radiopharmaceutical Production and Quality Control

B.-U. Jowanaridhi, T. Doungta, S. Hykunya, N. Chareonsin, S. Thida, C. Phaophang, T. Ngamprayad

Radioisotope Center, Thailand Institute of Nuclear Technology, Thailand

Corresponding Author: boonuma@tint.or.th

Background

Radioisotope Center, Thailand Institute of Nuclear Technology is the main organization providing and conducting research on radiopharmaceuticals used in Thailand. Somatostatin analogs have been increasingly used as radiopharmaceuticals for neuroendocrine tumor diagnosis and therapy. Lutetium-177 (177Lu) is a beta emitter with a half-life of 6.65 days which makes it one of the ideal radionuclides for theranosis. In this work, DOTA-TATE peptide was labelled with 177Lu. The technical data of the formulation and the quality control would be prepared for drug registration. The aims were to evaluate the radiochemical yield and the stability of 177Lu-DOTA- TATE and to study the effect of using a 18C cartridge for purification.

Methodology

DOTA-TATE was radiolabelled with 177LuCl3 as shown in Figure 1. The radiolabelling was performed by preparing the mixture of DOTA-TATE and Na-L-Ascorbate in sodium acetate buffer. To the solution was added 200 mCi of 177LuCl3 and this was incubated at 100°C for 20 min. After cooling to room temperature, to the reaction mixture was added diethylenetri- amine pentaacetate (DTPA) solution. Purification was done by using Sep-pak 18C cartridge and 0.22 µm Millipore was used to sterilise the radiolabelled compound as the last step. The product was determined by radioinstant thin layer chromatography (radio-ITLC) and radio-high performance liquid chromatography (radio-HPLC). The stability was investigated at room temperature for 4 days and the microbiology testing was conducted in accordance with GMP requirements. Moreover, biodistribution was studied in normal mice.

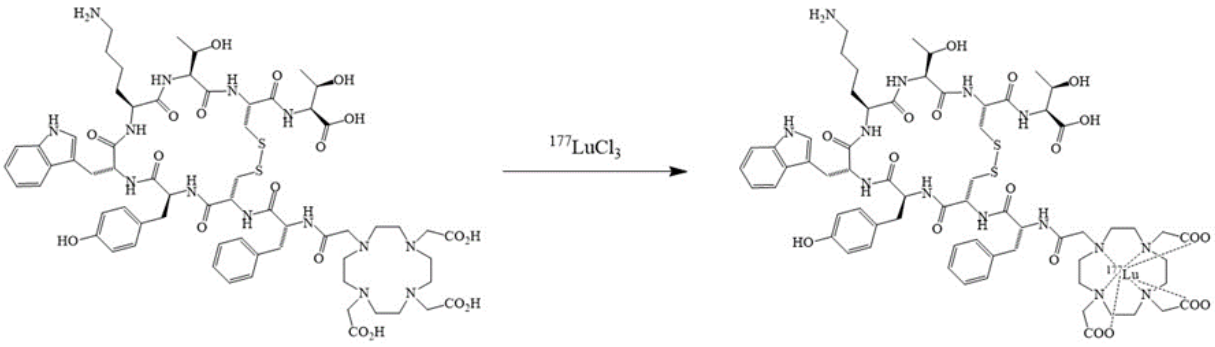

DOTA-TATE ^{177}Lu-DOTA-TATE

Figure 1: Radiolabelling of DOTA-TATE with 177LuCl3.

Results

Radiochemical yield of 177Lu-DOTA-TATE was more than 96% without purification. The radiolabelled compound was stable for at least 4 days at room temperature and was proved to be a sterile product. While the purified product obtained 98% radiochemical purity, the stability was lower. Radio-HPLC showed the loss of ascorbate resulted in the decrease of the product stability. Biodistribution study in normal mice demonstrated the uptake in pancreases.

Conclusion

This study presented the suitable radiolabelling condition of 177Lu-DOTA-TATE. The disadvantage of using the 18C cartridge for purification was found. Although free 177Lu was removed from the radiolabelled product, the stabilizer was trapped in the cartridge. Therefore, the radiolabelling should be performed without purification. However, if the purification step is required, it is highly recommended that a stabilizer such as gentisic acid or ascorbic acid should be added in the final product to maintain its stability.

IAEA-CN-285/17

Pre- and Post-Therapy Dosimetry of 177Lu-DOTATATE for Radioiodine-Refractory Differentiated Thyroid Cancer: First Personalized Patient Dosimetry in Indonesia

N. R. Hidayati[1], H. Budiawan[2], E. R. Harahap[2], R. Shintawati[2], A. R. Dewi[3], I. A. S. Mu'minah[4], A. H. S. Kartamihardja[2], P. Widodo[5]

[1] Center for Technology of Radiation Safety and Metrology, India
[2]General Hospital, India
[3]National Cancer Cneter, India
[4] Faculty of Mathematics and Natural Sciences, India
[5] Center for Technologyof Radiation Safety and Metrology

Corresponding Author: inn98@batan.go.id

Background
177Lu has been enormously utilized for radionuclide therapy worldwide. In Indonesia, the application of 177Lu for the clinical study has been performed started from 2017 in cooperation between The Center for Technology of Radiation Safety and Metrology-BATAN and Hasan Sadikin General Hospital, and with the support from IAEA CRP E23005, entitled Dosimetry in Molecular Radiotherapy for Personalized Patient Treatments. The objective of the study is to estimate the organ doses for kidneys, liver and spleen in the pre-therapy procedure and compare the doses after the therapy procedure.

Methodology
The study was performed on DTC patients who are refractory to I-131 with an average pre-dosimetry activity of 5.68±0.52 mCi. An amino acid infusion was performed prior to the administration of 177Lu-DOTATATE. Patients were scanned with the Infinia Siemens Gamma Camera with a scanning speed of 10 cm/min, equipped with a medium energy parallel hole collimator and a 15% window setting for the acquisition of whole-body scan (WBS). The images were quantified and analyzed by using the view conjugate method on planar images which were taken at 1, 24, 48 and 72 hours after the administration. The percentage of the injected dose were used as the input of OLINDA/EXM to produce the time-integrated activities coefficients (TIACs). Two months after the pre-dosimetry procedure, 3 patients have been selected for the therapy and administered with the activity of 177Lu-DOTATATE about ± 100 mCi. With the same procedure, the organ doses being evaluated and compared with the estimated organ doses as previously were estimated in pre-therapy dosimetry.

Results
The results show that the acquired organ doses for the post-therapy procedure in 2 out of 3 patients was less than the estimated organ doses in post-therapy.

Table 1. The result of estimated organ doses and acquired organ doses in post-therapy of [^{177}Lu]Lu-DOTATATE for radioiodine-refractory differentiated thyroid cancer patients.

ORGAN	P2 Dose (Gy)		P2 Dose (Gy)		P4 Dose (Gy)	
	estimated	acquired	estimated	acquired	estimated	acquired
Kidney	2.32	2.89	0.97	0.0002	1.85	1.03
Liver	0.72	0.38	0.02	0.00004	1.12	0.21
Spleen	6.24	9.22	0.16	0.0005``	3.79	0.64

Conclusion

The critical organs during the PRRT for radioiodine-refractory differentiated thyroid cancer patients are safe, since the estimation dose were taken was lower than the acquired dose in post therapy procedure.

IAEA-CN-285/21

The Role of the Hybrid Imaging Techniques SPECT-CT and PET-CT in the Diagnostic Algorithm and Optimization of the Therapy in Patients with Somatostatin Expressing Tumors

I. Kostadinova, M. Garcheva-Tzacheva, G. Mateva

University Hospital Acibadem City Clinic, Bulgaria

Corresponding Author: irdika.family@gmail.com

Background
Somatostatin receptor scintigraphy using 18F-FDG PET-CT is more frequently recommended for treatment planning of somatostatin expressing (SR) neuroendocrine tumors. The aim of our study was to apply both hybrid imaging techniques SPECT-CT and PET-CT within the period of one month in the same patient with a series of follow ups in the patients (Pts) with SR-expressing tumors for localization, staging, and restaging as a tool for choosing appropriate therapy.

Methodology
A total of 185 consecutive SPECT-CT and PET-CT examinations were performed on 48 patients (on average 3.8 exams) for the period 2016-2019, of which 32 were GEP tumors, 12-with lung and 4 –with other localizations. All investigated Pts have Ki 67 index >3%, in order to visualize differentiated and mixed/non-differentiated parts of the tumors. For SPECT-CT we have used the somatostatin analog 99mTc-HYNIC-TOC at activities between 550-600 MBq and for 18F- FDG PET-CT with an activity of 2.5 MBq/kg. The average level of chromogranin was 208 ng/ml and that of Ki 67 index-31%. Whole body and SPECT-CT scintigraphy were performed 2- 4h post and PET-CT– 45-90min post injection.

Results
In 27/48 Pts, with SPECT-CT exams only, more lesions were visualized than with PET-CT, in 8/48 with PET-CT exam only, more lesions were visualized than with SPECT-CT, in 5/48 equal numbers of lesions were detected in both scans, in 8/48 of the patients- both exams were negative (after surgery or drug therapy). During the follow up, in 10 Pts the tumor changes from differentiated to non/less differentiated and somatostatin positive scintigraphy became negative/less positive at the expense of more changes in PET-CT investigation. All patients with positive results were referred for surgery or further somatostatin therapy, chemotherapy, targeted chemotherapy, or PRRT, depending on the stage and the differentiation of the disease. The therapy plan had changed in 17 of the Pts -34.8%, which has proven that therapeutic strategies could be optimized by applying 18F-FDG PET-CT in some of the patients with less differentiated neuroendocrine tumors.

Conclusion

We consider that the application of both imaging techniques – SPECT-CT and PET-CT as a useful strategy for optimization of treatment in patients with somatostatin expressing neuroendocrine tumors. Serial follow up is important in order to see their differentiation and need for change in therapy.

IAEA-CN-285/22

The Role of 18F-FDG for Assessment of Tumor Response to Immunotherapy with PD-1/PD-L1 Blockage in Patients with Advanced Melanoma

I. Kostadinova

University Hospital Acibadem City Clinic, Bulgaria

Corresponding Author: irdika.family@gmail.com

Background
The advent of immune checkpoint inhibitors has revolutionized metastatic melanoma treatment as they have led to longer progression-free survival and overall survival rates. However, their introduction in clinics has raised the issue of appropriate treatment response evaluation since tumor responses are typically longer than in conventional treatment and are partially associated with immune-related adverse events. The aim of the study was to evaluate the treatment response of patients with metastatic malignant melanoma to check point inhibitors, using 18F-FDG PET-CT.

Methodology
We studied retrospectively 21 patients (12 women and 9 men), treated with pembrolizumab (18 patients) and with nivolumab (3 patients) for the period 2016-2019, performing 89 PET-CT investigations (on average 4.2 per patient), before and after the beginning of immunotherapy (the first scan performed at 3 months in order to avoid visualization of eventual early pseudoprogression). We used metabolic criteria PERCIST and morphological criteria -RECIST 1.1 and irRC for treatment response evaluation.

Results
Progression was registered in 7/21 patients with a 43.5% metabolic increase in activity of the target lesions on average (including new lesions) and the treatment was discontinued; complete response in 5/21 patients (without active lesions); partial response in 5/21 patients with 40.8% metabolic decrease of activity of the target lesions on average, and stable disease was registered in 4/21 patients. In 6 patients the therapeutic result was visualized earlier on PET than on CT (in some lymph nodes, bone marrow, peritoneum and muscles). Three patients with negative PET findings and residual lesions on CT had no signs of the progression in the following 2 years. Five patients showed adverse effects of the treatment such as sarcoidosis, pneumonitis, hypophisitis, colitis, and skin changes. From these, three were successfully visualized early with PET but not with CT and were treated later.

Conclusion
We consider PET-CT a promising tool for evaluating patients with metastatic melanoma under PD-1/PD-L1 blockage in order to optimize treatment. It could show an earlier therapeutic response and visualization of the adverse effects based on changed metabolism, compared to usage of CT only.

IAEA-CN-285/23

In Vivo Chemokine Receptors (CXCR4) Imaging in Newly Diagnosed Breast Cancer Patients Using 68Ga Labelled CXCR4 PET-CT

R. Kumar, B.T. Mittal, J. Shukla, H. Singh, V. Krishnaraju, Y. Rathore

Post Graduate Institute of Medical Education and Research Chandigarh, India

Corresponding Author: drrajender2010@gmail.com

Background
Chemokine receptors (CXCR4) over-expression is associated with numerous malignancies including breast cancer. It plays a major role in signalling pathways for tumor metastasis. The present study aimed to in vivo image chemokine receptors for potential surrogate markers for immune checkpoint inhibitor therapy (CXCR4-directed drugs).

Methodology
In this study, newly diagnosed cases of breast cancer were recruited prospectively for FDG PET-CT and followed by CXCR4-targeted PET-CT imaging with one-week intervals. Both the PET-CT images were evaluated by two expert nuclear medicine physicians visually and semi quantitatively with mutual consensus. Tracer uptake in the primary lesion more than the mediastinal blood pool activity was positive. The SUVmax of the lesion was compared with pathology findings, prognostic factors, and molecular subtypes. Immunohistochemistry for CXCR4 expression in the biopsy specimen was also done.

Results
A total of 50 patients (48 females, 2 males, meanage ±SD= 51.4±13, ranged 25-87 years) were recruited. Primary lesions were visualised in all patients on both the PET-CT images. The mean SUVmax of the primary lesion on CXCR4 receptor imaging ranged from 2.0-24.9 (mean ±SD= 6.5±4.2), while on FDG PET-CT imaging it ranged from 2.8-51.6 (mean ±SD= 13.9±8.7). CXCR4 receptor expression was also noted in all the metastatic sites visualised on FDG PET-CT. FDG PET-CT revealed higher SUV max when compared to CXCR4 PET-CT in primary as well as metastatic sites. Metastatic brain lesions in two patients were well visualised on CXCR4 PET-CT imaging as compared to FDG PET-CT imaging with no interfering Background activity in the normal brain parenchyma. No correlation was observed between SUVmax values of primary tumor on CXCR4 PET with breast cancer prognostic factors like estrogen receptor (ER), progesterone receptor (PR), human epidermal growth factor receptor 2 (HER2), proliferation index (Ki-67), tumor grade, or molecular subtypes.

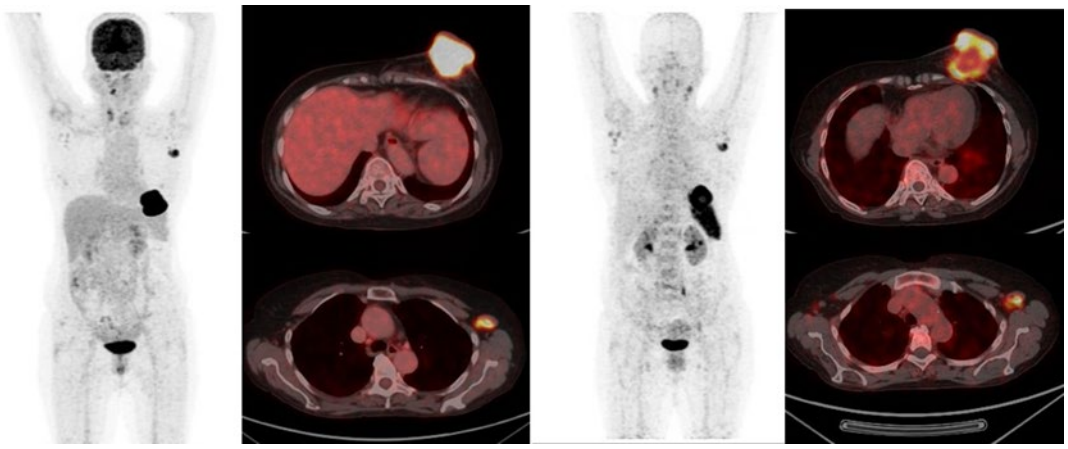

Conclusions

This study highlights the benefits of in-vivo imaging of CXCR4 receptor status in newly diagnosed breast cancer patients. CXCR4 imaging may act as a potential surrogate marker for CXCR4-directed drugs (i.e. Balixafortide) in such patients not responding to the conventional therapeutic regimen. Additionally, these patients may be promising candidates for further exploration of 177Lu labelled CXCR4 radionuclide therapy.

IAEA-CN-285/26

The Potential Role of Polyglutamate Folate in Mitigating off-Target Salivary PSMA Uptake in Molecular Radiotherapy

C. Kaoma[1], H. Ndlovu[2], I. Lawal[3], N. Mokgoro[3], M. Vorster[3], M. Sathekge[3]

[1] University Hospital, Lusaka, Zambia
[2] Steve Biko Academic Hospital, Pretoria, South Africa
[3] University of Pretoria, South Africa

Corresponding Author: chimbabantu@hotmail.com

Background
Prostate-specific membrane antigen (PSMA) molecular radiotherapy has shown promising Results in the treatment of metastatic castration-resistant prostate cancer (mCRPC). Most notable Results have been with an alpha particle-emitting radionuclide such as Actinium-225 (225Ac) which has shown great efficacy in late-stage patients. However, PSMA is also expressed in kidneys, lacrimal glands and salivary glands where specific uptake causes dose-limiting xerostomia. Recent evidence has shown that polyglutamate may prevent off-target PSMA uptake without affecting that in the tumors.

Methodology
The aim of the study was to establish the optimal dose and timing of polyglutamate before tracer injection that would block off-target salivary PSMA uptake. 14 patients with histologically confirmed prostate cancer presenting to our department for staging and restaging 68Ga-PSMA PET-CT were recruited to undergo a follow-up scan. 3 patients had 2 candies 30 minutes prior and 2 candies at the injection of the 68Ga-PSMA, 2 more had 3 candies 30 minutes prior and 3 candies at the time of injection. 3 more had 3 candies 60 minutes prior and 3 candies at the time of injection. 3 more had 3 candies at 120 minutes prior and 3 candies the time of injection. 3 more had 3 candies at 240 minutes and 120 minutes prior to injection.

Results
The non-significant change was noted in tracer uptake by visual inspection and in the form of SUV-max between the intervention and the control studies. The mean SUV-max of all the intervention groups except group 2, the second metastatic site, was noted to be moderately increased but however non-significant compared to control.

Conclusion
This study demonstrates no significant impact of polyglutamate folate on PSMA salivary uptake. Larger controlled studies are recommended to evaluate the optimal route of administration, timing, and dosing of the polyglutamate.

IAEA-CN-285/27

Evaluation of Suspect Lung Lesions through Percutaneous Biopsy: Differences in Diagnostic Accuracy Between PET-CT and CT

J. J. Cerci[1], M. Bogoni[1], M. Masukawa[1], C. Cunha Pereira Neto[1], J. V. Vítola[1]
R. Bar- Reiros[2], D. Sakamoto[3]

Corresponding Author: bogonimateos@gmail.com

Background
Lung biopsies can be performed through PET-CT or CT guidance. While CT provides purely anatomical information, PET-CT also analyzes metabolic features. The purpose of our study is to compare both groups' performances in guiding percutaneous biopsies with histological confirmation of lung lesions.

Methodology
We prospectively evaluated 404 patients of whom 211 underwent FDG PET-CT- guided biopsy and 193 underwent CT-guided biopsy. The pathology results, and complication rates in the two groups were evaluated.

Results
Of the 211 biopsies with PET-CT guidance, histology demonstrated 169 lesions (80.1%) to be malignant, and 42 (19.9%) benign; while of the 193 biopsies of the CT-guided group, 132 (68.4%) lesions were malignant and 61 (32.8%) were benign ($p < 0.001$). Of the PET-CT-guided biopsies, 31 (14.7%) were repeat biopsies due to a previous nondiagnostic CT-guided biopsy. During follow up of patients, a second biopsy was performed due to unreliable Results in 9/211 (4.2%) patients of the PET-CT-guided biopsy group, and in 16/193 (8.3%) patients in the CT group, with no significant statistical difference ($p=0.09$). The complication rate in the PET-CT-guided biopsy group was 14.7% (31 patients), while in the CT-guided group, was 14.5% (28 patients).

Conclusion
PET-CT-guided biopsy of lung lesions yielded higher malignant positive results than CT guided biopsy, with similar complication rates.

IAEA-CN-285/28

PET-CT-Guided Biopsy Presents Higher Malignant Positive Results than CT Guided Biopsy

J. J. Cerci[1], M. Bogoni[1], M. Masukawa[1], C. Cunha Pereira Neto[1], J. V. Vítola[1]
R. Bar- Reiros[2], D. Sakamoto[3]

Corresponding Author: bogonimateos@gmail.com

Background
Percutaneous biopsies can be performed through PET-CT or CT guidance. While CT provides purely anatomical information, PET-CT also analyzes metabolic features. The purpose of our study is to compare the performance of PET-CT and CT in guiding percutaneous biopsies of several different sites, with histological confirmation.

Methodology
We prospectively evaluated 1072 patients of whom 503 underwent FDG PET-CT guided biopsy and 569 underwent CT-guided biopsy. The pathology results, and complication rates in the two groups were evaluated.

Results
Of the 503 biopsies with PET-CT guidance histology demonstrated that 413/503 of lesions (82,1%) were malignant, and 90 (17,9%) were benign, while 394/5069 (69,2%) lesions were malignant and 175/569 (30,8%) were benign in the CT-guided group ($p = < 0.001$). Patients with a histological diagnosis of benign lesion had no recurrence of disease with a minimum of 6 months follow-up. Of the 188 PET-CT-guided biopsies, 35% were repeat biopsies due to a previous non-diagnostic CT-guided biopsy. The complication rate in the PET-CT-guided biopsy group was 8.2%, while in the CT-guided group, was 7.0% ($p = 0.4$).

Conclusion
PET-CT-guided biopsy presents higher malignant positive resultsthan CT guided biopsy, with similar complication rates.

IAEA-CN-285/30

Comparison of PET-CT and contrast CT in Peritoneal Carcinomatosis

M. Garcheva-Tsacheva, I. Kostadinova, G. Mateva

University Hospital Acibadem City Clinic, Bulgaria

Corresponding Author: marina.garcheva@gmail.com

Background
Peritoneal carcinomatosis (PC) is a potentially serious complication of some types of cancer such as ovarian cancer, colorectal cancer and other gynecological and gastrointestinal tumors. The therapeutic approach depends on the detection and the proper evaluation of the extent of the disease. The extent evaluation of peritoneal carcinomatosis is difficult, often possible only during surgical exploration. 18F-FDG-PET-CT was proposed as an option for diagnostics and follow-up additionally to other imaging modalities: contrast enhanced CT (ceCT) and magnetic resonance imaging.
The aim of the study is to determine the diagnostic value of PET-CT and compare PET-CT and ceCT in terms of diagnostic advantages and limitations in staging and follow-up of the disease.

Methodology
We evaluated retrospectively 67 patients by PET-CT. In 33 patients a comparison with ceCT has been done. Forty-three of the patients were women and 24 were men, aged from 41 to 77 years. Thirty-two patients were with gastrointestinal tumors (23 - with colorectal carcinoma); 33 with gynecological tumors (26 - ovarian). The other two patients were with primary peritoneal cancer and polyserositis. The contrast CT was performed in 32 patients in interval 2 ±1 month from PET-CT. All patients were with determined histology.

Results
There was a full coincidence between PET-CT and ceCT findings in 17/32 (53%) of patients.
The PET finding detectable in 64/67 of patients (96%) was peritoneal thickening with metabolic activity, and in 21 of them (31%) this was the unique finding of dissemination. Corresponding ceCT finding was detected in 28/32 patients (87%). The frequency of ascites on PET-CT images was 15% (10 patients), but as a unique finding it was detected only in 3 patients (4%). Recurrences were detected in 15 patients, 14 proved as true positive (21%), lesions in the surgical cicatrix - in 8 patients (12%), half of which disappeared on the follow-up studies (false positive). Additional spread findings as lymph nodes involvement (31%), lung and pleural lesions 15%, bone and bone marrow lesions (7%), liver lesions (6%), adrenal lesions (3%), leptomeningeal lesion (1%) were detected. The comparison with ceCT demonstrated detection of 12% more recurrences by PET-CT (14 vs 10); detection of more scar implants (4 of which were true positive, 12%) and detection of more distant metastases. PET permitted the determination of the metabolic activity of some peritoneal lesions without dynamics on corresponding ceCT and of lymph nodes without enlargement. The false positive PET-CT results were related to peritoneal metabolic activity without substrate (n=1), to inflammation (n=1) and 4 false positive cicatrix implants.

Conclusions

Due to its whole-body character, PET-CT detected more lesions (including peritoneal) related to the presence and dissemination of the disease. By determination of the metabolic activity, the effect of therapy also can be evaluated. False positive PET-CT findings always had to be taken into consideration especially in the ileocecal and scar's regions.

IAEA-CN-285/32

Aplastic Anaemia After I-131 Therapy of Metastatic Differentiated Thyroid Carcinoma: A Case Report

S. Abubakar[1], A. Isah[2], R. Steyn[3], E. Verburgh[3]

[1]University of Ilorin Teaching Hospital, Nigeria
[2]Usmanu Dan Fodio University Teaching Hospital, Nigeria
[3] University of Cape Town, South Africa

Corresponding Author: abubakar.yinka@yahoo.com

Background
In differentiated thyroid carcinoma, radioactive iodine therapy is a well-established adjuvant treatment which improves disease specific and disease-free survival more so in patients with metastatic or residual disease. Most patients with metastatic disease require high and multiple doses of ra- dioactive iodine thus increasing their risk of significant adverse effect. Aplastic anaemia is a very rare adverse effect. We report the first case of such in our facility.

Case Report
A 68-year-old woman presented with 2 years history of painless slow growing neck mass. FNAC and CT of the neck and chest showed malignant cytology and evidence of metastatic disease in the neck and lungs. She subsequently had total thyroidectomy, laryngectomy and bilateral neck dissection. Histology showed a 45 mm papillary thyroid carcinoma with extensive vascular and lymphatic invasion, extrathyroidal soft tissue and surrounding skeletal muscle invasion, 10 positive neck nodes with extracapsular extension in some of the nodes. She was classified as a high-risk patient and referred for I-131 therapy.
She had a diagnostic I-123 scan which showed iodine uptake in the thyroid bed, paratracheal nodes and multiple lung nodules. She then had 7.6GBq I-131 therapy. Admission was uneventful. Two months after the first therapy, her stimulated thyroglobulin decreased from 4777µg/l pre-treatment to 2362µg/l.
Follow up I-123 diagnostic scan at 6 months showed decreased uptake in the neck, mediastinum and lungs. She had a second dose of 8.1GBq of I-131. Admission was uneventful. She had a drop in her stimulated thyroglobulin from 1835µg/l to 394µg/l.
She presented about 1 month after her second I-131 therapy with petechial rashes on the tongue and thighs. Full blood count showed pancytopenia (Table 1). Bone marrow aspirate and trephine biopsy was aplastic with estimated overall cellularity of <5%. A diagnosis of severe acquired aplastic anaemia was made. Over the next month, she required repeated blood transfusions on 5 occasions. Thereafter there was a gradual return of the peripheral blood indices to normal over the course of the next year.

IAEA-CN-285/34

99mTc PYP Scintigraphy in the Diagnosis of Transthyretin Cardiac Amyloidosis

M. Garcheva-Tsacheva[1], M. Gospodinova[2], G. Mateva[1]

[1]AcibademCity Clinic, Bulgaria
[2]Medical Institute -Ministry of Interior, Bulgaria

Corresponding Author: marina.garcheva@gmail.com

Background
Transthyretin cardiac amyloidosis is a devastating disease, more common than previously thought. Early diagnosis is vital for timely treatment and better prognosis. Endomyocardial biopsy (EBM) with amyloid typing is the gold standard for diagnosis, but it is an invasive procedure with the potential risk of fatal complications. Bone scintigraphy is approved in the non-biopsy diagnostic algorithm for transthyretin cardiomyopathy.

Methodology
Thirty-seven patients (28 male, 9 females, aged 39-78 years) with suspicion for cardiac amyloidosis from clinical examinations, electro and echocardiography were submitted to bone scan with 99mTc-PYP in order to determine the eventual myocardial uptake of bone seeking radiotracer. Two planar projection up to 750 K counts and SPECT-CT were registered on GE Discovery NM/CT 670 Pro at the 1st hour after the injection of 10-15 mCi of 99mTc-PYP. The visual Perugini score was used for qualitative evaluation of cardiac uptake and the ratio heart to the contralateral region (H/CL) for semi-quantitative evaluation. SPECT-CT images were important to discriminate the blood pool activity from myocardial activity especially in patients with renal insufficiency.

Results
Twenty-three patients had a score of 0-1 and H/CL 1-1.2. Ten patients had a score of 2-3 and H/CL 1.5. Four patients scored between 1.25-1.40. Transthyretin cardiomyopathy was confirmed by genetic analysis in 6 pts, in 1- a wild type of the disease, all of them with H/CL 1.5. Three patients from this group were false positive, two - with light chain amyloidosis (AL), according to parallel haematological examinations. SPECT-CT demonstrated blood pool uptake in one of them, helping the nonconclusive result. Not one of the patients with H/CL 1-1.4 had Transthyretin amyloidosis, AL was proved in 3 of them.

Conclusion
Bone scan by 99mTc PYP is a reliable method for the diagnosis of the transthyretin cardiac amyloidosis with low rate of false positive results. SPECT-CT helps the diagnosis of myocardial deposition of the bone seeking agent. This non-invasive examination reduced significantly the percentage of patients with unclear diagnosis, which needed EMB.

IAEA-CN-285/35

Should 18F-FDG PET-CT be used in Staging of Early Breast Carcinoma? Impact of 18F-FDG PET-CT in Different Clinical Stages of Breast Cancer

S. Gandhi

Zydus Cancer Center. Ahmedabad, India

Corresponding Author: gndsunny@gmail.com

Background
Role of 18F-FDG PET-CT is well established in locally advanced and metastatic breast carcinoma for staging. Current guidelines do not recommend 18F-FDG PET-CT for staging in early breast carcinoma (clinical stage I, II and operable stage III). We wanted to assess the impact of PET-CT in initial staging of breast cancer across various clinical stages and to investigate the potential utility in the initial staging of patients with early breast cancer.

Methodology
160 patients with biopsy-proven breast cancer with various clinical stages presented within last 2 years, who underwent 18F-FDG PET-CT scan for staging purpose, were retrospectively analyzed. Whole body PET-CT images were obtained from vertex to mid-thigh using dedicated PET-CT scanner. Diagnostic CT scan was acquired using non-ionic iodinated intravenous contrast medium as a part of PET-CT study.

Results
Out of total 160 patients, 2 patients had clinical stage I disease and 1 patient had clinical stage IV disease and PET-CT did not change clinical stage. But it was useful in detecting all metastatic sites in stage IV disease. Out of 113 patients of clinical stage III patients, 66 patients (58%) had change in clinical stage post PET-CT. Out of theses 66 patients, 55 (48.6%) had change in clinical management plan. Out of 44 patients of clinical stage II patients, 06 patients (13.6%) had change in clinical stage post PET-CT. Out of theses 06 patients all had change in clinical management plan.

Clinical Stage	Total No. of Patients	No. of Patients with change in clinical stage	% change in clinical stage	No. of Patients with change in clinical management	% change in clinical management
Stage I	**02**	**00**	**00%**	**00**	**00%**
IA	02	00	00%	00	00%
Stage II	**44**	**06**	**13.6%**	**06**	**13.6%**
IIA	15	02	13.3%	2	13.3%
IIB	29	04	13.8%	4	13.8%
Stage III	**113**	**66**	**58%**	**55**	**48.6%**
IIIA	51	29	56.8%	22	43.1%
IIIB	31	11	35.4%	08	25.8%
IIIC	31	26	83.8%	25	80.6%
Stage IV	**01**	**00**	**00%**	**00**	**00%**

Conclusion

PET-CT can detect extra-axillary lymph node involvement (supra-clavicular, internal mammary and other distant) with better sensitivity and can uncover occult distant metastases in a significant percentage of patients. Although chances of detection of extra-axillary nodes and distant metastasis is more with locally advanced and metastatic disease, early breast cancer can also present with extra-axillary nodal and distant metastasis in reasonable number of patients. Whenever detected, it can have significant impact on patient management as shown in our study. Therefore, in the era of personalized medicine, initial PET-CT can enable better treatment planning for patients with early breast cancer (Stage II and operable stage III) excluding stage I disease.

IAEA-CN-285/37

Clinical Outcome of Radioligand Therapy with 177-Lu-PSMA in Metastatic Prostate Cancer: An Initial Experience from an Indian Tertiary Care Cancer Hospital

M. Gupta[1], P. S. Choudhury[1], G. Garthikeyan[2], V. Talwar[1], C. Sudhir[1]

[1] Rajiv Gandhi Cancer Institute and Research Centre, India
[2] Amity University, India

Corresponding Author: docmanojgupta@yahoo.com

Background
Metastatic castration resistant prostate cancer (mCRPC) is an inevitable stage in the management of prostate cancer. Eventually, all advanced prostate cancer patients develop resistance to known standard drugs and most of them end up with rising PSA, high volume of disease, and diffuse bone pain. Hence, novel drugs with better efficacies are desired for patient palliation. One such possible hope to these patients is to use the 'Theranostic' approach using prostate specific membrane antigen (PSMA) as a target. In this study, we analysed the clinical outcome of 177-Lu-PSMA in mCRPC patients in the Indian population.

Methodology
Twenty-five mPC patients were treated with 177-Lu-PSMA on compassionate bases. Pre- and 8- 10 weeks post-treatment PSAs, Eastern cooperative oncology group (ECOG) performance status, Visual analogue scale (VAS), and Analgesic quantification scales (AQS) were recorded for clinical outcomes. Based on three PSA response groups (partial response PR, stable disease SD, progressive disease PD), patients were categorised into responder (PR+SD) and non-responder (PD). Wilcoxon signed-rank, and Kruskal–Wallis test, Kaplan Meier with Log rank test were computed by MedCalc Statistical Software version 19.1.5. P value < 0.05 was considered statistically significant.

Results
Twenty-five mPCa patients with a median Gleason score of 8.3 (range 7-10) with a median 69 years of age (range 45-81) were treated with a median 7.4 GBq (range 3.7-7.7 GBq) 177Lu-PSMA. Overall PR, SD, and PD were 24%, 60%, and 16% respectively. Sixteen patients who received a $\geq$ 7.4GBq 177-Lu-PSMA dose, had PR and SD Results of 31.2% and 68.8% respectively. We had 84% responders and 16% non-responders. Statistically significant difference ($P < 0.05$) was seen in pre and post ECOG (Z value -2.5), VAS (Z value -3.9) and AQS (Z value -3.5) parameters on Wilcoxon signed- rank test while it was statistically insignificant for PSA (P value 0.170, Z value -1.6). We found that the 177-Lu-PSMA dose was the only significant factor (P 0.024) on Kruskal–Wallis test for a PSA response outcome. Overall, median PFS was 24 weeks (95% CI: 9-52) in our study. Two years PFS of PR, SD and PD response group was 50%, 37.3%, and 0% respectively. Significant difference was seen in the PFS of responder and non-responder groups (P value 0.0003 and Hazard ratio 0.16).

Conclusion

We concluded that 177Lu-PSMA was a fair palliative option in heavily pre-treated mPCa patients for both pain and PSA response despite poor performance status. It has the potential to become a valid treatment option for these patients, however proper randomised studies are required.

IAEA-CN-285/42

Determination of Patient Doses and Biokinetic of 68Ga-PSMA 11 PET-CT Imaging in Metastases Prostate Cancer Patients

K. Khamwan, P. Chamnan, Y. Thinka, S. Shiratori

Chulalongkorn University, Thailand

Corresponding Author: kitiwat.k@chula.ac.th

Background
Prostate cancer is one of the most common cancers worldwide among the male population. 68Ga-PSMA-11 radiopharmaceutical was recently used as the cutting-edge imaging to diagnose for metastasis prostate cancer patients. However, there is no relevant research regarding the radiation dose for prostate cancer patients using 68Ga-PSMA-11 in Thailand. This study aimed to evaluate patient doses and the biokinetic distribution of 68Ga-PSMA-11 PET-CT examination in prostate cancer patients in order to establish the preliminary baseline dosimetry of Theranostics in Thai patients.

Methodology
Sixteen metastases prostate cancer patients aged between 54 and 83 years-old (mean±SD; 68.9±6.8) were administered intravenously with 89–224 MBq of 68Ga-PSMA-11 (mean±SD, 153.87±36.98 MBq). Whole–body PET-CT static scan at 1-hour post injection was acquired by Siemens Biograph
16 PET-CT system at King Chulalongkorn Memorial Hospital (KCMH), Bangkok. Contours were drawn on fused PET-CT images using the PMOD program for brain, salivary glands, thyroid, lungs, heart wall, liver, gallbladder, spleen, adrenal glands, kidneys, red marrow (L3-L5), urinary bladder, and muscle (right thigh) by placing ROI over the portion of the organ uptake with 68Ga-PSMA to calculate the time-integrated activity coefficients in source organs. The mass of organ in each patient was interpolated by scaling the organ mass from the reference man according to ICRP Publication 89. The absorbed dose coefficients in target organs were calculated according to Medical Internal Radiation Dose (MIRD) scheme using OLINDA/EXM version 2.0, based on non-uniform rational B-splines (NURBS) computational phantoms. Tissue weighting factors from ICRP 103 were used in effective dose calculations.

Results
The highest absorbed dose coefficient of 0.12±0.05 mGy/MBq was found in kidneys, followed by the adrenal glands, salivary glands, spleen and urinary bladder of 0.075±0.03, 0.057±0.02, 0.032±0.01 and 0.031±0.01 mGy/MBq respectively. The average whole-body effective dose coefficient of 68Ga-PSMA-11 of 11±3.2 μSv/MBq was obtained. The highest activity uptake was observed in the muscle approximately 6.32%. Additional organs with high uptake were found in kidneys (4.60%), liver (4.54%) and urinary bladder (1.45%), respectively. The effective dose coefficient calculated by NURBS phantom using OLINDA/EXM 2.0 was lower than the Cristy-Eckerman stylized computational phantom using the OLINDA/EXM version 1.0 by -17%.

Conclusion

Kidneys were the critical organ for 68Ga-PSMA-11 radiopharmaceutical. The effective dose coefficient of 11 μSv/MBq obtained in this study was slightly lower than other previous studies as the single-time point image-based method was employed. The resulttsobtained in this study can be used as the preliminary reference data for 68Ga-PSMA-11 dosimetry and its biokinetic in Thai patients.

IAEA-CN-285/44

Development of a New 64Cu-Semicarbazone Complex: Potential Theranostic Radiopharmaceutical for Hypoxic Tumor

I. Aljammaz[1], N. Alhokbany[2], B. Alotaibi[1], S. Okarvi[1]

[1] King Faisal Specialist Hospital & Research Centre, Arabia Saudí
[2] King Saudi University, Arabia Saudí

Corresponding Author: jammaz@kfshrc.edu.sa

Background
Heterocyclic thiosemicarbazones, semicarbazones and their metal complexes have been extensively investigated as potential anti-tumor agents. Most studied thiosemicarbazones and semicarbazones were the pyridine-based compounds which might be attributed to their resemblance to pyridoxal metabolites that attached to co-enzyme B6-dependent enzymes and caused enzyme inhibition. Varieties of metallic PET and SPECT radionuclides were incorporated into thiosemicarbazones chelates. Among these radionuclides, 67/68Ga and copper-62/64 (62/64Cu) have shown considerable success for targeting hypoxic and normoxic tumor xenografts in athymic mouse models. In comparison with their corresponding thiosemicarbazone, semicarbazone complexes possess enhanced anti-neoplastic activity. A recent study demonstrated significant tumor uptake and favourable pharmacokinetics of 68Ga-semicarbazone over 68Ga-thiosemicarbazone radiotracers. In addition, the physical property of the positron emitter 64Cu together with the well-known coordination chemistry makes it one of the most attractive radionuclides for PET imaging and possibly therapy. We report the synthesis, characterization and preclinical evaluation of new 64Cu-semicarbazone (64Cu-[APSC]2) as a potential PET imaging agent for hypoxic tumor.

Methodology
The synthetic approach for the preparation of 64Cu-[APSC]2 was simple and straightforward. Solution of 64CuCl2 (37-300 MBq) was reacted with APSC in acetate buffer (pH ~4.5) at 80oC and 20 min. Work up of this reaction gave 64Cu-[APSC]2 in quantitative radiochemical yields and purities as assessed by TLC and HPLC in less than 30 min. The stability of 64Cu-[APSC]2 was determined in human plasma and revealed that this radiotracer remained stable during incubation at 37oC for at least 4 h.

Results
Biodistribution studies in nude mice bearing MDA-MB-231 cell-line xenografts demonstrated substantial tumor uptake (~12%, ID/g) after 2 h post injection. In vivo imaging using animal PET-CT is in progress and will be reported.

Conclusion
This result demonstrates that 64Cu-[APSC]2 radiotracer may be useful as theranostic radiopharmaceutical for hypoxic tumor. However, further evaluation is warranted.

IAEA-CN-285/45

Diagnostic Value of 99mTc-Ethambutol in the Management of Pulmonary Tuberculosis

Y. Kurniawati[1], A. Kartamihardja[2], A. Y. Soeroto[2], J. S. Masjhur[2]

[1] University Andalas/Dr.M.Djamil Hospital, Indonesia
[2] University Padjad- Jaran/Dr.Hasan Sadikin Hospital, Indonesia

Corresponding Author: yuliakurniawati79@gmail.com

Background
A survey of tuberculosis prevalence in some countries since 2000 showed that most of undiagnosed of pulmonary tuberculosis (pulmonary TB) was negative smear sputum microscopic that increased prevalence of pulmonary TB by about 15-20%. Ethambutol labelled 99mTc-pertechnetate (99mTc- Ethambutol) was specifically uptaked by Mycobacterium tuberculosis (M. tuberculosis) and can be used to detect tuberculosis lesion. The aim of this study was to determine the diagnostic ability of 99mTc-Ethambutol scintigraphy in identify M. tuberculosis infection of pulmonary TB.

Methodology
A case control study was conducted on 43 subjects with suspected pulmonary tuberculosis who came to the Pulmunology Clinic of Dr. Hasan Sadikin Hospital regularly. These subjects were diagnosed based on clinical symptoms, thorax x-ray and sputum microbiology, then divided into two groups consisting of 25 subjects of pulmonary TB as the case group and 18 subjects of non-pulmonary TB as the control group. 99mTc-Ethambutol scintigraphy was performed on all subjects at 1, 4, and 24 hours post injection of radiopharmaceutical. Qualitative analysis was done by observing the uptake of 99mTc-Ethambutol by the lungs at 1, 4 and 24 hours.

Results
The sensitivity, specificity, positive predictive value, negative predictive value and ac- curacy of 99mTc-Ethambutol scintigraphy were 92%, 72%, 82%, 87% and 84% respectively. False negative and false positive were observed due to variation of 99mTc-Ethambutol uptakes based on characteristic of tuberculosis lesions.

Conclusion
99mTc-Ethambutol is a promising diagnostic modality which showed good performance in detecting pulmonary tuberculous lesions.

IAEA-CN-285/48

99mTc Labeled HPG (Hyperbranched Polyglycerol) Probe as Multimodal Imaging with Fluorescence/Single Photon Emission Computed Tomography and in Vitro Affinies with K562 Myelogenous Leukemia Cells

P. Unak, S. Ay, V. Yasakci

Ege University, Turkey

Corresponding Author: perihan.unak@gmail.com

Background
In the pursuit of dendrimer alternatives, hyperbranched polymers have attracted increasing attention from academia and industry in a wide range of fields due to their topological and synthetic advantages. Hyper-branched polyglycerol (HPG), as its name implies, is a 50-65% hyper-branched polymer with dendrimeric structure. Because of its safety profile and multifunctionality, HPG has been extensively studied for different biomedical applications such as macromolecular therapeutics, multivalent inhibitors / scavengers, controlled drug delivery systems, organ preservation, dialysis and cell surface engineering, imaging agents and therapeutics.

Methodology
We developed a 99mTc labelled SPECT/ Fluorescent (99mTc-SPECT/FL) multifunctional diagnostic probe to display blood cells in this work. Hyperbranched polyglycerol (HPG) was synthesized by anionic ring opening polymerization due to its global nature, functionality in terms of versatility and excellent biocompatibility profiles. Succinic anhydride was used for the functionalization of the polymer. Deferoxamine was selected as the chelating agent and linked to succinate functionalized (SS-HPG). Indocyanine green (ICG) was bound to HPG for fluorescence imaging and then radiolabelled with 99mTc. K562 myelogenous leukemia cells were used as model for red blood cells. A conventional WST-8 setup was established to investigate the cell viability responses and IC50 (concentration range causing 50% mortality) values of the synthesized nanoparticles in a dose-dependent way.

Results
Indocyanine green (ICG) was bound to HPG with 73.59% yield. The structural properties were determined by Fourier Transform Infrared Spectroscopy (FT-IR), dynamic light scattering (DLS) and scanning probe microscopy (SPM). The molecular weight determination of HPG was determined by high pressure liquid chromatography (HPLC) and found to be 10,371 Da. The hydrodynamic diameter of HPG nanoparticles dispersed in water was recorded as 190.1 nm and the polydispersity index as 1,000. Radiolabeling yield was found to be 100% according to HPLRC and TLC analyses. The 99mTc radiolabeled HPG-ICG-DFO was stable for 6 hours in SF.
In vitro examination of the biological behaviour of HPG-ICG-DFO samples K562 chronic myeloid leukaemia cells were used. Cytotoxicity study showed that cytotoxicity increased with increasing substance concentration. The highest cell viability was observed at a concentration of 5 µg / mL. Time variation of the binding efficiency of 99mTc (HPG-ICG-DFO) samples to K562 cells was investigated. As a result, the

percentage of binding was increased over time and found 30% at 6 hours. IC50 values were found to be 55,78±1 for 24 hrs.

Conclusion

The results showed that fluorescent stained HPG samples showed a promising study of the visualization of blood cells and the presence of bleeding focus.

Acknowledgement

This work was supported by Ege University Research Fund with the project number of 18FBE-006.

IAEA-CN-285/49

Enhancement of Education and Communication in Nuclear Medicine Society by Telemedicine: Indonesian Experience

H. Budiawan[1], B. Suhardiman[2], B. Hidayat[1], A. H. S. Kartamihardja[1], B. Dar- Mawan[1], E. Af- Fandi[1], S. L. Dong[3]

[1] Hasan Sadikin Hospital, Indonesia
[2] Bandung Institute of Technology, Indonesia
[3] Seoul National University Hospital

Corresponding Author: dvn_b@yahoo.com

Background
With a population of more than 260 million spread over thousands of islands, the need for nuclear medicine facilities is increasing. Although the number of services has been increasing year on year, the main constraints are the nuclear medicine facilities. This includes the issue of human resources insufficiently allocated due to non-homogenous spread. One way to overcome this is by establishing well-equipped telemedicine projects between departments that allow us to share cases and knowledge and conduct virtual case discussions.

Methodology
Through the project of Enhancement of Nuclear Medicine Performance in Asian Countries by Asi@Connect (TEINCC/ Trans-Eurasian Information Network Cooperation Center), 10 cam-kits have been delivered to 10 nuclear medicine centres in 10 different cities on 3 main islands (Bandung, Jakarta, Jogjakarta, Solo, Semarang, Surabaya, Medan, Padang, Samarinda, and Makassar in Java, Sumatera, and Kalimantan islands) in 2019.

Results
Since starting Asi@Connect, some scientific meetings and dissemination of training results have been delivered more often in our nuclear medicine education center and broadcast online via the TEIN telemedicine network to other departments. Nuclear medicine physicians living in areas far from our education center were more exposed to the development of nuclear medicine. By using video conference equipment, two-way communication could be performed well.

Conclusion
Scientific meetings can be performed more often, attended by people from remote areas. This effort can promote nuclear medicine in a broader area, not only in big cities, and will enhance and accelerate the progress of nuclear medicine services.

IAEA-CN-285/50

Peptide Receptor Radionuclide Therapy in Radioiodine Refractory Differentiated Thyroid Cancer based on pre-Therapy Imaging using 177Lu-DOTATATE

H. Budiawan[1], N. R. Hidayati[2], E. R. Harahap[1], R. Shintawati[1], B. Darmawan[1], B. Hidayat[1], E. Afandi[1], A. R. Dewi[3], A. H. S. Kartamihardja[1]

[1] Sadikin Hospital, Indonesia
[2] BATAN
[3] Dharmais National Cancer Center, Indonesia

Corresponding Author: dvn_b@yahoo.com

Background
Most patients with differentiated thyroid carcinoma undergo near-total thyroidectomy followed by I-131 ablation of the thyroid remnant, which reduces the recurrence rate, improves survival, and facilitates follow-up. However, in the course of the disease, some of them become less differentiated and refractory to I-131 ablation. Less differentiated carcinomas tend to express a greater variety of SSTR subtypes in contrast to normal thyroid follicular epithel. Based on this fact, peptide receptor radionuclide therapy (PRRT) can be a promising modality for radioiodine refractory differentiated thyoid cancer (RrDTC). The pre-therapy diagnostic imaging is usually performed using 68Ga-DOTA-somatostatin analog PET scan, but it cannot be used as a dosimetry tool due to the short half-life. In this study, pre-therapy imaging was performed using 177Lu DOTATATE, as well as pre-therapy dosimetry.

Methodology
Subjects of this study were RrDTC patients. Diagnostic scan was performed with 5 mCi 177Lu DOTATATE. Two months after this imaging, patients with lesions showing significant uptake would undergo PRRT, except patients with kidney impairment, compromised bone marrow, and severe acute concomitant illness. One litre of modified amino acid solution was administered intravenously within 1 hour before and 5 hours after 177Lu DOTATATE injection both for imaging and therapeutic purposes.

Results
16 RrDTC subjects, 6 males and 10 females (mean age: 57.6 years old) underwent pre-therapy scan. Of the 16 patients, 5 patients (31.25%) showed significant uptake of 177Lu DOTATATE, 1 (6.25%) with faint uptake, and 10 (62.50%) without uptake. Based on this image, 3,700 Mbq 177LuDOTATATE was administered to 4 patients with significant uptake; 1 patient with significant uptake was excluded because of anemia and leukopenia. Biodistribution of post-therapeutic 177LuDOTATATE imaging was similar with the pre-therapeutic 177Lu DOTATATE imaging. No serious side effect was observed until 2 months of therapy.

Conclusion

Not all RrDTC patients showed significant uptake on 177Lu DOTATATE scan. Similar biodistribution was observed between pre-therapeutic 177Lu DOTATATE scan and post-therapy 177LuDOTATATE scan. The advantage of using 177Lu DOTATATE for pre-therapy scan is dosimetry can be performed before therapy which uses the same radiopharmaceutical and can be used when PET-CT scan is not available.

Acknowledgement: This work has been done as CRP E23005, entitled Dosimetry in Molecular Radiotherapy for Personalized Patient Treatments.

IAEA-CN-285/52

Synthesis, Characterization and Theranostic Evaluation of 99mTc Labelled Multifunctional Superparamagnetic Iron Oxide Nanoparticles: Dual Labelled DPAPA (3,5-Bis (Diphosphono Amino) Pentanoic Acid) Conjugated Iron Oxide Prop as a Prostate Cancer Theranostic Agent

V. Yasakci, B. Karatay, E. Tutun, P. Unak

Ege University

Corresponding Author: volkanyasakci@gmail.com

Background

We aimed to prepare fluorescence labelled ICG (Indocyanine green), conjugated DPAPA (3,5-bis (diphosphono amino) pentanoic acid), and 99mTc radiolabelled targeted Super Paramagnetic Iron Oxide (SPIO) nanoparticles for diagnosis and therapy of bone metastases of prostate cancer. DPAPA is a derivative of EDTMP (Quadramet, Cytogen) and is a radiopharmaceutical designed for deposition into bone metastases of prostate cancers. When stable magnetic DPAPA radio bioconjugate labelled with theranostic radionuclides, it can be used for aggressive prostate cancer. Additionally, it is seen that the second therapeutic method that the investigators plan to apply is the so-called magnetic hyperthermia and photodynamic therapy. It is expected that the obtained Results could be used for other multimodal magnetic radiopharmaceuticals applied in the simultaneous SPECT and NMR diagnosis, photodynamic therapy, radionuclide therapy, and localized magnetic hyperthermia.

Methodology

Iron oxide nano cubes were prepared by heating a solution of iron (III) acetylacetonate (Fe(acac)3), decanoic acid, and dibenzyl ether. 1 mmol of Fe(acac)3 was mixed with decanoic acid in dibenzyl ether. 75% of C-MNPs were used for silication. After adding TEOS (tetraethyl orthosilicate) to the synthesized C-MNPs, 10% of 2.5 mL NH3 was added. The reaction was carried out at 40°C for 12 hours. Hyper-branched polyglycerol (HPG) was synthesized with an anionic ring polymerization. Succinic anhydride was used for the functionalization of the polymer. Indocyanine green (ICG) was bound to HPG for fluorescence imaging. DPAPA was synthesized using a modified Mannich-type reaction using phosphoric acid, ethylenediamine and formaldehyde in the presence of HCl. Phosphoric acid and concentrated HCl was mixed in a container, then heated by adding L-ornithine on hydrochloric acid. An aqueous solution of formaldehyde (37%) was added dropwise. After heating for 4 hours at 100°C, the boiling suspension was filtered under vacuum. Then DPAPA was conjugated with magnetic iron oxide nanoparticles according to the EDC/NHS chemistry method and the nanoconjugates were optically labelled with ICG (Indocyanine Green) using CDI conjugation. In order to use the synthesized molecule for diagnostic purposes, 99mTc radiolabelling was made using the SnCl2 reduction method. PC3 prostate cancer cell affinities and cytotoxicity were determined using in vitro cell culture assays.

Results

FTIR (Fourier-transform infrared spectroscopy) analyses confirmed expected molecular structures. SEM and TEM images presented that nanoparticles are cubic formed nanostructures. Cytotoxicity studies were done with PC3 human prostate cancer cell line.

Conclusion

These nanoparticles might allow lesions to be identified with higher accuracy describe 99mTc-DPAPA linked nanoconjugates interactions, providing the detail of the complexes together with their stabilities, and might be useful when designing more effective theranostics.

IAEA-CN-285/53

Brain Perfusion SPECT Changes in Major Depressive Disorder Patients Treated with Statins in Addition to Standard SSRIs Therapy, Using Neurostat Software

B. Riedel De Juan[1], T. Massardo Vega[1], J. C. Quintana Fresno[2], J. Spuler Fernandez[1], G. Castro Muñoz[1], D. Muñoz Villanueva[1], D. Vicentini Harboe[2], R. Lastra Vallejos[1]

[1] University Hospital, Chile
[2] Pontificia Catholic University, Chile

Corresponding Author: riedel.md@gmail.com

Background
Patients with major depressive disorder (MDD) present abnormal brain perfusion in different regions, usually in prefrontal and temporal areas. The standard therapy includes specific serotonin inhibitor receptor (SSRIs); however, there is a significant proportion of refractoriness and relapse with a high social cost. As part of research which studied the inflammatory effect of statins in MDD as an addition to SSRIs, we evaluated the brain perfusion SPECT changes with a Neurostat program in patients submitted to placebo or rosuvastatin. Our goal was to recognize the major regional changes in different brain areas when using statins compared with placebo in MDD submitted to standard SRRIs therapy.

Methodology
We evaluated 20 MDD patients, 59% female with median age of 34 years old; all free of specific therapy with Hamilton Depression Rating Scale with 17 items (HAM-D17) score >15, self-applied Beck´s questionnaire ≥12 and brain perfusion SPECT with 99mTc-ethylcisteinate dimer. We used Neurostat 3D-SSP program iSSP3.5 version to analyze the data [normal values Z score -2 to +2]. All patients received SSRIs, half with rosuvastatin 10mg daily and half placebo, during 3 months, randomized. We compared with student t test the brain areas related with mood, neurocognition and emotions.

Results
In all patients there was a significant diminution in HAM-D17 ($p<0,0001$) and Beck ($p<0,0001$) scores at 3 months, with a major difference in the Beck score of the statin group.
We found significant differences ($p<0,05$) and some trends in the brain perfusion of the statin group, mainly in bilateral frontal regions (ventromedial and dorsolateral), left temporal middle and parietal inferior gyrus, all with basal decreased perfusion, and in both temporal entorhinal cortex with increased basal perfusion. In all of the regions mentioned above there was a trend to normalize the Z score after 3 months of SSIR and statin therapy (See table 1).
When we evaluated the brain perfusion changes in Brodmann areas (BA) related to mood, we found differences in the statins group in areas related to planification, like left BA47 ($p<0.0096$) and right BA46 ($p<0.0625$), and in one area related to emotions, left BA25 ($p<0.0189$), all with decreased basal perfusion that normalized after therapy.
There were no significant differences in all brain regions and BA evaluated in the placebo group comparing the basal perfusion versus 3 months therapy.

Table 1.
Significant brain perfusion regional differences after three months of therapy with placebo or statins in addition to standard therapy

Hemisphere	Region		Baseline – 3 months	
			Placebo	Rosuvastatin
Left	Frontal	Ventromedial	ns	0.0054*
		Dorsolateral	ns	0.0394*
	Temporal	Enthorrinal	ns	0.0625
		Middle gyrus	ns	0.0455*
	Parietal	Inferior	ns	0.0061*
Right	Frontal	Ventromedial	ns	0.0430*
		Dorsolateral	ns	0.0531
	Temporal	Enthorrinal	ns	0.0195*

Conclusion

The addition of statins to the standard SSRIs therapy in MDD seems to improve the clinical response and trend to normalize some of the brain perfusion abnormalities, related to neurocognitive functions like planification and emotions. Neurostat iSSP3.5 proved to be a very helpful tool to analyze the regional brain perfusion and to provide us with a quantitative parameter to control and compare the therapy response and with other patients

(We count with written authorization of Dr. Minoshima, owner of the tool, to publish this work funded by National Grant FONDECYT 1160885).

IAEA-CN-285/54

Usefulness of 18F-FDG PET-CT in aVery Rare Pulmonary Artery Leiomyosarcoma: A Case Report

T. Kaewchur, W. Pongwiwattanachai, S. Namwongprom, M. Ekmahachai,

Faculty of Medicine, Chiang Mai University, Thailand

Corresponding Author: tawika.k@cmu.ac.th

Background
Pulmonary artery leiomyosarcoma is a very rare malignancy characterized by malignant endothelial lining of pulmonary artery. This disease is often misdiagnosed as pulmonary thromboembolism. Symptoms at presentation are similar to pulmonary embolism as well as diagnostic CT features. Since leiomyosarcoma shows as metabolically active, 18F-FDG PET-CT plays an important role to make a diagnosis and evaluate distant metastasis.

Case Report
This is a report of a very rare case of pulmonary leiomyosarcoma in a 45-year-old woman. The patient was diagnosed with leiomyosarcoma of the pulmonary valve in 2005 and underwent open heart surgery to remove the tumor, excise the pulmonary valve, and had a Devega annuloplasty. Adjuvant chemotherapy was given. In 2019, she presented with acute dyspnea and clinical heart failure. The echocardiography showed right ventricular outflow tract obstruction. An urgent 18F-FDG PET-CT was performed under a prolonged fasting period of 15 hours and low carbohydrate diet for 48 hours. The 18F-FDG PET-CT showed a hypermetabolic intracardiac mass occupying the right ventricular apex, right ventricular outflow tract, and right pulmonic valve ring. Another focus of hypermetabolic tumor was also found occupying in pulmonary trunk and right main pulmonary artery without any extrathoracic distant metastasis.

Conclusion
18F-FDG PET-CT is of value to differentiate between malignant intraluminal mass and pulmonary thromboembolism and it is also a useful tool for accurate disease staging.

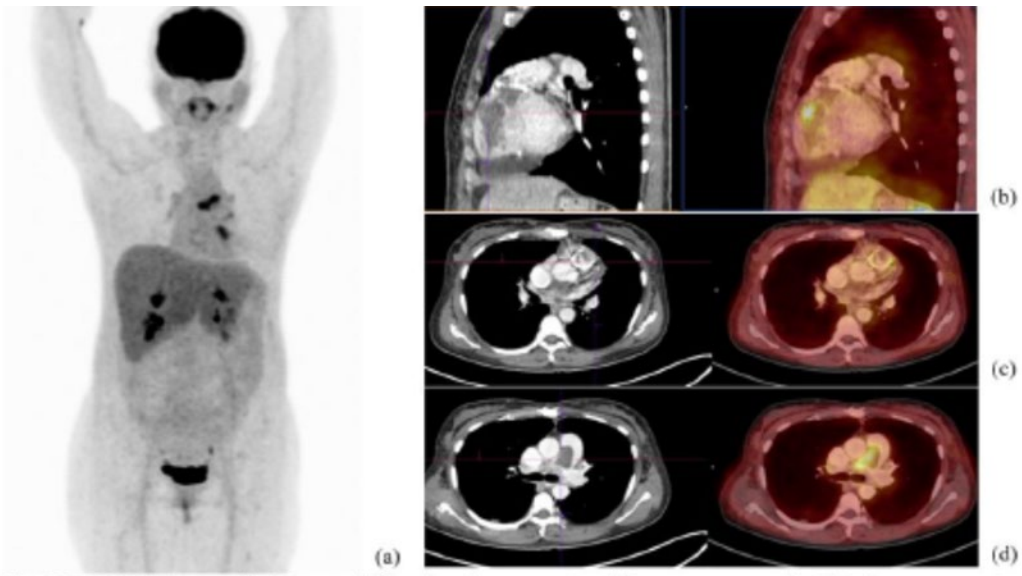

Fig.1 FDG PET/CT scan of a 45 year-old female pulmonary artery leiomyosarcoma patient (a) shows recurrent hypermetabolic tumor occupying in the right ventricle, right ventricular outflow tract (b) and pulmonary valve ring (c). Also seen another one skip malignancy at the pulmonary trunk and right main pulmonary artery (d).

IAEA-CN-285/55

Combined versus Subtraction-Only Technique in Parathyroid Scintigraphy

J. S. Mugisha[1], J. Warwick[2], A. Doruyter[2]

[1] University of Science and Technology, Uganda
[2] Stellenbosch University and Tygerberg Hospital, South Africa

Corresponding Author: jsmugisha2003@yahoo.com

Background
Parathyroidectomy is the main form of treatment for patients with primary and tertiary hyperparathyroidism. Scintigraphic, pre-operative localization of hyper-functioning parathyroid tissue depends on either a delayed washout technique, a subtraction technique, or a combination of the two. The rationale frequently given for adopting a combination approach is its presumed superior sensitivity, but there is limited evidence to support this strategy at the cost of patient inconvenience and impact on departmental workflows. The aim of this study was to determine whether a combined technique detects any additional hyper-functioning parathyroid tissue compared to using the subtraction technique alone in patients with hyperparathyroidism being considered for surgery.

Methodology
A retrospective analysis was performed of parathyroid scans at Tygerberg Hospital between January 2012 and April 2018. Scans were re-interpreted by consensus by three readers, blinded to the original interpretation. A McNemar discordant pairs analysis was then performed.

Results
A total of 97 participant scans were reviewed (female: 71; mean age: 50.8 years). The number of patients with primary, secondary, and tertiary hyperparathyroidism were 63, 21, and 13, respectively. A total of 192 lesions were identified in this study. While both the combined and subtraction-only approaches identified hyper-functioning parathyroid lesions, only four lesions were identified using the combined technique that were missed by the subtraction technique. This result was not statistically significant ($p=0.125$).

Conclusion
Based on our findings, the combined parathyroid scintigraphic technique does not improve lesion detection and may be dispensed with. Doing so will enhance patient convenience and comfort and improve departmental workflows without compromising lesion detection.

IAEA-CN-285/56

PSMA Theranostic in Castration Resistant Prostate Cancer (CRPC) Case with Benign Brain Tumor Mimicking Brain Metastasis: Case Report

B. Khiewvan, S. Chiewvit, P. Danchaivijitr

Siriraj Hospital, Bangkok, Thailand

Corresponding Author: bkhiewvan@yahoo.com

Case Report

An 81-year old man is presented here with history of metastatic castration resistant prostate cancer and multiple bony metastases post radical prostatectomy, radiation therapy, hormonal treatment and 6 cycles of Ra-223 dichloride. He firstly developed progressive bony metastases, progressive bone pain and rising prostate specific antigen (PSA) level. His PSA level was rising from 0.15 ng/ml to 58.3 ng/ml during one year. Patient was referred for Lutetium-177 prostate specific membrane antigen (PSMA). The Gallium-68(68Ga)-PSMA positron emission tomography/ computed tomography (PET-CT) was performed before therapy. 68Ga-PSMA PET-CT showed multiple PSMA avid bony metastases at T5-T6 vertebrae, bilateral proximal humeri, left iliac bone and left proximal femur. In addition, there is PSMA avid well-defined enhancing mass at right temporal lobe, sized about 3.2X2.1 cm which is suspicious of brain metastasis. MRI brain was performed to evaluate brain lesion before 177Lu PSMA treatment. MRI brain showed meningioma at right temporal lobe. The benign or malignant brain lesions can take up PSMA due to neovasculature of the tumor tissue. Meningioma is one of the most common benign brain tumors and has been reported to uptake PSMA. It is important to differentiate from brain metastasis in prostate cancer patient who underwent PSMA PET-CT. CT or magnetic resonance imaging (MRI) can help to confirm diagnosis. Then, patient received Lutetium-177-PSMA 200 mCi without brain symptoms. The PSA was decreasing to 1.44 ng/ml since the first dose of 177-Lu-PSMA treatment.

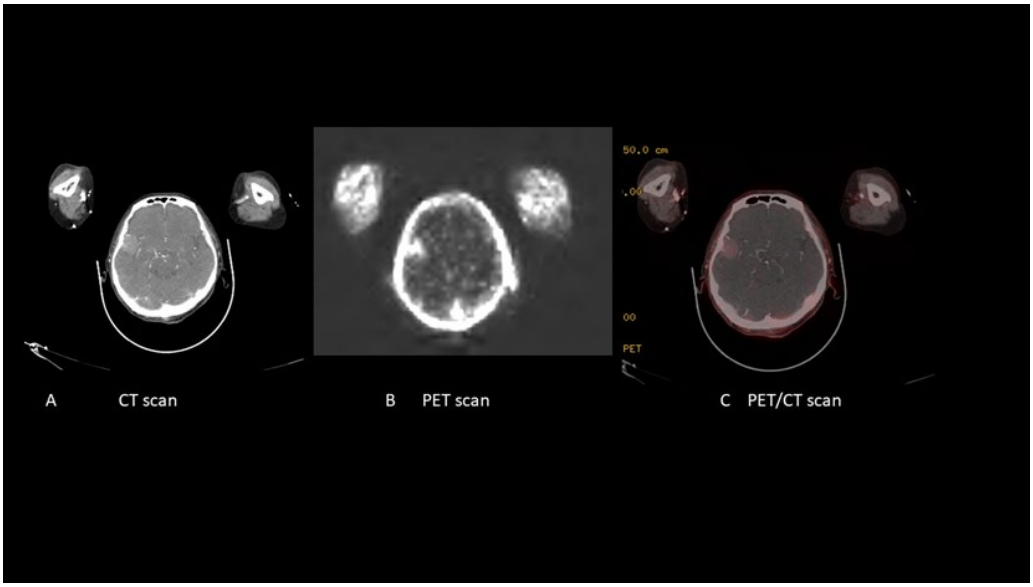

IAEA-CN-285/57

Health-Related Quality-of-Life Outcomes with 225Ac-PSMA-617 Therapy in Patients with Heavily Pre-Treated Metastatic Castration Resistant Prostate Cancer

A. Sood, S. Satapathy, B. Mittal

Postgraduate Institute of Medical Education and Research (PGIMER), India

Corresponding Author: sood99@yahoo.com

Background
Prostate cancer (PCa) is ranked currently as the second most frequent cancer and the fifth leading cause of cancer-related death in males. Localised PCa is reported to have better prognosis, however, metastatic castration resistant PCa (mCRPC) accounts for the substantial pro- portion of PCa related morbidity and mortality. Despite a number of approved therapies showing a survival benefit in mCRPC, quality of life remains an essential patient-centric issue. In recent times, 225Ac-PSMA-617 has emerged as a novel and promising treatment modality in the manage- ment of mCRPC with remarkable efficacy and safety profile. However, its impact on the quality of life of the patients' needs to be evaluated. The aim of this study was to assess the impact of 225Ac-PSMA-617 therapy on the quality of life of patients with heavily pre-treated mCRPC using the National Comprehensive Cancer Network-Functional As- sessment of Cancer Therapy-Prostate Symptom Index-17 (NCCN-FACT-FPSI-17) questionnaire.

Methodology
This was a retrospective single-centre study where data of consecutive heavily pre-treated mCRPC patients treated with 225Ac-PSMA-617, was collected and analysed for biochemical response, quality-of-life outcomes and treatment-related toxicity.

Results
Eleven heavily pre-treated mCRPC patients received a median cumulative dose of 8.3 MBq (IQR 5.6 – 20.4 MBq) 225Ac-PSMA-617 over 1-4 cycles. Five patients (46%) showed a $\geq$ 50% decline in PSA, while stable values and PSA progression were observed in three (27%) patients each. Pre- and post-therapy NCCN-FACT-FPSI-17 questionnaires revealed statistically significant improvement in the total FPSI score (median 29.8 versus 41.3, p=0.003) as well as the disease-related symptoms-physical (median 16 versus 22.5, p=0.004) and disease-related symptoms-emotional (median 1 versus 3, p=0.046) subscores. Among the physical symptoms, significant improvement was noted with respect to pain (p=0.003), difficulty in urination (p=0.020), bone pain (p=0.007), fatigue (p=0.016) and restriction in physical activity (p=0.016). No significant changes were noted in the treatment side-effects and function/well-being subscores. Of the treatment-related adverse effects, grade 3 dryness of mouth, anaemia & nephrotoxicity were observed in one patient (9%) each and grade 3 thrombocytopenia in two patients (18%).

Conclusion
Health-related quality-of-life of the mCRPC patients improved significantly with 225Ac-PSMA-617 therapy despite extensive pre-treatment and advanced nature of the disease.

IAEA-CN-285/67

Internal Dose Assessment of Lymphoma Patients Administered with 18F-FDG Radiopharmaceutical in PET-CT Examination

M. K. Abdul Karim

National Cancer Institute, Malaysia

Corresponding Author: khalis.karim@gmail.com

Background

Nuclear medicine is based on the use of radioactive tracers which provides specific images of the human body and its pathologies. However, the use of radioactive pharmaceuticals carries potential risk toward biological effects. This could be potentially the case with Positron Emission Tomography (PET) examination administered with 18F-FDG tracer. Te aim of this study was to evaluate the internal dose assessment involving absorbed dose and effective dose using the IDAC-Dose 2.1 program. IDAC-Dose 2.1 was developed by the International Commission of Radiological Protection (ICRP) to estimate the internal dose of patients' organ or tissue in diagnostic nuclear medicine based on the newest model of kinetics of radiopharmaceuticals in the human body proposed in ICRP Publication.

Methodology

Data of 30 lymphoma patients administered with 18F-FDG for PET-CT scan (Siemens Biograph 64-slice, Germany) examinations at our institution were collected retrospectively. The data collected including patients' age, weight, fasting blood glucose (FBG), height, BMI, race, gender, date of scanning, type of examination and scan duration. In addition, the administered activity of radiopharmaceutical used and its biokinetic data were also recorded. The biokinetic data of 18F-FDG was in the form of cumulated activity per administered activity Ã/Ao. Based on the current practice, the dosage of 18F-FDG administration depends on the patient's blood glucose level. If the level was <7.0 mmol/L, a dosage of 8 mCi 18F-FDG was injected to the patient with weight of 40 kg and above. For a patient with weight below 40 kg, a dosage of below 8 mCi of 18F-FDG was administered. If the level is >7.0 mmol/L, a further investigation by physician was required. The administered activity was determined by measuring the residual in the syringe. Subject's absorbed dose and effective dose were calculated using the IDAC-Dose 2.1 program. The program has listed 83 source regions and 47 target tissues or organs. In this work, adrenals, brain, breast, kidneys and liver were included for measurement. All data was further analysed using a statistical method such as Pearson correlation coefficient and Spearman rank correlation for correlation analysis. Analysis of variance (ANOVA) was used to evaluate the statistical significance between groups with p-value set at 0.05.

Results

The effective dose for all patients was found out to be 4.85±0.37 mSv while the ratio of effective dose to administered activity was 1.611×10-2 mSv/MBq. Thus, the radiation exposure in PET examination practiced by our institution was considered safe according to ICRP Publication 106 as the ratio of effective dose to administered activity did not exceed 1.9×10-2 mSv/MBq. As for the relationship between effective dose and weight of patients, there was a significant difference threshold for 40 kg of patient's weight.

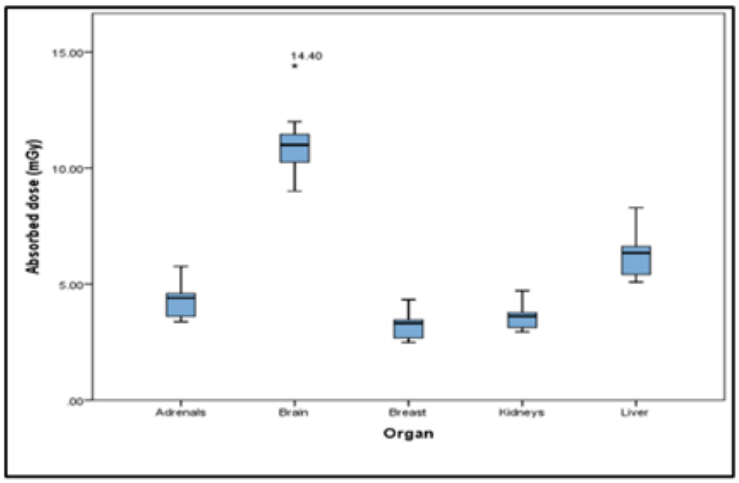

Figure 1 shows box-plot graph of selected organ absorbed dose received from PET/CT examinations.

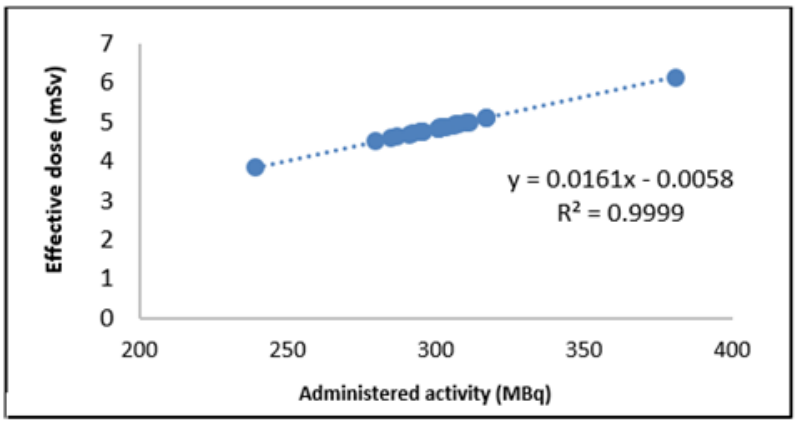

Figure 2: The scattered plot graph of effective dose against administered activity.

Conclusion

The radiation dose from the PET-CT examinations has been obtained and found to have high correlation activity with high "goodness of fit".

IAEA-CN-285/77

Correlational Study on Relationship Between Suv-Derived Parameters Assessed on 18F-FDG PET-CT and EGFR Mutation Subtypes in Patients with Lung Adenocarcinoma

R. F. Wang, X. H. Liao, M. Liu, X. Q. Chen, Y. G. Cui, L. J. Di, L. Yin, Z. H. Tong, H. Zheng, H. W. Sun, C. X. Wu.

Peking University First Hospital, China

Corresponding author: rongfu_wang@163.com

Background
It's well known that fluorine-18Fluorodeoxyglucose (18F-FDG) positron emission to- mography/computed tomography (PET-CT) plays a significant role in differential diagnosis, stag- ing and restaging, evaluation of efficacy and prognosis in lung cancer.The purpose of the study is to explore the relationship between 18F-FDG standardized uptake value (SUV)-derived parameters and mutation subtypes (deletions in exon 19 and a mutation in exon 21) in lung adenocarcinoma patients with mutant EGFR gene.

Methodology
Data of 64 patients who underwent 18F-FDG PET-CT scans and EGFR gene mutation test for diagnosed lung adenocarcinoma were collected. The relationships between subtype mutation of EGFR gene with four parameters of primary lesion based on 18F-FDG PET-CT (maximum standardized uptake value (SUVmax), average of standardized uptake value (SUVmean), metabolic tumor volume (MTV) and total lesion glycolysis (TLG) and clinical characteristics were evaluated respectively through univariate and multivariate logistic regression.

Results
The mutant ratio of exon 19 and exon 21 was 23:41. When the parameters were continuous variables, univariate logistic regression showed exon 21 mutations were found more frequently in the EGFR-positive patients with shorter maximum diameter of primary lesion (OR=0.942, 95%CI: 0.890-0.998) and low level of MTV of primary lesion (pMTV) (OR=0.957, 95%CI: 0.923-0.991). As dichotomous variables, in univariate regression shorter maximum diameter of primary lesion (diameter 26.5 mm: OR=3.759, 95%CI: 1.284-11.005), high level SUVmean (≥4.35: OR=4.267, 95%CI: 1.088-16.726), low level pMTV (diameter 11.2 cm3, OR=7.000, 95%CI: 1.798-27.253) would be significantly related to mutant exon 21. The multivariate logistic regression displayed that low level of pMTV were found more frequently in exon 21 mutations.

Conclusion
The primary-lesion SUV-derived parameters from 18F-FDG PET-CT of lung adenocarcinoma patients with EGFR-gene mutation could be associated with the mutant subtypes (exon 19 and 21 mutation) to some extent, but this correlation might be limited.

IAEA-CN-285/80

123/131I-Labeled Reduced Nano-Graphene Oxide Sheets as a Novel Tumor Theranostic Agent

T. M. Hafe, M. F. Elsabagh

Egyptian Atomic Energy Authority

Corresponding Author: moh_pharma2008@yahoo.com

Background
Functionalized nanographene with ultra-high surface area has been used as a nanocarrier for loading and delivery of various drugs and genes. In vivo applications of nano-graphene for cancer therapy have been further explored, with encouraging therapeutic Results in animal models. The potential toxicity of graphene has also been investigated, and it is generally agreed that the toxicity of graphene is closely associated with its surface chemistry. We explored the use of nano-graphene for in vivo tumor targeting and quantitatively evaluated the pharmacokinetics and tumor targeting efficacy through serial non-invasive positron emission tomography (PET) imaging.

Methodology
Synthesis of GO:
Natural graphite powder (particle diameter≤40 μm, Sigma-Aldrich) was utilized to synthesize graphite oxide suspension by a modified Hummers' method. In a typical procedure (as previously reported by our group [11]), at first, 1.0 g graphite and 1.0 g NaNO3 were added in 50 mL H2SO4. The mixture was then stirred in an ice bath for 10 min. Following this, 6 g KMnO4 was slowly added while it warmed up to room temperature. The suspension was stirred continuously in an oil bath at 35 °C for 2 h. The prepared suspension was then diluted by 100 mL deionized (DI) water. During the diluting, the temperature of the suspension was maintained at less than 60 °C. Finally, 6 mL H2O2 (30%) diluted by 200 mL DI water was added into the suspension in order to reduce residual permanganate to soluble manganese ions to stop the gas evolution of the suspension. The residual acids and salts of the graphite oxide suspension were removed by centrifuging the suspension at 6000 rpm for 10 min.
Labeling of reduced nano-graphene oxide sheets with 123/131I:
All radioactive materials were handled according to approved protocols at the laboratory for radioisotopes, Na131I was purchased from RPF, EAEA as a high concentration solution in 0.1 M NaOH. Reduced nano-graphene oxide sheets were radiolabeled with 123/131I by a modification of the chloramine T method.
In-vivo biodistribution:
The distribution of the radiolabeled complex among tissues of rats bearing fibrosarcoma tumor was determined immediately after imaging.

Results
Synthesis and characterization of GO conjugates:
Schematic structures of the four GO conjugates are shown in Fig. 1. Based on AFM measurements, GO-PEG, are small sheets within a size range of 10-50 nm, which was corroborated by DLS data that determined the average diameters of GO-PEG.

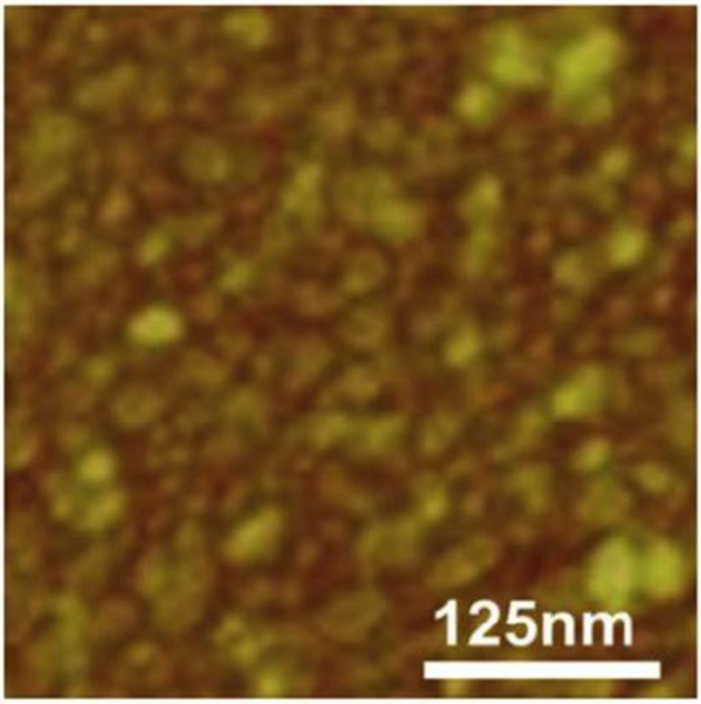

Fig. (1) Based on AFM measurements, GO-PEG Biodistribution study
Biodistribution studies were carried out the %ID/g values obtained from non-invasive PET imaging against radioactivity distribution measured ex vivo. At 24 h p.i.,

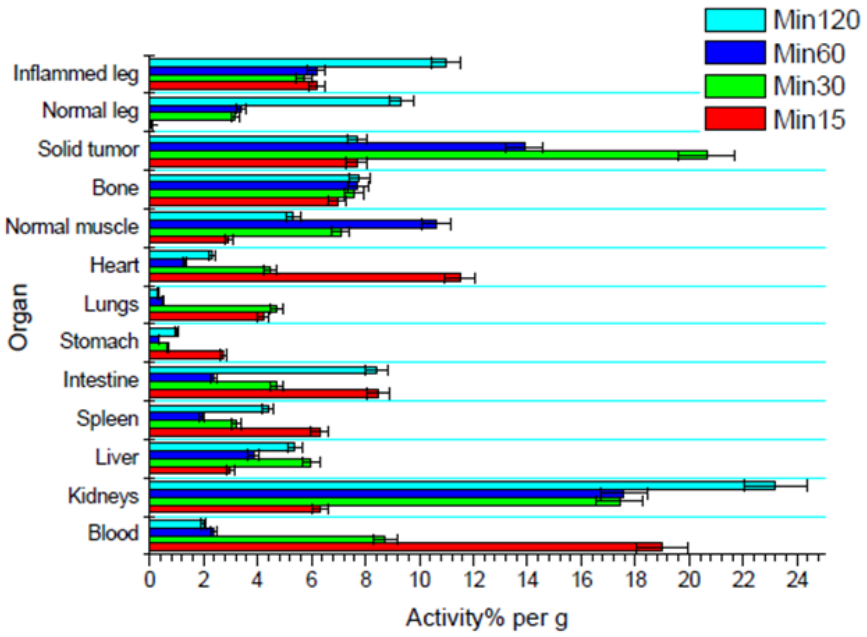

Fig. (2): Biodistribution of 123/131I - NGO-complex in Albino mice bearing EAC.

Conclusion

Herein we demonstrated that 123/131I labeled reduced nano-graphene oxide sheets with significant radioactivity retention in tumors, may provide a new approach of targeted imaging and therapy towards tumors.

IAEA-CN-285/82

Direct Radiolabeling of Iron Oxide Nanoparticles with 68-Gallium for Dual Modality PET/MR Imaging: Initial Studies on Blockade of RES Organs

M-A. Karageorgou[1], E-A. Salvanou[1], A. Apostolopoulou[1], D. Bouziotis[1]
X. Xanthopoulos[1], M. P. Petsotas[1], D. Stamopoulos[2], C. Tsoukalas[1], P. Bouziotis[1]

[1] National Center for Scientific Research "Demokritos", Greece
[2] National and Kapodistrian University of Athens, Greece

Corresponding Author: bouzioti@rrp.demokritos.gr

Background
The development of novel imaging tools with improved imaging characteristics would lead to an early identification of disease and consequently, to improved patient management. Nanoparticles possess unique characteristics that make them well-suited as probes for molecular imaging. Radiolabeled nanoparticles can circulate for longer periods of time than small molecule SPECT/PET tracers, thus carrying a larger radionuclide payload. Dual-modality contrast agents, such as radiolabeled nanoparticles, are promising candidates for a number of diagnostic applications, since they combine the advantages of two different imaging modalities, namely SPECT or PET with MR imaging. The benefit of such a combination is to more accurately interpret disease and abnormalities in vivo, by exploiting the advantages of each imaging technique, i.e. high sensitivity for SPECT/PET, high resolution anatomical information for MRI. This, in combination with hyperthermic capabilities of magnetic nanoparticles, can lead to highly effective cancer theranostic agents. In this study, we describe the direct labeling of iron oxide nanoparticles (NPs), with the positron emitting radionuclide 68Ga (T1/2=67.8 min) and their subsequent in vitro and in vivo evaluation. The aim of the study was to evaluate the efficacy of the developed magnetic nanoparticles in passive tumor targeting. Furthermore, the blockade of the reticuloendothelial system (RES) organs (liver, spleen, lungs) was evaluated by administration of commercially available radiopharmaceutical Phytate in healthy mice.

Methodology
For the preparation of 68Ga-labeled iron oxide NPs, the NPs were mixed with sodium acetate buffer pH 4 and 100 μL of 68Ga eluate (~80 MBq, 30 min at 90°C). In vitro stability of 68Ga-NPs was assessed in saline and serum. Radiolabeling and stability were assessed by TLC (ITLC-SG in citric acid solution 0.1M). The in vivo behavior of the radiolabeled compound was evaluated in SCID mice bearing 4T1 breast cancer xenografts, at 30, 60 and 120 min post-injection of the 68Ga-NPs. For the Phytate blocking study, healthy mice were injected with 10mg/kg body weight of Phytate (0.2 mg Phytate per mouse) 10 min prior to 68Ga-NP injection. The mice were then injected with 68Ga-NPs and biodistribution was assessed at 60 min p.i.

Results
Successful labeling of the NPs was achieved with 68-Gallium (RCP ~ 93%), which was stable at RT up to 180 min post-preparation. The radiolabeled NPs exhibited slow metabolic degradation in human serum (~82% at 120 min). Biodistribution studies in tumor-bearing SCID mice showed that the 68Ga-NPs were mainly concentrated in the reticuloendothelial system (liver, spleen and lung). Moderate passive NP

accumulation in tumor was observed with minimal uptake in other major organs. RES blockade with Phytate resulted in a significant decrease in liver, spleen and lung uptake.

Conclusions

In this study we have proven the feasibility of labeling bare iron oxide nanoparticles with 68Ga as a potential dual-modality imaging agent for diagnostic applications. This imaging radiotracer demonstrated high radiolabeling efficiency and satisfactory in vitro stability, as well as moderate passive NP accumulation in 4T1 breast cancer tumors. Phytate blocking of the RES organs will be further investigated in tumor-bearing animal models.

IAEA-CN-285/83

Radiolabeling of Gold Nanoparticles with 68-Gallium: In Vitro/In Vivo Evaluation

A. Apostolopoulou, D. Bouzioti, M-A. Karageorgou,
B. E-A. Salvanou, X. Xanthopoulos, C. Tsoukalas[1], P. Bouziotis

National Center for Scientific Research "Demokritos", Greece

Corresponding author: madoapostol@gmail.com

Background
Radiolabeled gold nanoparticles can be used as imaging agents in both Positron Emission Tomography (PET) and Single Photon Emission Computed Tomography (SPECT). In this study, gold nanoparticles (Au NPs) of different sizes (2 nm and 20 nm) were evaluated after their radiolabeling with the positron-emitter 68-Gallium (68Ga, t1/2 = 67.7 min).

Methodology
Initially, gold nanoparticles (Au NPs) were functionalized with the chelator mal-NOTA-MPAA after the NPs were coated with dimercaptosuccinic acid (DMSA). The resulting NOTA-DMSA-NPs were purified by centrifugation and further used for radiolabeling with 68Ga. Radiolabeling was performed by mixing 50 uL of each NP suspension, 350 uL of sodium acetate buffer (0.2M, pH 4), and 100 uL of 68Ga-Cl3 and incubating at 70°C for 30 min. The radiolabeling yield was determined by thin layer chromatography analysis (ITLC-SG). The radiolabeled sample was purified by centrifugation and the % radiochemical purity of 68Ga-NOTA-DMSA-NPs was determined by ITLC-SG. In vitro stability of 68Ga-NOTA-DMSA-NPs was assessed in presence of phosphate-buffered saline (PBS) for up to 2 h. For the stability experiment, 100 μL 68Ga-NOTA-DMSA-NPs were incubated with 900 μL PBS at RT for 30, 60 and 120 min and then analyzed by ITLC-SG. The radiolabeled AuNPs were then assessed in vivo, in tumor-bearing mice. For the development of experimental tumor models, female SCID mice of 8 weeks on the day of inoculation were subcutaneously inoculated with 4T1 cells (1 × 107 cells). Approximately 7 days after inoculation, ex vivo biodistribution studies were performed on the tumor-bearing mice. Each mouse received 100 μL (~0.5 MBq) of the radiolabeled NP. The animals were euthanized 90 min post-injection.

Results
68Ga-NOTA-DMSA-NPs were radiolabeled after 30 min incubation at 70 °C. The radiochemical yield was assessed by ITLC and was found to be ~85 %. The radiolabeled NPs were subjected to purification by centrifugation with ultracentrifugation filters. ITLC assessment demonstrated a radiochemical purity of > 92 % for the radiolabeled NPs. In order to assess the in vitro stability of 68Ga-NOTA-DMSA-NPs in various solutions, the radiolabeled sample was incubated with PBS for 120 min at RT, and was found to be practically stable (>90% retention of the radiolabel for all NP species), as evaluated by ITLC analysis. Further assessment was not possible, due to the short half-life of 68Ga.
Both radiolabeled Au NP species demonstrated fast blood clearance, with ~ 2% ID/g remaining in the bloodstream at 2h p.i., while the excretion route was primarily the hepatobiliary system. Nonetheless, there

is an estimable clearance via the urinary tract. Apart from the liver and kidneys, no major uptake in all analyzed tissues is noted (<1.5% ID/g from 30 min p.i.). Finally, both radiotracers demonstrated moderate passive accumulation in the tumor at 90 min p.i.

Conclusion

The preliminary Results of this study warrant the need for further development of these 68Ga- radiolabeled nanoparticles, as possible PET imaging agents.

IAEA-CN-285/84

Correlation Between 18F-FDG Brain Uptake Patterns and Immunotherapy Treatment Outcome in Advanced Melanoma Patients

M. Namías[1], H. Daniel[2], L. Zurbriggen[3], A. Weisman[2], T. Bradshaw[2], M. Albertini[3], R. Jeraj[2]

[1] Nuclear Diagnostic Center Foundation, Argentina
[2] University of Wisconsin, United States
[3] Carbone Cancer Center, United States

Corresponding Author: mnamias@fcdn.org.ar

Background
Immunotherapy with immune checkpoint inhibitors has been shown to improve outcomes for patients with advanced melanoma, but reliable biomarkers of response have yet to be determined. 18F-FDG-PET scans are used for initial staging and for quantitative treatment response assessment. The immune system may interfere with brain function, and the central nervous system may also influence the activity of the immune system. In this context, we analysed patterns of brain 18F-FDG uptake through group-based t-score images and their relationship with immune checkpoint inhibitors treatment outcome.

Methodology
134 18F-FDG PET-CT scans from 20 melanoma patients were included in the analysis. Patients were treated mainly with pembrolizumab and nivolumab. Scans were divided into two groups based on final treatment outcome: progressive disease (PD) and non-progressive disease (NPD) which includes stable disease, partial response and complete response. PET scans were quantitatively harmonized and then normalized to the MNI standard space using SPM12 software. A group-level t-score image was derived, after voxel-wise removal of the brain uptake linear correlation with age, gender, uptake time and age-gender interaction for each scan. Scores for the pattern expression of individual brain scans were estimated as the inner product (vector product) between the pattern and the individual scan. Leave-one-out cross-validation was performed, leaving out all the scans of a particular patient from the pattern derivation for each fold and using those scans for pattern validation. Brain scores were transformed to Z-Scores and a Wilcoxon rank-sum test was used to assess difference between groups. Conventional cluster-level analysis was also performed with SPM12, using an uncorrected p-value threshold of 0.001.

Results
64 and 70 scans were included in the PD and NPD groups respectively. Leave-one-out cross-validation of the brain pattern achieved an area under the curve (AUC) of 0.93 to classify treatment outcome, with 0.92 sensitivity and 0.80 specificity for detecting PD.
The differences in Z-scores between groups was statistically significant ($p<0.0001$). Two clusters were identified where PD patients had higher uptake than NPD patients. The regions involved were the right middle temporal lobe, right middle occipital lobe, the left inferior parietal lobe and the left angular gyrus ($p<0.001$).

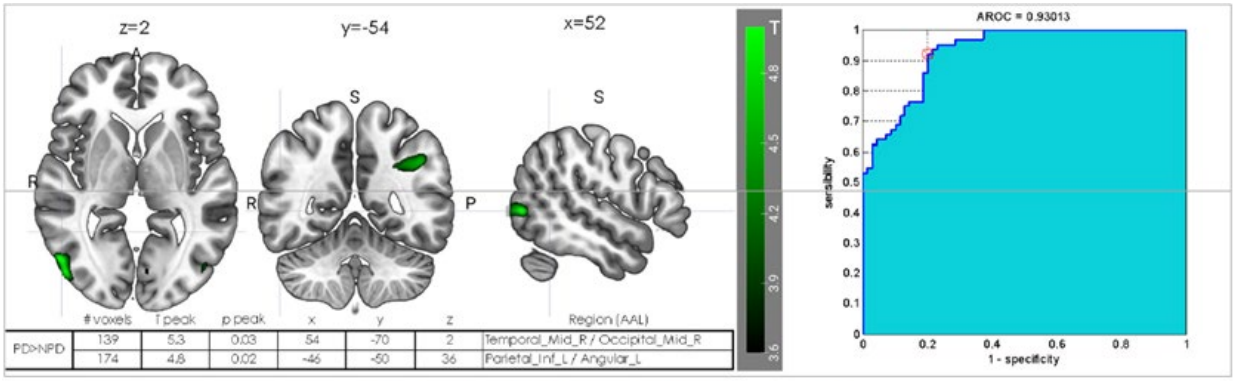

	# voxels	T peak	p peak	x	y	z	Region (AAL)
PD>NPD	139	5.3	0.03	54	-70	2	Temporal_Mid_R / Occipital_Mid_R
	174	4.8	0.02	-46	-50	36	Parietal_Inf_L / Angular_L

Figure 1. Cluster-level and ROC analysis results.

Conclusion

18F-FDG PET-CT brain uptake patterns were able to classify melanoma patients by immunotherapy treatment outcome with high sensitivity and specificity. Future work should test the causal relation of this pattern and assess if it is specific for immunotherapy patients or a more general pattern.

IAEA-CN-285/85

First Experience of Using 68Ga-PSMA-11 PET-CT in Detection of Prostate Cancer in Central Asia

M. Maksudov, U. Khaydarov, M. Khodjibekova

Fedorovich Clinical Sanatorium, Tashkent, Uzbekistan.

Corresponding Author: dr.mfmaksudov@gmail.com

Background
The aim of our work is to present the data on this novel, highly promising imaging technique in primary staging and detection of recurrence of prostate cancer.

Methodology
62 patients were examined, 45 with a primary tumor and 17 with biochemical recurrence of the disease after radical treatment. All patients underwent PET-CT with 68Ga-PSMA-11 according to the whole-body protocol. Interpretation of images was carried out visually and quantitatively with the calculation of SUVmax.

Results
High focal (24 patients) or diffuse (21 patients) 68Ga-PSMA-11 uptake was found in the parenchyma of the prostate gland in all patients with primary prostate cancer, which corresponded to the tumor focus. In 18 patients, metastases were additionally diagnosed. PET-positive results were obtained in 14 of 17 patients with biochemical relapse. PET-negative results were observed in 3 of 7 patients with low PSA values (less than 1.0 ng / ml). In patients with PSA level more than 1.0 ng/ml PET-positive results were obtained in all cases. Significant correlation was found between the frequency of obtaining PET-positive results and the stage of tumor according to T category.

Conclusion
68Ga-PSMA-11 PET-CT has a high potential in the workup of prostate cancer patients, including primary diagnosis, staging and localization of the tumor process in biochemical recurrence. The probability of obtaining PET-positive Results in cases of biochemical recurrence is affected by a PSA level above 1 ng/ml and a high stage of the disease according to the T category (T3-T4).

IAEA-CN-285/97

Inclusion of PET in Radiation Treatment Planning in Lung Cancer: Are There Clinical Impacts?

R. Buecker[1], E. Fricke[2], U. Schaefer[1]

[1]Radiation Oncology, Germany
[2]Nuclear Medicine, Germany

Corresponding Author: rebecca.buecker@klinikum-lippe.de

Background
The success of radiation therapy in the treatment of lung cancer depends on the accurate definition of the planning treatment volumes (PTV). For that reason, PET is included in the radiation treatment planning. The purpose of this study is to analyze whether the accuracy of PET-based planning correlates with the clinical outcome.

Methodology
The data of 287 patients with histological diagnosis of lung cancer were analyzed retrospectively in the period between 1 January 2010 and 1 January 2019. 68% of patients had NSCLC and 32% SCLC. Range of age of patients was between 41 and 89 years with a median of 66,9 years. 97 patients underwent surgery and 190 received definitive treatment. For radiation treatment planning, 116 patients received an additional PET examination. Follow-up with analysis of survival were analyzed using follow-up data from the hospital information system. Any local or regional relapse outside or close to the treatment fields were defined as error of planning target volume (PTV-error). The influence of additional PET for radiation treatment planning on recurrence free and overall survival was estimated with Kaplan-Meier-Analysis (Log rank test).

Results
The median follow-up period was 21 months (range 0 – 108 months). 169 of 287 (59%) patients with local or regional recurrences were detected, 55 (19%) of them were classified as PTV-error, 20 /55 (36%) with additional PET planning und 35/55 (64%) without. Mean progression-free survival and mean overall survival of patients with PET planning was 34.1 months and 60.3 months compared with 31.4 months and 56.2 months without PET planning. These differences did not reach the expected level of significance.

Conclusion
In our retrospective study, we failed to demonstrate a significant clinical benefit in terms of progression free survival or overall, all survival for the additional use of PET in the radiation treatment planning of patients with lung cancer, although PTV-error occurred less frequently with additional PET. A possible reason is that lung cancer is an aggressive disease with a high rate of regional and distant spreading.

IAEA-CN-285/98

18F-FDG PET-CT in Electrical Status Epilepticus in Sleep (ESES) – An Emerging Role

M. K. Srivastava, S. A, Jabeen, T. Katragadda, K. Nalla- Pareddy

Nizams Institute of Medical Sciences

Corresponding author: drmadhur77@yahoo.co.in

Background
Electrical status epilepticus in sleep (ESES) is described as a near continuous bilateral (occasionally lateralized) slow spike and wave discharge on electroencephalogram (EEG) occupying more than 85% of non-REM sleep with at least three or more records over one month of time. It is also known as continuous spikes and waves during sleep (CSWS) or epileptic encephalopathy with marked sleep potentiation of epileptiform activity in the transition from wakefulness to sleep. Seizures almost always disappear with age but the longer the duration, the more cognitive impairment there is. Little is known about the pathophysiology of ESES. However, thalamus may play a role in synchronizing of ESES. MRI imaging is helpful only in a small subset of cases with structural abnormalities. There are very few studies on the role of PET-CT in ESES. We formulated this study to examine the role of PET-CT in MRI negative ESES patients.

Methodology
This was a prospective observational study performed in a tertiary care institute over a one-year- period with children (Group A), aged 2-16 years, with EEG, fulfilling the criteria for ESES having normal MRI and normal milestones. All patients underwent PET-CT as per institute protocol and their history and demographic data were recorded. A control group (Group B) was formed of children undergoing PET-CT study for non-neurologic indication and no prior history of any developmental or psychiatric disorders. The region of interests (ROI) were drawn on frontal, parietal, temporal (lateral and medial), occipital, midbrain, thalamus, caudate, lentiform nuclei and cerebellum on PET-CT images, and their Maximum Standardized uptake values (SUVmax) was noted. Absolute asymmetry index (AAI) for thalami was calculated as (RT-LT) *100/[(RT+LT)/2].

Results
In all, PET-CT was performed on 14 patients in Group A and 13 patients in Group B. The mean age of group A was 8.2 ± 2.7 years and group B was 11.6 ± 3.2 years (p = 0.008). Focal seizure was the most common presentation (n=8; 57%) and the mean age of onset of seizures was 4.5 ± 1.7 years, while mean duration of seizures was 6 ± 2.8 years. There was moderate negative correlation between duration of seizures and IQ (Pearson correlation r2 -0.47) with a trend towards significance (P value 0.08). On PET-CT imaging, 12/14 patients (85.7%) showed visual thalamic abnormality, either unilateral or bilateral. However, the SUVmax values of various cortical and subcortical structures and AAI in both Group A & Group B did not show any statistical difference. As the duration of ESES prolongs multiple number of cortical and subcortical structures are involved in the form of decreased 18F-FDG uptake and which was statistically significant, reason might be because of ongoing insult due to prolonged ESES.

Conclusion

Our study confirms the role of thalamic abnormality in ESES and that as duration of ESES increases, there is more cortical involvement leading to neurocognitive regression. Hence, PET-CT may be useful in doubtful cases of ESES with normal MRI where early treatment is important to preserve neurocognitive development.

IAEA-CN-285/100

18F-FDG PETCT Imaging of Extra Pulmonary Tuberculosis Immune Reconstitution Inflammatory Syndrome

O. Evbuomwan[1], J. Momodu[2], K. Purbhoo[2], M. di. T. Vangu[2]

[1] University of Free State, South Africa
[2] University of The Witwatersrand, South Africa

Corresponding Author: moreli14@yahoo.com

Background
Immune reconstitution inflammatory syndrome (IRIS) results from rapid restoration of immune responses to opportunistic infections, causing either deterioration of a treated infection or presentation of a previously subclinical infection. It usually complicates antiretroviral therapy (ART) in patients who also have pulmonary tuberculosis (TB), with worsening of fever and pulmonary symptoms. Extra pulmonary TB is common in patients with pulmonary TB who are immunocompromised, thus we decided to study the metabolic pattern and frequency of extra pulmonary TB IRIS in immunocompromised patients.

Methodology
18F-FDG PET-CT image findings of 14 HIV positive patients with confirmed pulmonary tuberculosis and no other comorbidities were retrospectively collected for the study. Each patient had a baseline 18F-FDG PET-CT scan before initiation of ART and a follow up scan 2-3 months after initiation of ART. Only 2 patients had a third scan at the end of TB therapy. The criteria used for identification of IRIS was worsening of disease (increased metabolic activity using the SUV max) between the baseline scan and the follow up scan. Follow up scans were also compared with the end of TB therapy scan for those who had a third 18F-FDG PET-CT scan after therapy, to confirm complete resolution of disease.

Results
All fourteen patients had EPTB on 18F-FDG PET-CT imaging. These included lymph node (cervical, axillary, mediastinal, hilar and abdominal), membranous (peritoneal and pleural) and organ (spleen) involvement. All the patients showed increased metabolism (SUVmax) in the sites of EPTB on their follow up scan after initiation of ART, in keeping with IRIS. The only two patients with an end of anti TB therapy scan showed complete resolution of disease in both pulmonary and extra pulmonary sites of tuberculosis, further strengthening the fact that initial findings were in keeping with IRIS. The average increase in SUVmax following IRIS in the cervical, axillary, mediastinal, hilar and abdominal lymph nodes were 55%, 64% ,47%, 59% and 42% respectively. The average increase in SUVmax following IRIS in membranous tissue and spleen was 47% and 54% respectively. Of significant interest was splenic disease on an initial follow up scan that was not evident on the baseline scan but completely cleared after anti TB therapy (as shown in figure 1).

Conclusion
Metabolic imaging with 18F-FDG PET-CT was able to demonstrate extra pulmonary TB IRIS in all 14 patients. The most striking findings were visceral disease in the spleen that were not present or mild on the

baseline scan but worsened on the follow up scan with complete resolution at the end of anti TB therapy. These are findings which usually will go unnoticed during the treatment of immunocompromised patients with TB.

Pictorial illustration of metabolic imaging of TB IRIS with splenic involvement

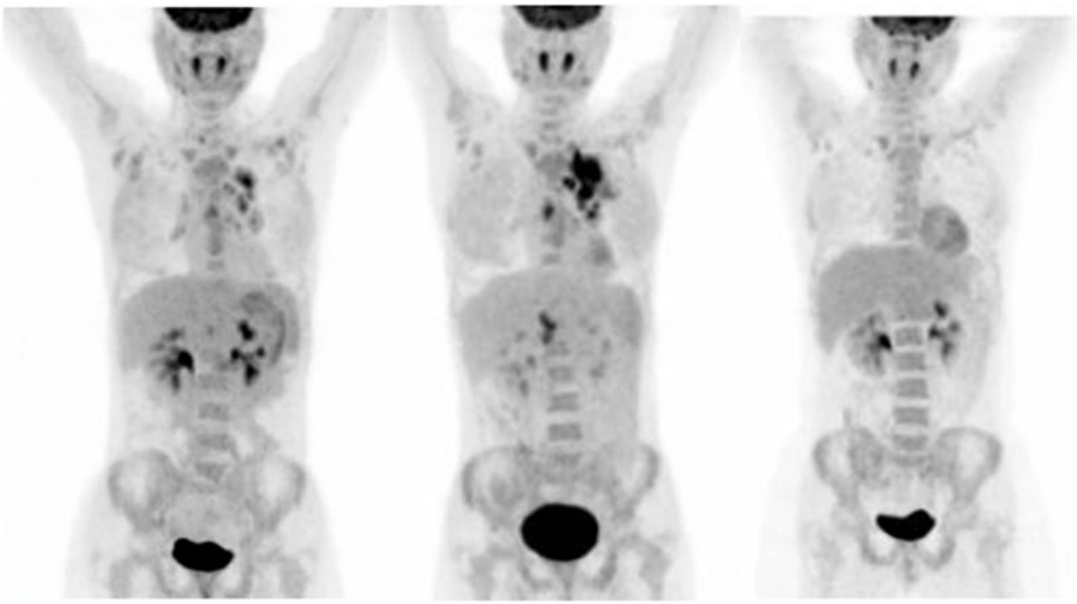

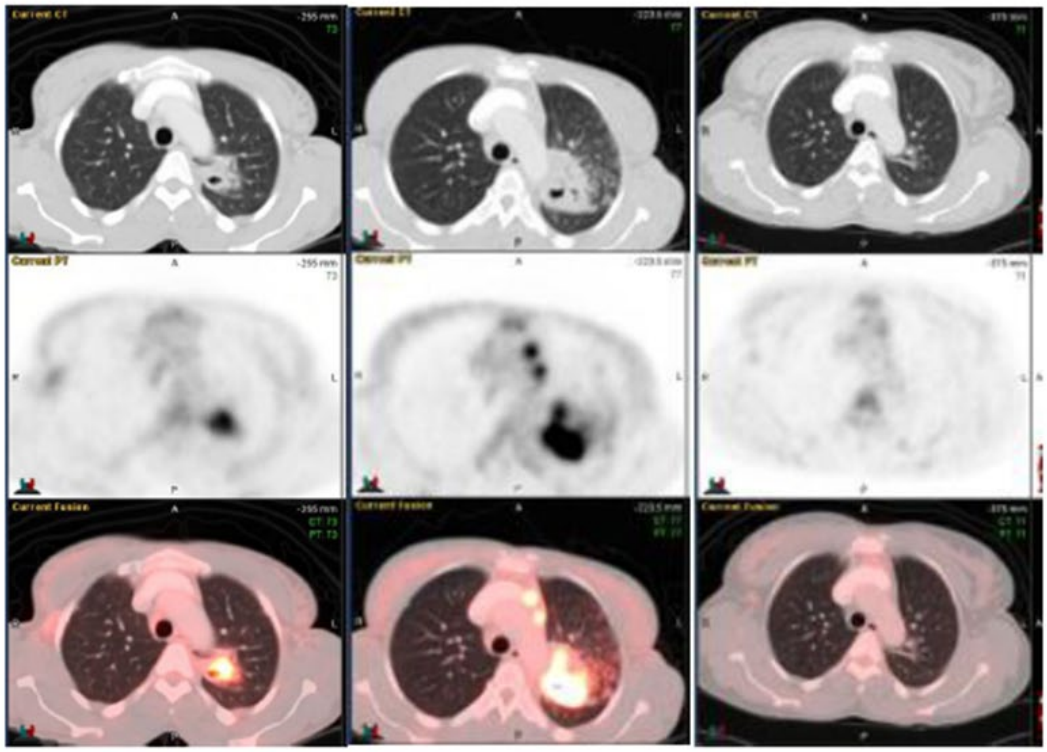

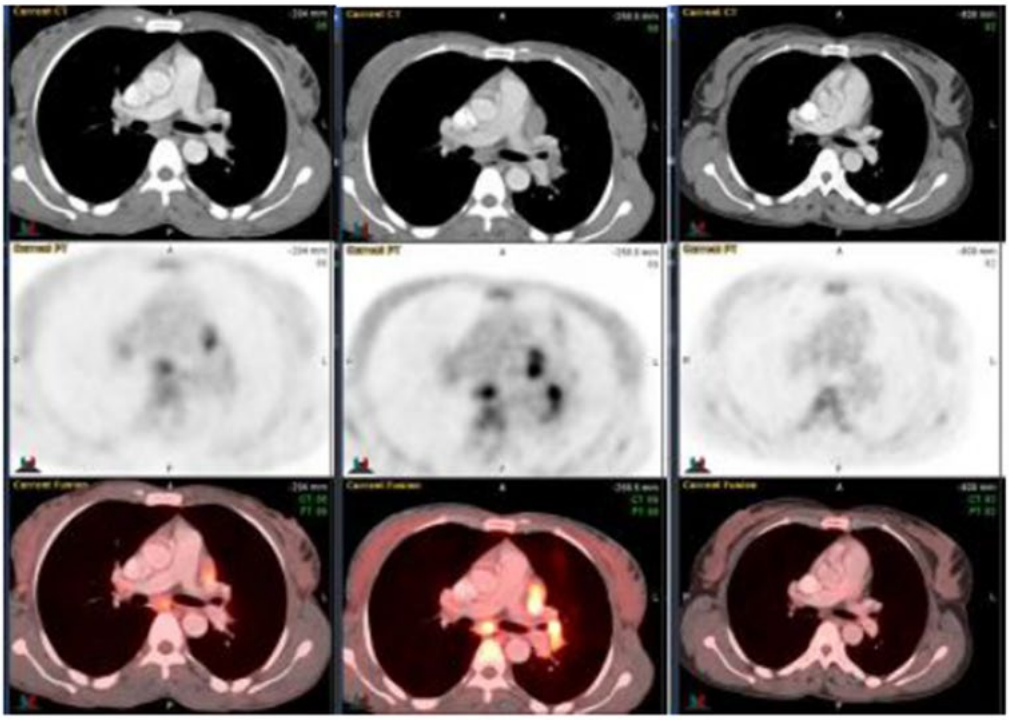

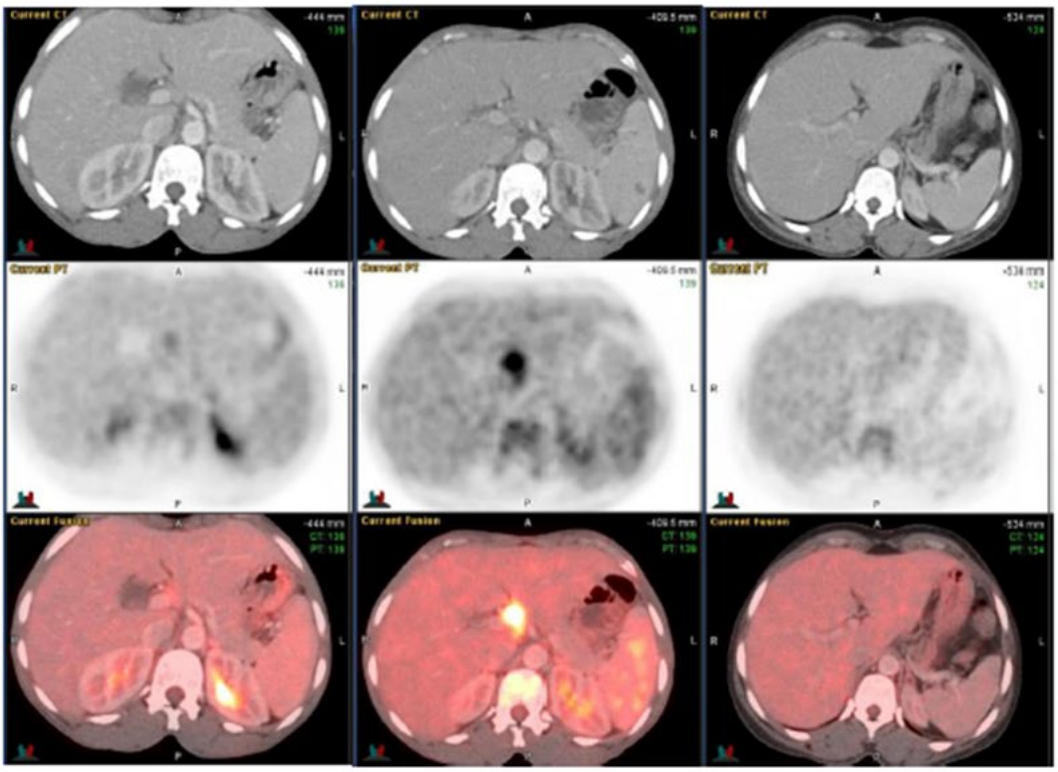

IAEA-CN-285/101

Progressive Accumulation of Radiolabelled White Cells in Scans Performed for Suspected Vascular Prosthetic Graft Infections

J. A. Jooma[1], J. M. Warwick[2], A. G. G. Doruyter[3]

[1] Ministry of Health and Population, Malawi
[2] Tygerberg Hospital, Stellenbosch University, South Africa
[3] Stellenbosch University, South Africa

Corresponding Author: jeffreyjooma@gmail.com

Background
Vascular prosthetic graft infection (VPGI) can be diagnosed using radiolabelled white cell scintigraphy (WCS). The EANM guideline on WCS recommends acquisition profiles and interpretation criteria for multiple indications. Regarding suspected VPGI (SVPGI), the guideline does not specify a role of 24-hr imaging. Erba et al demonstrated the benefit of 24-hr imaging in other infections. Therefore, this paper aimed to investigate the value of dual point acquisition and interpretation of WCS in cases of SVPGI.

Methodology
A retrospective analysis was performed of all WCS scans performed for SVPGI from January 2004 - June 2018. Studies were included if imaging was complete up to 24-hrs. 3-hr images were classified as positive or negative based on presence or absence of white cell activity at the site of the vascular graft. Next, by comparing 24-hr and 3-hr images, studies were scored as either positive or negative based on the presence or absence of progressive white cell accumula tion, both visually and using an accumulation index. A reference standard for the final diagnosis was based on a combination of microbiological, clinical and imaging follow up. Accuracy of interpretation methods was compared using pairwise comparisons of receiver operating characteristic curves.

Results
Twenty-three studies (n=23) of 24 SVPGIs were included. Infection was proven in 18 and excluded in 6. Visual interpretation of 3-hr images alone classified 23 cases correctly and resulted in 1 false positive. Visual interpretation of white cell accumulation over 24-hrs classified 18 cases correctly and resulted in 1 false positive and 5 false negatives. Finally, interpretation based on an accumulation index alone correctly classified 12 cases but resulted in 3 false positives and 9 false negatives. Visual interpretation at 3-hrs was statistically more accurate than visual assessment for accumulation over 24-hr ($P = 0.0106$).

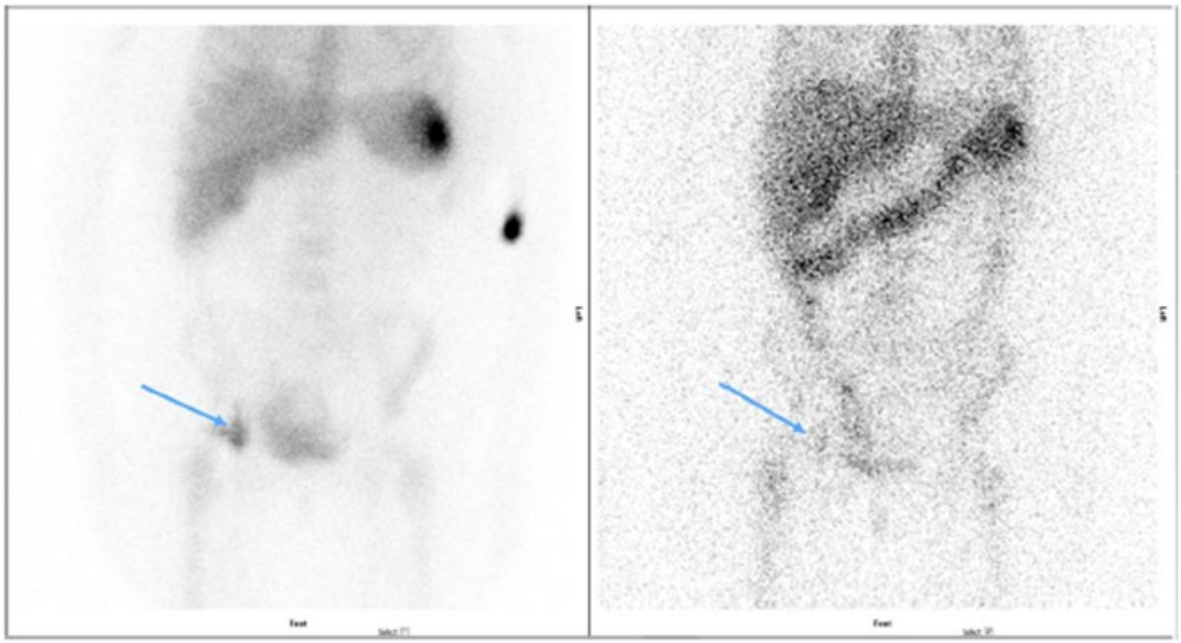

Fig. 1: White cell scintigraphy performed for suspected vascular prosthetic graft infection. The study is positive on visual analysis of the early images but negative on visual analysis of early and late images & semi-quantitative analysis. This patient had an aorto-bifemoral graft insertion 1 year prior to study and presented with a right inguinal draining sinus. ESR and CRP were raised – 21mm/hr. and 23 mg/L respectively. Visual analysis at 3 hours was positive. At 24 hours, visual analysis and the accumulation index were scored as negative. The patient underwent re-operation and a localised infection was present. Microbiology cultured *Pseudomonas aeruginosa*. Thus, visual analysis at 24 hours and use of the accumulation index resulted in a false negative.

Conclusion

Dual point interpretation of WCS does not improve diagnostic accuracy of WCS for SVPGI.

IAEA-CN-285/106

Role of 18F-FDG PET-CT in the Evaluation and Staging of Hepatocellular Carcinoma

S. Qasim[1], N. Younas[2], A. Qureshy[2], A. B. Shahid[2], S. Shah, I. Fatima[2] J. Alli[2]

[1]Swat Institute of Nuclear Medicine, Oncology and Radiotherapy (SINOR) Pakistan
[2]Institute of Nuclear Medicine and Oncology Lahore (INMOL). Pakistan

Corresponding Author: shahzad.qasim73@gmail.com

Background

18F-FDG PET-CT has proven to be a valuable tool in the initial diagnosis, staging, and re staging of a variety of cancers. The potential use of FDG-PET in the evaluation and management of hepatocellular carcinoma (HCC) continues to evolve. The purpose of this study was to investigate the effectiveness of 18F-FDG PET-CT for the detection and staging of HCC. In addition, we also assessed the correlation between 18F-FDG PET positivity and SUV based parameters, tumor size, Alpha fetoprotein levels (AFP) and grade of cirrhosis.

Methodology

All patients on the hepatobiliary and liver transplant service with radiologically proven HCC (LI-RADS 5) that underwent 18F-FDG PET-CT at INMOL between November 2017 and July 2018 were studied prospectively. Results of the FDG-PET-CT scan were compared with other imaging studies [computed tomography (CT), magnetic resonance imaging (MRI), ultrasonography (USG)], tumor size, AFP levels, cirrhosis grade, local and peripheral metastases.

Results

Of the 30 patients who underwent 18F-FDG PET-CT, increased FDG uptake (Grade III) was noted in primary HCC lesions in 23 scans (77%), FDG non-avid primary HCC lesions (Grade I) in 5 (17%) scans and FDG uptake equal to the surrounding normal liver parenchyma (Grade II) was observed in 2 scans (6 %). Similarly, 49 metastatic lesions were identified by PET-CT in 21 (70%) HCC patients against only 23 metastatic lesions identified by conventional imaging [CT, MRI, USG] in 12 patients. Total 43 (88%) out of 49 metastatic lesions were FDG avid and showed mild, moderate or intense FDG avidity. FDG-PET had 100% sensitivity for primary HCC lesion > 30 mm in size and all these lesions showed intense FDG avidity while the sensitivity for primary HCC lesion < 30 mm was 46%. The FDG-PET scans with AFP levels <100 ng/ml were positive in 6 of 11 patients (sensitivity 55.6%).

In patients with AFP levels >100 ng/ml, 17 of 19 patients (Sensitivity 89.4%) had positive scans. Only two of our patients underwent liver transplant during the course of study hence histopathological correlation with FDG avidity could not be made. There was a strong correlation of FDG uptake with tumor size and elevated AFP levels. However, no correlation was seen between FDG avidity, cirrhosis and portal vein thrombosis.

Conclusion

The 18F-FDG PET-CT is a valuable addition to conventional imaging in staging of HCC as it can alter patient management due to the detection of new extrahepatic metastatic lesions. It can also be helpful in evaluation of HCC with larger tumor size and elevated AFP levels when conventional imaging shows equivocal results.

IAEA-CN-285/107

Initial Experiences with Selective Internal Radiation Therapy (SIRT) in Hungary: The Value of Hybrid Imaging

S. Czibor, Z. Bánsághi, G. Taba, T. Györke

Semmelweis University, Hungary

Corresponding Author: czibors@gmail.com

Background
SIRT is a multidisciplinary treatment option performed in primary or metastatic liver tumours. It is based on the intraarterial injection of microspheres labelled with beta-emitting isotopes which results in prolonged local irradiation from the deposited spheres. We report our early experience with SIRT in Hungary.

Methodology
SIRT was performed in six patients, four with metastatic disease (colon adenocarcinoma, pharyngeal squamous cell carcinoma, oculary melanoma, and nonseminomatous testicular cancer as the primary tumour) and one each with primary hepatocellular carcinoma (HCC) and cholangiocellular carcinoma. In five cases, 18F-FDG PET-CT, and in the HCC case, 67Ga-SPECT-CT was performed as baseline imaging. At pretreatment diagnostic angiography, 99mTc- labelled macroaggregates of albumin (MAA) were injected in the appropriate hepatic artery to determine the lung shunt ratio (LSR) and SPECT-CT images were performed for evaluation of potential extrahepatic MAA deposition and for treatment dose planning. After injecting the ther- apeutic 90Y-microspheres PET-CT imaging was performed for treatment safety evaluation and dosimetry calculation. Patient follow-up was performed with 18FFDG PET-CT or, in case of non- FDG avidity, with contrast-enhanced CT or MRI.

Results
LSR remained under 10% in each patient. MAA-SPECT-CT showed extrahepatic (gallbladder wall) activity in one case, leading to the change of catheter position at treatment. It was also useful for therapy dose planning and helped confirm the biarterial (left and right hepatic branch) supply in two cases and in one patient where part of the left liver lobe tumour mass was fed by the left gastric artery. 90-Y PET dosimetric data yielded mean absorbed doses ranging 45-124 Gy. 18FFDG PET-CT proved useful in early (1-month post-treatment) follow-up, showing initial response (38-69% decrease in metabolic tumour volume at the treated area) in three patients and definitive progression in another patient (with decreased metabolic activity at the treatment site).

Conclusion
Hybrid imaging methods can facilitate the therapy planning, dosimetry, and follow-up of patients treated with SIRT.

IAEA-CN-285/108

Skeletal MTV Comparison of 68Ga-PSMA PET-CTwith 18F-FDG PET-CT for Multiple Myeloma Patients

M. E. S. Takahashi, S. De Souza, F. C. Frasson, F. Pericole, C. D. Ramos

University of Campinas, Brazil

Corresponding Author: mseren@unicamp.br

Background
18F-FDG PET-CT is used for assessing multiple myeloma (MM) including its bone involvement. Moreover, 68Ga-PSMA PET-CT has being proposed as potential alternative tracer for evaluating these patients. Total or partial skeletal segmentation of 18F-FDG PET-CT is used to access the metabolically active bone tissue in MM patients. The aim of this study was to compare the skeletal metabolic tumour volume (SMTV) measured using 68Ga-PSMA PET-CT (PSMA-SMTV) with SMTV measured using 18F-FDG PET-CT (FDG-SMTV) in MM patients.

Methodology
Nine MM patients were submitted to both whole-body 18F-FDG PET-CT (4.4 MBq/kg) and 68Ga-PSMA PET-CT (1.5 MBq/kg), with an interval of 1 to 8 days between exams using a Biography mCT40 PET-CT scanner (Siemens Medical Solutions Inc., Knoxville, Tennessee, USA). PET images were reconstructed using an iterative method (3D-OSEM+PSF+TOF) with 2 it- erations and 21 subsets with scatter and attenuation correction. CT images were acquired with 120-140kV, 120mA, transaxial FOV 700mm, rotation time 0.8s and slice thickness 2.1mm. Applying a CT-based segmentation, the bone tissue was segmented on 68Ga-PSMA PET and the tissue with uptake above the left atrium mean SUV was selected for the PSMA-SMTV. On 18F-FDG PET, SMTV was also calculated using the hepatic uptake as reference, but this time excluding the patient skull to avoid the high interference from 18F-FDG physiological brain uptake. In one of the patients, (Fig. 1) there were lesions in the skull, in which case, they were manually added to the FDG-SMTV. Correlation between PSMA-SMTV and FDG-SMTV were examined using the Spearman´s test.

Results
PSMA-SMTV was consistently higher than FDG-SMTV (mean values of 275.0±147.3ml and 44.0±63.3ml, respectively), with a very strong correlation between them ($r=0.897$, $p<0.001$).

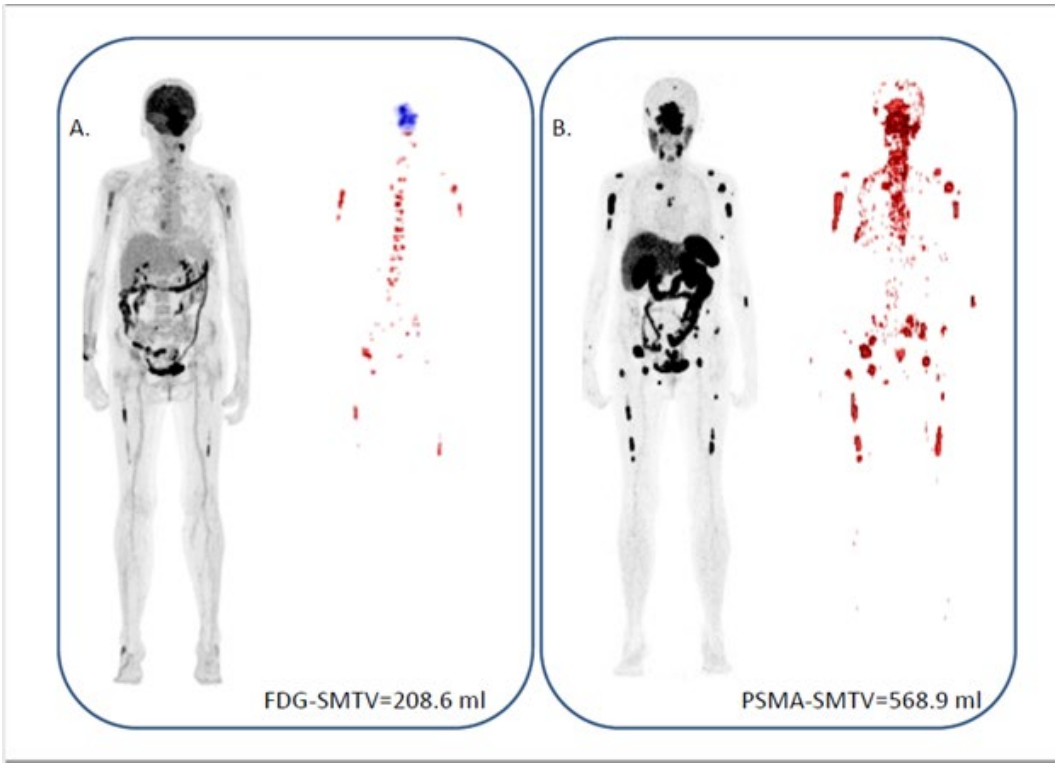

Conclusion

68Ga-PSMA images had higher volumes of metabolically active MM skeletal lesions than 18F-FDG images, with strongly correlated results. Large series of patients should be studied to evaluate PSMA-SMTV as possible alternative to FDG-SMTV to quantify active bone lesions of patients with MM.

IAEA-CN-285/110

Development of aNuclear Gamma Cascade Correlations Based Medical Imaging System - A Novel Modality with Potentials for Replacement of SPECT and PET

C. Rangacharyulu[1], L. T. K. Ly[2], K. Olshanoski[1], S. Santosh[3], L. Nkuba[4], T. Fukuchi[5], M. Fukuda[6], H. Kanda[6], P. Msaki[7], K. Sai[3], N. Takahashi[6]

[1] University of Saskatchewan, Canada
[2] Department of Nuclear Physics and Nuclear Engineering, HCMUS, Viet Nam
[3] Department of Physics, SSIHL, India
[4] Atomic Energy Commission, Tanzania
[5] RIKEN Center for Life Science Technologies, Japan
[6] Research Centre for Nuclear Physics, Osaka University, Japan
[7] Department of Physics, University of Dar es Salaam

Corresponding Author: leonid_nkuba@yahoo.co.uk

Background

Several limitations to PET and SPECT medical imaging are due to their inherent inability to identify the decay vertices of individual decay emissions of isotopes [1].

Methodology

It has been suggested that the non-collinear angular correlations of gamma-ray cascades emitted in individual decays of beta emitters are likely candidates to overcome this deficiency [2]. This novel modality can be implemented in the existing PET systems, with the additional retrofit of a collimator as in SPECT imaging assemblies and rewriting the PET imaging software to accommodate the non-collinear angular correlations. Though the introduction of physical colli- mator in PET Results in reduced geometrical acceptance, it may be more than offset by the unique advantage that each event is an image point with a well-defined decay vertex. In present-day PET/SPECT imaging, several hundred/thousands of decays must be recorded, and they resort to back-projection techniques.

Results

We identified the 617 keV and 372 keV gamma-ray cascade pair of 43K isotope β- decay (T1/2 = 22.3 hours) as a good test candidate [2,3,4]. The daughter nucleus being a stable 43Ca, which is easily absorbed by the neighboring cells. We produced the isotope by the 44Ca(p,2p) reaction at the AVF cyclotron of the RCNP, Osaka University, and confirmed that the gamma-ray cascade of our interest exhibits maximum non-collinearity [2,4]. We have implemented the collimator geometry in a MICROPET simulation program based on GATE of GEANT4.

Conclusion

Our current efforts are to optimize the collimator geometry with respect to the dimensions of collimator walls to minimize the scattered photons entering the detector area mimicking the full energy and maximize the detection efficiency. Future plans are to construct the collimator and attach it to the MicroPET of RIKEN facility in RIKEN/Kobe Japan and perform prototype imaging to this end.

IAEA-CN-285/111

Radiomics Based on 18F-FDG PET-CT in Breast Cancer Detection Using Deep Learning: A Preliminary Study

S. Tonpe, S. Tonpe

Cancer Hospital, India

Corresponding Author: sudhanshutonpe@gmail.com

Background
A convolutional neural network is an artificial intelligence technique based on physiological principles underlying the human visual cortex. Transfer learning is the practice of applying previously trained machine learning algorithms to new (but related) problems. 18F-FDG PET-CT findings of breast cancer are loco-regional and unsuspected distant metastatic hypermetabolism that affects management. This study aims to evaluate the potential of a deep learning algorithm to be used for the evaluation of these hypermetabolic areas for breast cancer detection.

Methodology
18F-FDG PET-CT conducted at a tertiary hospital between May 18 and April 20 were studies with equivocal findings excluded resulting in 190 studies. Test set of 45 images was randomly selected from initial sample (27 abnormal, 18 normal) and were not used in training process. A further 37 abnormal scans were randomly excluded resulting in a training set of 54 normal and 54 abnormal studies. Equal number of images were required in each group for optimal network training and converted to JPEG format image. The initial sample was amplified 26- fold using a combination of horizontal flip, size alteration, and rotation. The pre-trained Inception v3 network was then retrained using the amplified images. Training data was randomly split with 80% for training, 10% for validation, and 10% for final testing. The model was trained over 2000 iterations with a learning rate of 0.01. The area under the receiver operator curve was calculated using the web-based analysis tool.

Results
The proportion of abnormal PET-CT images was 62%. The area under the receiver operator curve for this CNN as a diagnostic test was 0.87 demonstrating a high level of diagnostic test accuracy. The output from CNN produces a continuous score of between 0 (abnormal) and 1 (normal). Setting the threshold to 0.395 as the output score resultsin a test sensitivity of 96.3%, specificity of 66.7%, and positive predictive value of 81.3% and a negative predictive value of 92.3%.

Conclusion
This proof of concept study demonstrates that high diagnostic test accuracy can be achieved in an automated analysis of 18F-FDG PET-CT in diagnosing locoregional and distant metastasis in patients suspected with breast cancer. In this study CNN could never outperform radiologists since radiologist's opinion was the ground truth. Future studies could attempt to use superior ground truth by using a consensus of many experts and histological data. This technique could be adopted across many different imaging investigations and may

be very useful in improving workflow efficiency and automatically flagging abnormal scans for urgent review reducing diagnostic delay.

IAEA-CN-285/113

Dynamic Evaluation of Volumetric Parameters with 68Ga-DOTA-NOC in Patients with Neuroendocrine Tumors who Received Therapy with 177Lu-DOTA-TOC

M. Acuña Hernandez[1], F. C. Goyzueta Aycho[2], F. O. García Pérez[2]

[1]Universidad Autónoma de Bucaramang, Colombia
[2] National Cancer Institute, Colombia

Corresponding Author: nandu152@hotmail.com

Background
Neuroendocrine tumours are a heterogeneous group of tumours showing overexpression of somatostatin receptors (SSTRs) on their cell membrane.
68Ga-tetraazacyclododecanetetraacetic acid (DOTA)–peptide (TATE, TOC or NOC) PET-CT is a imaging modality of SSTR, used for initial diagnosis, selection of patients for peptide receptor radionuclide therapy, and localization of unknown primaries.
In the last years, quantitative and semiquantitative parameters are used as prognostic factors for survival, considering the standardized uptake value (SUV), somatostatin receptor density (SRD) and total lesion somatostatin receptor expression (TLSRE). Currently, there are no studies evaluating the behaviour of quantitative and semiquantitative parameters with 68Ga-DOTA-NOC after peptide receptor radionuclide therapy with 177 Lu-DOTA-TOC.

Methodology
This is a retrospective cohort study, including patients of both genders, over 18 years of age who received therapy with177Lu-DOTA-TOC between January 1, 2016 to May 1, 2020. Response to therapy was assessed with 68Ga-DOTA- NOC. Analysis of variance (ANOVA) was employed to evaluate the tendency of the semi and quantitative parameters and Kaplan-Meier values to establish the survival.

Results
27 patients who met the inclusion and exclusion criteria were recruited. 74% of the participants were women and the average age was 58.6 ± 12 years. Regarding the most relevant primary tumour, 37% of cases came from the pancreas, 25.9% unknown site and 18.5% from the lung. 77.2% had WHO 1 histological grade and 70% a Ki67 between 1 and 2%. The means and standard deviations for the SUVmax, SRD and TLSRE were established, which are described in the following table. No statistically significant values were found; although the values in function of the SRD presented F = 3.19 and p 0.07. Finally, a statistically significant association was found using the Kaplan-Meier method between the greatest number of days of survival as a function of the decrease in SUVmax values (p 0.0003) and TLSRE (p 0.009), but not for SRD (p 0.08).

Parameter	Mean	Standard deviation
SUVmáx initial	37.3	± 30.2
SUVmáx follow up 1	27.6	± 20.9
SUVmáx follow up 2	34.0	± 29.3
SUVmáx follow up 3	38.5	± 30.4
SUVmáx follow up 4	40.0	± 28.3
SRD initial	104.1	± 193.9
SRD follow up 1	112.4	± 185.3
SRD follow up 2	112.6	± 184.3
SRD follow up 3	95.3	± 165.4
SRD follow up 4	27.3	± 36.4
TLSRE initial	2072.0	± 3682.6
TLSRE follow up 1	1432.5	± 2372.7
TLSRE follow up 2	2083.1	± 3265.2
TLSRE follow up 3	1790.9	± 2862.3
TLSRE follow up 4	817.1	± 1425.1

Conclusion

There are statistically significant differences in the decrease in SUVmax and TLSRE values and survival in patients undergoing therapy with 177 Lu-DOTA-TOC.

IAEA-CN-285/118

Preparation and Preclinical Studies of 64Cu-NOTA-antiCD20 for Clinical Use in PET Imaging of Non-Hodgkin's Lymphoma (NHL)

B. Alirezapour[1], H. Yousefnia[1], A. Bahrami Samani[1], N. Soltani[2], G. R. Aslani[1]

[1] Nuclear Science and Technology Research Institute, Iran
[2] Pars Isotope Company, Iran

Corresponding Author: behroz_a2000@yahoo.com

Background
Radiolabeled monoclonal antibodies have shown great promise for cancer diagnosis and therapy. Rituximab is a monoclonal chimeric antibody which has been approved by US FDA for immunotherapy of Non-Hodgkins' lymphoma (NHL). In the present study, we prepared Rituximab as an anti-CD20 antibody via identical chelator, NOTA (p-SCN-Bn-NOTA) labeled with 64Cu (T1/2 = 12.8 h, β+ = 17%, β− = 39%, EC = 43%) and performed preliminary biodistribution studies in mouse bearing Raji cell line.

Methodology
Rituximab (5 mg) was conjugated with NOTA (Macrocyclics B-605), the average number of the chelator conjugated per mAb was calculated and total concentration was determined by spectrophotometrically. NOTA–Rituximab was labeled with 64Cu (6 mCi, 0.22 GBq) then Radiochemical purity and immunoreactivity by Raji cell line and serum stability of 64Cu– NOTA–Rituximab were determined. The biodistribution studies and radioimmunoscintigraphy were performed in female BALB/c mouse bearing Raji cell (64Cu – NOTA– Rituximab i.v., 100 microl, 20±5 µg mAb, 6, 12, 24 and 48).

Results
64Cu–NOTA–Rituximab was prepared (RCP 99% ± 0.5, Specific activity 4.3 ± 0.7 µCi/µg). Conjugation reaction of chelator (50 molar excess ratio) to antibody resulted in a product with the average number of chelators attached to a mAb (c/a) of 4.4 ± 0.4. Labeling yield with 64Cu in 400µg concentration of bioconjugate was 93.2% ± 2.1. Immunoreaction of 64Cu– NOTA–Rituximab complex towards CD20 antigen was determined by RIA and the complex showed high immunoreactivity towards CD20. In vitro and in vivo stability of radioimmunoconjugate was investigated respectively in PBS and blood serum by RTLC method. In vitro stability showed more than 90% ± 2.6 in the PBS and 79% ± 1.2 in the serum over 24 h. The Immunoreactivity of the radiolabeled anti- CD20 towards Raji cell line was done by using Lindmo assay protocol. Under these conditions, the immunoreactivity of the radioimmunoconjugate was found to be 0.79. The biodistribution of 64Cu–NOTA–Rituximab complex in normal and tumor bearing mice at 6, 12, 24 and 48 after intravenous administration, expressed as percentage of injected dose per gram of tissue (%ID/g). Biodistribution and imaging studies at 24 and 48 h post-injection revealed the specific localization of complex at the site of tumors.

Conclusion

64Cu–NOTA–Rituximab is a potential compound for PET imaging of Non-Hodgkin's Lymphoma (NHL) in oncology.

IAEA-CN-285/123

An Overview of PET-CT and Cyclotron Facilities in Bangladesh - Present Status and Experiences

MD. N. Hossain, T. A. Biman, F. Begum

National Institute of Nuclear Medicine & Allied Sciences (NINMAS), Bangladesh

Corresponding Author: nahidhssn@yahoo.com

Background
PET-CT is a powerful and very sensitive diagnostic tool that integrates functional and anatomical imaging into one combined scanning system. Patients will benefit from PET-CT imaging with accurate diagnosis, staging and management of cancer. PET-CT technology in Bangladesh is a dynamic field where new procedures and techniques are continuously being introduced through manpower development obtained by training and workshops under technical cooperation with IAEA.

Methodology
The first PET-CT was installed in a private hospital named United Hospital, Dhaka at 2011. Establishment of a PET-CT facility in the government sector was somewhat delayed compared to the private sector. In the government sector, the first PET-CT was installed in the National institute of Nuclear Medicine & Allied Sciences (NINMAS) under the Bangladesh Atomic Energy Commission (BAEC) at 2015. Currently there are a total of eight PET-CT machines installed in different hospitals, five being in the government side and other three in private hospitals. The first medical cyclotron was installed in 2011 at the United Hospital, Dhaka. This one is still the only cyclotron (9.6 MeV energy from GE) which is supplied the PET tracers to all PET-CT establishments. United Hospital routinely operates the cyclotron only two days per week. This cyclotron can currently manage the demands of PET tracers in the country. But increasing the application of PET-CT imaging, more PET-CT facilities will be established within a short time. A cyclotron is urgently required in the government sector.

Results
Considering the necessity of a cyclotron, the government took the initiative to establish a cyclotron facility a few years ago under a government ADP project. Selection of the type of cyclotron to set up was crucial. Accumulating the information regarding expenditure and time required, expert opinions from IAEA were sought, then the decision was finalized to have a cyclotron of around 16-20 MeV within our budget. Following completion of the tender procedure, it was decided to install a 18/9 MeV cyclotron from IBA. Construction of the building was completed, and the cyclotron was installed in the facility. The radiochemistry and QC lab were also prepared. After final commissioning of the cyclotron and other auxiliary equipment, the final production is awaited. It is expected that production will be started within very short time. After starting production from this cyclotron, the needs of PET tracers can easily be fulfilled in our country.

Conclusion

All PET-CT and Cyclotron facilities so far were established in Dhaka, the capital city of Bangladesh. Considering the demand of PET-CT scan and the necessity to expand the facilities outside of Dhaka, the government has taken the initiative to establish another two PET-CT and three cyclotron facilities in the country. It is expected that within three years these facilities will be established. Several PET-CT facilities will also be established in the private sector. Due to the large population of the country (164 million), it will not be sufficient to cover the entire country, but we are trying to expand this facility as much as possible.

IAEA-CN-285/127

Current Status of Nuclear Medicine in Sri Lanka

V. Ramanathan

General Sir John Kotelawala Defence University

Corresponding Author: vijitha.r@kdu.ac.lk

Background
Nuclear medicine is widely used in oncology, cardiology and neuroscience. With the advent of hybrid imaging facilities, nuclear medicine has more popular worldwide. Implementing advanced imaging technology in middle- and lower-income countries is a challenging task. Sri Lanka recently graduated to an upper middle-income country with a GDP [Gross Domestic Product] per capita of USD 4,102 and a total population of 21.7 million. The purpose of this study is to analyze the current status of nuclear medicine in Sri Lanka.

Methodology
The data collected was pertinent to nuclear medicine facilities in government and private sectors in Sri Lanka by on-site visits, telephone conversations, and from the website of Ministry of Health and Atomic Energy Authority of Sri Lanka (AEA).

Results
In Sri Lanka, a nuclear medicine unit was established in 1972 at University of Peradeniya with the support of International Atomic Energy Agency (IAEA). The practice of nuclear imaging was initiated in 1978. Currently there are seven gamma cameras available, of which six are in government hospitals and one is in the private sector. With regard to hybrid imaging facilities, two PET-CT are functioning in two different private sectors organisations. Recently, the National Cancer Institute (called Apeksha Hospital) received a PET-CT from a public donation with help from Fight Cancer Team. It is a great support for Sri Lankans since the majority of patients who belong to the poor social economy are unable to bear the cost of a PET-CT scan. Moreover, radioisotopes are imported from India as there is no cyclotron facilities in Sri Lanka. It is a significant shortfall.

Conclusion
Currently, there are seven gamma cameras and three PET-CT machines available in Sri Lanka for approximately 22 million people. According to the Sri Lanka's population, 45 gamma camera machines are needed if following the international standard of a gamma camera per 400,000 inhabitants. Installing more gamma camera/PET CT machines and establishing a cyclotron facility for radioisotopes production are an essential and current need for our country to provide first-class health care in Sri Lanka.

IAEA-CN-285/129

Evaluating Accuracy in Hybrid and 3D Internal Absorbed Dose Estimation Protocols in 177Lu-DOTATATE Molecular Radiotherapy Using Monte Carlo Simulated Images with SIMIND Code

A.F. Calderón Marín[1], J. J. González González[1], C. Gonzalez Espinosa[1]
L. A. Torres Aroche[2], J. P. Oliva González[1], M. Pérez Benítez[1]

[1] Oncology and Radiobiology Institute, Cuba
[2] Direction of Clinical Research

Corresponding Author: cfcalder@infomed.sld.cu

Background
Individualized internal dose estimations (I-IDE) are mandatory for molecular radiotherapy planning, becoming essential to the the evaluation of I-IDE accuracy in clinical conditions. Frequently, hybrid I-IDE protocols combining whole-body (WB) and tomographic (SPECT or PET) imaging are used instead of 3D I-IDE, often due to time availability in the imaging systems. SIMIND is Monte Carlo code for simulation of SPECT systems. Our purpose was to evaluate the accuracy of I-IDE using hybrid and 3D protocols regarding the tools and methods for reconstruction, image processing, corrections and segmentation using MC simulated images and bootstrapping methods.

Methodology
The gammacamera MEDISO AnyScan SC was simulated with SIMIND (v6.2) for image acquisitions of 177Lu with energy windows of 20% centred at 113keV and 208keV plus two of 10% adjacent to each one and the MEGP collimator. Image quality in uniform projections and planar images was evaluated for 50-250 million photons histories. Measurements of parameters (sensitivity, spatial resolution and contrast recovery) were simulated. The 177Lu-DOTATATE biodistribution were simulated using the Zubal phantom considering kidneys, spleen, liver, urinary bladder and tumour (neck or liver) as sources and the rest as background. Images were generated at: 4-8h, 24-30h, 48-52h, 96-100h and 120-125h. Iterative reconstructions were done with TheratomoQ (Mediso) and CASToR (v3.0.1). The images were corrected for scattering, attenuation and count rates in ROIs also for background and overlapping. FIJI/ImageJ (v1.52p) and 3D-slicer (v4.11) were used for image processing. Data sets were generated for each protocol, with the SPECT for hybrid protocol at 24-30h and 48-50h. For I-IDE estimations: MIRD methodologyfor WB images and local energy deposition or voxel S value methods for SPECT. Bootstrapping algorithms were implemented for random sampling to obtain sets of biodistribution profiles and segmentation (manual or threshold) for evaluating the influence of random errors on accuracy.

Results
The lower noise in the uniform images was found for <150 million of photon histories. In general, the relative differences between the performance parameters were lower than 5%. This gammacamera can produce SPECT slices that cover wide anatomical regions by acquiring projections sets moving the table in overlapping length steps in each cycle. It was also simulated obtaining a similar image quality to real one.

These images where used to perform 3D I-IDE in normal organs in this work. A “free effect” simulated image (WB or SPECT) was used as reference during evaluation of activity quantification step. The differences for hybrid I-IDE protocols were dependent of corrections to WB images. The differences in mean absorbed dose in organs for both protocols ranged between 5-15%. The 3D I-IDE have better accuracy because some corrections are not needed in SPECT, however the implementation of hybrid I-IDE protocols with good accuracy in clinical routine is achievable.

Conclusion

The tool presented could be useful for evaluating the accuracy, and even uncertainties, of I-IDE for particular scenarios (instrumentation, image corrections, reconstruction, registration and segmentation). It could be easily extended to any therapeutic radiopharmaceutical, as well as educational resource and training.

Acknowledgements

Supported by IAEA CRP E2.30.05.

IAEA-CN-285/131

Role of PET-CT With 68Ga-Somatostatin Analogues in the Evaluation of Congenital Hyperinsulinism

L. Salazar Vargas, P. Orellana Briones

Pontificia Universidad Catolica de Chile

Corresponding Author: lsalazarv@gmail.com

Background
Congenital hyperinsulinism (CHI) is the most common cause of hyperinsulinemic hypoglycemia (HH) in neonates and infants. It is characterized by symptoms of severe hypoglycemia in the presence of inadequately elevated hyperinsulinemia. CHI compromises a group of different genetic disorders with the common finding of recurrent episodes of hypoglycaemia due to inappropriate insulin secretion. The estimated incidence of CHI is 1/50,000 live births and up to 1/2500 in areas with high rates of consanguinity It carries a high risk of significant neurological sequelae, such as cognitive impairment. Early treatment is madatory in order to prevent neurological damage and long-term complications. First-line therapy is pharmacological, but in cases of poor response, pancreatectomy is the only available alternative. Differentiating whether the alteration is focal or diffuse predict clinical evolution and define whether the neonate is a candidate for medical or surgical management and the type of surgery required (lumpectomy with minimally invasive surgery vs. subtotal pancreatectomy).
PET-CT with 18F-DOPA and genetic markers are currently the studies of choice in these patients since they allow distinguishing between the different subtypes (focal / diffuse / mixed) and eventually, determining the anatomic location of the lesion. However, these studies are not available in many medical centers in our region. Based on the known overexpression of somatostatin receptors in pancreatic islets, 68Ga bound peptides to somatostatin analogues had been proposed as an alternative for the differential study of these patients.

Methodology
We retrospectively evaluated the usefulness of PET-CT with 68Ga-DOTATATE in ten patients with hypoglycemia refractory to first-line treatment. 5 boys aged between 28 days and 1 year old. PET-CT with 68Ga-DOTATATE and low-dose CT was performed. The patients were referred for medical or surgical management.

Results
There were six positive studies. Two with diffuse abnormal overexpression of SST receptors and four with a single or multiple focal overexpression. Neonates with focal abnormalities underwent laparoscopic partial pancreatectomy with good overall response, without new episodes of hypoglycemia. Neonates with diffuse alteration were managed with 2nd and 3rd line pharmacological therapy, with a concordant genetic study, and none underwent pancreatectomy. Only one false negative was obtained in a patient reported without significative pancreatic alteration but with retroperitoneal abnormal uptake due to a severe thrombosis of

the renal vein. This case was subsequently confirmed with CHI as a result of a compatible genetic alteration. In the other three negative PET-CT CHI was discarded. No false positive cases were found in this series.

Conclusion

PET-CT with 68Ga-Somatostatin peptide analogues closely correlated with the clinical evolution and the histological and genetic results performed. In countries where 18F-DOPA is not available, 68Ga-DOTA PET-CT should be considered as a useful alternative to help define diffuse versus focal forms of CHI and start prompt therapy.

IAEA-CN-285/132

Incidence and Patterns of Pancreatic Metastasis on FDG PET-CT

V. Agarwal, S. Chandra

Vimhans Nayati Hospital, India

Corresponding Author: stanley2005vishal@yahoo.com

Background
Pancreatic involvement by metastases from other primaries is rare and accounts for approximately 2% to 4% of pancreatic tumors and is found in 12% of patients with advanced malignancy, at autopsy. Metabolic imaging can be a convenient noninvasive method of early detection of recurrence and in monitoring metastatic disease during follow-up.

Methodology
The most frequent primary sites include lung, breast, kidney and GIT. Metastases do not appear to show a predilection for a particular part of the pancreas. A retrospective study was done comprising of the last 2000 PET-CT WB cases to look for incidence and pattern of these metastases in our oncology patients.

Results
In total, 1.2% (24 cases) of cases showed pancreatic involvement, mostly (> 90%) in advanced stages (III/ IV) with mainly three patterns: first and most common (0.8% - 16 cases) that of an FDG avid single localized mass either isodense or hypodense on corresponding unenhanced CT images. Distortion, compression, or obstruction of the CBD/ MPD was seen in two cases, simulating primary pancreatic adenocarcinoma. Rarely, vascular involvement with splenic vein obstruction and varices can be observed as per literature, but none was observed in our study. A second pattern (0.3% - 6 cases) was of multiple FDG avid pancreatic nodules. In the third type (0.1% - 2 cases), FDG avid diffuse pancreatic enlargement, with smooth or lobulated contour, was seen. The morphologic and enhancement features of pancreatic metastases on corresponding CT images closely resembled those of the distant primary neoplastic source in 30% of total cases. More than 75% of metastases exhibit enhancement; larger lesions showing peripheral enhancement, whereas masses smaller than 1.5 cm diameter showing more homogeneous enhancement. Renal carcinoma (2 cases) metastatic to the pancreas exhibited rapid enhancement on the arterial phase beginning 25 sec from the start of injection with no relation to the size; and washout in the delayed phase images.
Other sites of metastases were also frequently noticed (> 95%) on PET-CT which in fact, reinforced the likelihood that the pancreatic mass seen represents metastasis.

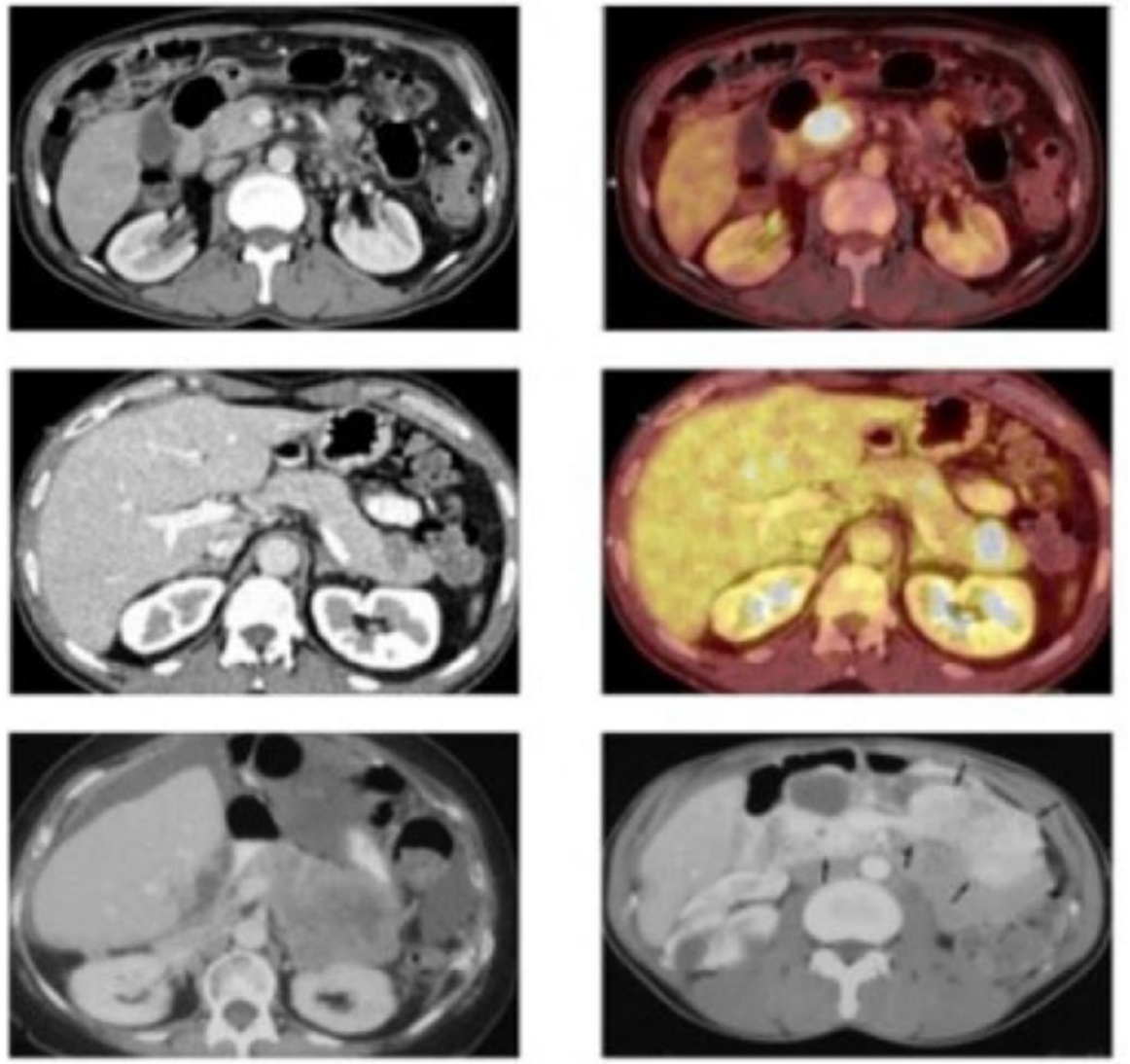

Conclusion

Symptomatically speaking, most patients (83%) are free of organ-specific complaints when the metastases is detected incidentally on conventional imaging and that's why, interval from diagnosis of an extra-pancreatic primary tumor to subsequent detection of a pancreatic metastases varies between 1 and 3 years, which can be significantly reduced with PET-CT incorporation in oncology surveillance. Pancreatic metastases usually develop late in the course of a generalized malignant process, leaving room only for palliative measures; but with 90% sensitivity of FDG PET in detecting recurrence/ metastases in patients, especially with asymptomatically elevated tumor markers and/or equivocal conventional imaging results, FDG PET-CT definitely has the role both in showing the presence of pancreatic metastases and in providing guidance to obtain a definitive tissue diagnosis.

IAEA-CN-285/138

First Experience with 177Lu-PSMA-617 in Patients with Metastatic Castration-Resistant Prostate Cancer in Uruguay

G. Dos Santos[1], E. Silvera[2], M. Rodriguez[1], C. Juan Carlos[2], M. Terán[3], W. Golomar[4] E. De Marco[2], F. Coppe[2], H. Balter[1], V. Trindade[1], S. Rodriguez[2], O. Alonso[1]

[1]CUDIM, Uruguay
[2] Hospital de Clinicas. Uruguay
[3] Facultad de Quimica.Uruguay
[4] INCA.Uruguay

Corresponding Author: gabyaguaa@gmail.com

Background
177Lu-PSMA-617 is an increasingly used new radioligand therapy (RLT) in metastatic castration- resistant prostate cancer patients (mCRPC). The aim of this study was to evaluate treatment response and safety in patients undergoing RLT with 177Lu-PSMA-617 for mCRPC.

Methodology
Between October 2017 and May 2020, 15 patients (mean age 66.8 years, range 50-79 years; median PSA level 100 ng/ml, range 6-1000 ng/ml) with mCRPC were prospectively enrolled to undergo 177Lu-PSMA therapy.
68Ga-PSMA-11 PET-CT was performed in all patients 1-week prior to therapy to confirm PSMA expression in metastatic lesions and after two cycles and at the end of treatment to assess response.
Hematologic parameters, clinical data and serum prostate specific antigen (PSA) levels were documented before and after therapy.
Therapy response was evaluated with serum total PSA and imaging findings using PSMA PET Progression (PPP) criteria. Clinical response was assessed in terms of the severity of pain and usage of analgesics after treatment cycles.
Biochemical and hematological toxicity was graded according to Common Toxicity Criteria for Adverse Events (CTCAE version 4.03).

Results
15 patients underwent a total of 42 intravenous doses of 177Lu-PSMA-617 (mean activity 7.16 GBq/cycle; range 6.6-7.6 GBq/cycle) at intervals of 8 weeks (n=7) or 6 weeks (n=8).
All patients received 1 to 5 cycles of therapy (1 cycle n=2, 2 cycles n=2, 3 cycles n=9, 4 cycles n=1 and 5 cycles n=1). Eleven patients (73.3%) completed three cycles of therapy.
Before therapy, all patients showed PSMA-avid metastatic lesions on 68Ga-PSMA-11 PET-CT.
All patients (100%) had bone involvement. Ten patients (67%) presented lymph node metastasis, 2 patients liver metastasis (13%), two patients lung metastasis (13%) and one patient adrenal metastases (7%).
Seven patients (46.7%) showed any PSA decline. Four patients (26.7%) showed a PSA decline of

≥ 50% (biochemical response), 2 patients (13.3%) showed changes in PSA level between -50% and +25% (stable disease) and 7 patients (46.7%) showed increase in PSA level of ≥25% (progressive disease). We documented xerostomia (n=2), nausea (n=3) and fatigue (n=5). Moderate thrombocytopenia occurred in two (13%) patients. There was no hepatotoxicity and nephrotoxicity documented. 7 patients (47%) reported symptomatic pain relief.

177Lu-PSMA-617 showed mean absorbed doses (Gy) below the recommended ones in critical organs namely red marrow (0.97), kidneys (4.6), liver (2.4) and whole body (0.4). These values confirm the safety of the radiopharmaceutical for non target tissues.

The analysis of PET-CT images with 68Ga-PSMA-11 in patients who completed three cycles or more showed disease progression (n=9) and partial remission (n=4).

Those patients who showed progressive disease received less dose activity (6.6 GBq) at 8-week intervals.

From October 2017 to May 2020, a total of 7patients (46.7%) died during this observation period.

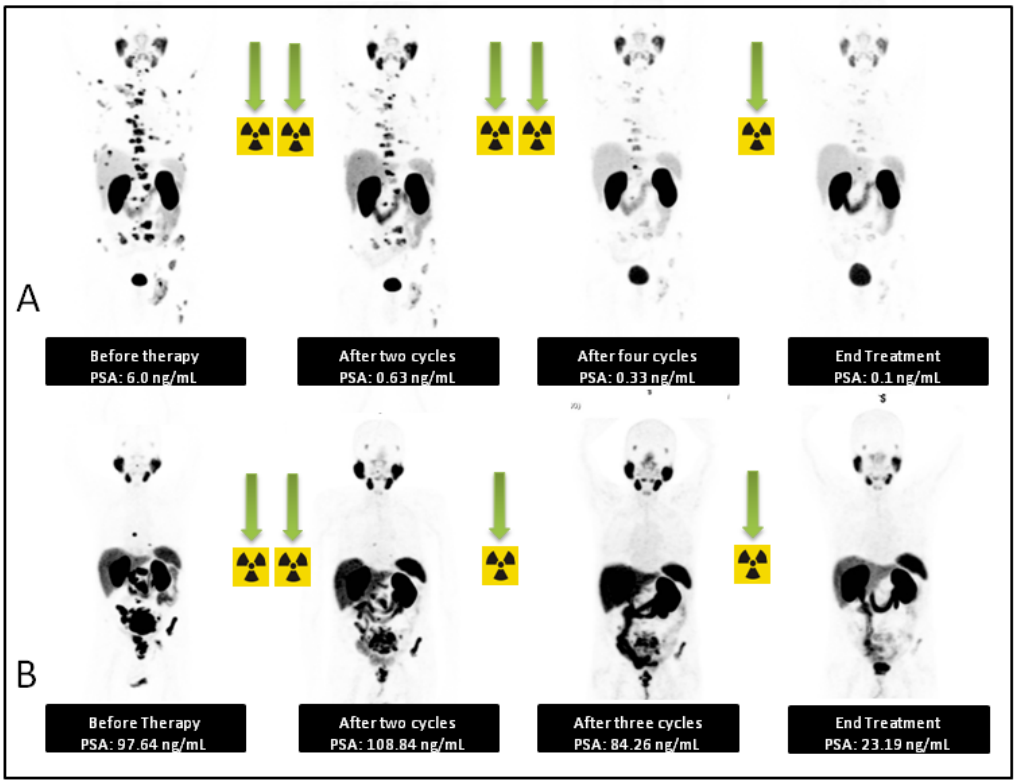

Figure 1. Sequential ^{68}Ga-PSMA-11 PET 1 h p.i. (MIPS) in patients 9 (A) and 11 (B). Note the *continuing PSA decline and partial response* in ^{68}Ga-PSMA PET images after five and four cycles of therapy, respectively

Conclusion

Our first clinical experience with 177Lu-PSMA-617 therapy shows that RLT is a safe and well tolerated therapeutic option for patients with mCRPC.

We highlight that the best therapeutic results were obtained at higher therapeutic doses and shorter time intervals between them.

IAEA-CN-285/141

Diagnostic Usefulness of 18F-PSMA PET-CT in Patients with Hepatocellular Carcinoma, Comparison versus 18F-FDG

U. Cancino Ramos[1], F. O. Garcia Perez[2], Q. G. Pitalúa Cortés[2]

[1]National Institute of Neurology and Neurosurgery, Mexico
[2]The National Cancer Institute, Mexico

Corresponding Author: uvicamo@hotmail.com

Background
Hepatocellular carcinoma is the most common primary liver cancer in Mexico. Cirrhosis is the most important risk factor. The diagnostic method is computed tomography and magnetic resonance with sensitivities greater than 90%. PET-CT with 18F-FDG has limited role for detection with a sensitivity of 40% -50, currently other radiotracers are being sought that offer better detec tion, especially in early stages. We evaluate the diagnostic efficacy of PET-CT with the radiotracer 18F-PSMA versus 18F-FDG in patients with hepatocellular carcinoma.

Metodology
Observational, analytical, cross-sectional, retrospective study in patients diagnosed with hepatocellular carcinoma determined by tomographic study and pathology report. Nine patients were evaluated with age range between 24 and 71 years and who had PET-CT with 18F-PSMA and 18F-FDG were included. Visual analysis of the studies was carried out to determine whether they were positive or negative, as well as SUVmax and tumor / background ratio (T / N), a chi-square test was performed on each radiotracer to determine the association between the level of differentiation and uptake.

Results
Nine patients were included; the average age was 53.5 (24-71) years. The six patients with the most differentiated histological grades (Grades I-II) were all positive with 18F-PSMA and negative in the three patients with the less differentiated histological grades (Grades III-IV). In the PET-CT with 18F-PSMA, a T / N ratio > 1.11 was recorded for positive studies and T / N values <0.68 for negative ones. The positives for 18F-FDG were Grades III-IV. Chi-square test was performed to determine association between level of differentiation and uptake, for PSMA a value of 9 was obtained with a P of 0.029.

PSMA	Grade I (n=2)	Grade II (n=4)	Grade III (n=2)	Grade IV (n=1)
SUVmax Tumor	24.97 ± 13.25	21.54 ± 9.38	2.50 ± 0.42	9.7
SUVmax Liver	7.65 ± 0.63	10.0 ± 5.23	13.85 ± 9.54	14.17
Tumor / background ratio (T / N)	3.34 ± 2.01	3.0 ± 2.20	0.25 ± 0.20	0.68
Diameter (mm)	36.5 ± 0.70	63.5 ± 15.84	114.5 ± 26.16	21

FDG	Grade I (n=2)	Grade II (n=4)	Grade III (n=2)	Grade IV (n=1)
SUVmax Tumor	3.81± 0.69	6.2 ± 3.34	17.9 ± 6.03	11.9
SUVmax Liver	2.67 ± 0.03	2.75 ± 0.95	3.15 ± 0.35	3.79
Tumor / background ratio (T / N)	1.42 ± 0.24	2.38 ± 1.13	5.83 ± 2.57	3.14
Diameter (mm)	36.5 ± 0.70	63.5 ± 15.84	114.5 ± 26.16	21

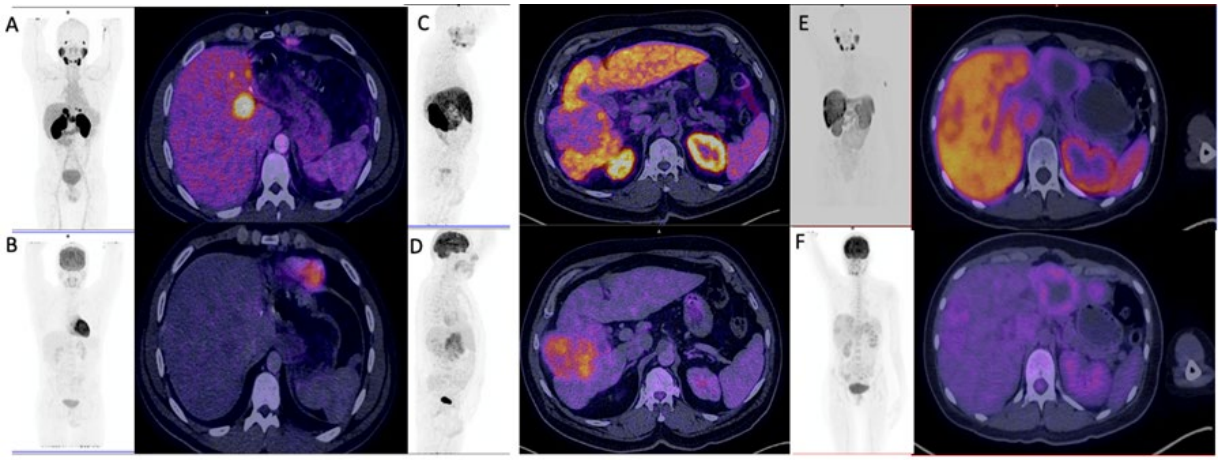

Fig 1. PET/CT ^{18}F A) PSMA (+) B) FDG (-) C) PSMA (-) D) FDG (+) E) PSMA (+) F) FDG (-)

Conclusion

PET-CT with 18F-PSMA can be considered as an effective non-invasive diagnostic tool providing information on the degree of differentiation of hepatocellular carcinoma.

IAEA-CN-285/143

Biological Evaluation of Radiolabeled Gemcitabine Loaded Polymeric Nanoparticles

S. Teksoz[1], C. İçhedef, I. Sarikavak[1], B. Aydin[1], O. Çetin[1], Y. Parlak[2], B. Sayit Bilgin[2]

[1] Ege University, Turkey
[2] Celal Bayar University

Corresponding Author: steksoz@hotmail.com

Background
The main objective of this study is to design a multi-functional drug carrier system as a prototype product. For this purpose, Gemcitabine that is used for multiple kinds of tumor therapy, and technetium(I)-tricarbonyl core [99mTc (CO)3]+, was incorporated to the PLA-PEG-COOH (polylactic acid-polyethylene glycol-carboxyl) polymeric structure. It is thought that cytotoxic side effects of drug in non-target tissues may be reduced and in specific tissues both imaging and therapy can be performed. A nucleoside analog gemcitabine is a chemotherapeutic agent which has increasing the use in pancreatic, bladder, ovarian and breast cancers. Nowadays, polymeric structures are preferred drug delivery systems. Technetium-99m has got ideal half-life and gamma energy, which is why it is widely used in nuclear medicine for diagnostic purposes.

Methodology
At first, PLA-PEG-COOH co-polymer was synthesized using esterification reaction and the product was characterized by Fourier transform infrared (FTIR) spectroscopy and Nuclear Magnetic Resonance (1H-NMR). Gemcitabine loaded PLA-PEG nanoparticles were prepared by double solvent diffusion method. The particle size, zeta potential and the nanoparticle morphology were characterized with Dynamic Light Scattering (DLS), Zeta Potential Analysis and Scanning Electron Microscopy (SEM) imaging, respectively. And then, radiolabelling efficiency of gemcitabine loaded radiolabeled PLA-PEG nanoparticles (99mTc (CO)3-PLA-PEG-Gem) were observed by Thin Layer Radiochromatography (TLRC) method. The biological activity of this radiolabeled system was determined in vivo by biodistribution and gamma camera imaging on Wistar Albino rats.

Results
The synthesis of PLA-PEG copolymer was performed successfully according to the 1H-NMR and FTIR Results. The particles size of the Gemcitabine loaded nanoparticles were found as 100-250 nm. The radiolabeling of drug loaded nanoparticles was efficiently carried out. The radiolabeling efficiency was found to be 94 ± 3.24 %. According to in vivo imaging Results radiolabeled polymeric nanoparticles showed higher uptake in the lung and liver at all selected time points.

Conclusion
Nuclear medicine and molecular imaging have provided a multidisciplinary collaboration, making it a stimulating and hugely varied area in which to make a career in chemistry. Systems formed by drug, polymer and radionuclide combination offer the most promising opportunities in the diagnosis and treatment of many diseases.

Acknowledgement
This study was carried out by funding support of Celal Bayar University Scientific Research project numbered 2017-001.

IAEA-CN-285/144

Radiolabeling of Drug Loaded Mesoporous Silica Nanoparticles and In Vitro Evaluation

S. Hamurişçi, B. Aydin, S. Teksoz, C. Çiğdem

Ege University, Turkey

Corresponding Author: cigdem_ch@yahoo.com

Background
In recent years, interest in the development of biodegradable nanoparticles has been increasing for drug targeting purposes. Imaging and therapy studies with radiolabeling of these nanoparticles also attract great attention. Mesoporous silica nanoparticles can provide precise control of surface chemistry to achieve drug or chemical loading and region-specific targeting. In addition, thanks to its features such as biocompatibility and low toxicity, silica nanoparticles make it a desired carrier system for biomedical imaging and therapeutic applications. In this study, cyclophosphamide, an anticancer agent, which is used in the treatment of breast cancer, bladder cancer, skin cancer and secondary acute leukemia, was encapsulated into the mesoporous silica nanoparticles and biological evaluation was performed by in vitro.

Methodology
In this study, cyclophosphamide (CPH), an anticancer drug used in breast cancer treatment, loaded mesoporous silica nanoparticles (MSN) was synthesized. Characterization of the drug loaded carrier system was performed with Fourier Transform Infrared Spectrophotometer (FTIR), Dynamic Light Scattering (DLS) and Scanning Electron Microscope (SEM). Then the synthesized CPH loaded mesoporous silica nanoparticles were radiolabeled with 99mTc in order to evaluate the breast cancer diagnosis potential of the drug delivery system. Cytotoxicity and cell uptake of the radiolabeled cyclophosphamide loaded mesoporous silica nanoparticles on cancerous cell lines were investigated in vitro.

Results
It was found that the particle size of the CPH loaded mesoporous silica nanoparticles were about 125 nm according to DLS measurements. SEM analyses also proved that they have homogenous spherical size. The radiolabeling yield of the silica nanoparticles were determined by thin layer chromatography with a high yield of above 95%.

Conclusion
It can be concluded that the optimized drug delivery system synthesized in this study will contribute to the development of new drug delivery systems for anticancer drugs.

Acknowlegement
This project was funded by Ege University Scientific Research Project numbered FYL-2019-20684.

IAEA-CN-285/145

Radiolabeled Zonisamide and its Incorporation on SH-SY5Y Cells

E. Derviş, B. Karatay, F. Z. B. Muftuler, A. Yurt Kilçar

Ege University, Turkey

Corresponding Author: ayfer.yurt.kilcar@ege.edu.tr

Background
Many patients (approximately one-third of the overall population with epilepsy) continue to have seizures in spite of receiving antiepileptic drug (AED) treatment. The prevalence of active epilepsy, 5-10/1000, is one of the highest among serious neurological disorders with more than 50 million people affected worldwide. Seizures are debilitating and burdensome for the health care system. Patients with seizures have higher medical expenses, lower employment rates, and barriers to social participation. Seizures lead to longer hospital stays and increased health care costs. The risk of new-onset seizure for a patient with a brain tumor is between 20%–90%. AEDs have been used to decrease the rate of postoperative seizures.
Zonisamide (ZNS) is an AED used to treat the symptoms of epilepsy and Parkinson's disease. It has been approved by the FDA since 2000 as an adjunctive treatment in refractory partial seizures. It acts by blocking T-type calcium channels and sodium channels. Additionally, it has serotonergic and dopaminergic activity. ZNS has specific efficacy for reducing tremors. ZNS is also a newer generation AED with demonstrated efficacy for the treatment of partial seizures, including simple and partial seizures even with secondary generalization. ZNS may also directly inhibit the indirect pathway through delta-opioid receptors.
In the current study, it is aimed to determine the radiolabeling potential of ZNS with Technetium-99m (99mTc) which is an optimum radioisotope for imaging. Furthermore, it is aimed to determine the in vitro incorporation potential of the radiolabeled AED (99mTc-ZNS).

Methodology
ZNS was radiolabeled via 99mTc by SnCl2 as reducing agent and quality control studies were performed by using radio chromatographic methods. Also, in vitro stability in PBS and lipophilicity of the 99mTc-ZNS were determined. In addition, the in vitro incorporation potential of the radiolabeled AED was investigated on SH-SY5Y neuroblastoma cell line, which is often used as in vitro models of neuronal function and differentiation.

Results
The radiolabeling yield of 99mTc-ZNS was over 95 %. It's seen that radiochemical purity in PBS was stable for four hours. LogP value of the 99mTc-ZNS was determined as -2.98 ±0.42 (n=6). The 99mTc-ZNS group was demonstrated 2.53- and 3.83-times higher incorporation values than the control group (99mTc) at 120 and 240 minutes, respectively.

Conclusion
Radiolabeling of ZNS as an AED may be initiative for the discovery of novel promising brain imaging agents. Further studies on animal models should be performed.

IAEA-CN-285/146

Development and Characterization of Copper-64 Radioresistant GBM Lines: Contributing to Theragnostic Radiopharmaceuticals

S. Valentini[1], G. Ravegnini[2], S. Angelini, P. Hrelia[2]

[1]Acom-Advanced Center Oncology Macer- Ata-Srl, Italy
[2]University of Bologna, Italy

Corresponding Author: s.valentini@acompet.it

Background
Copper-64 is a new promising theragnostic agent that has shown its diagnostic and therapeutic capabilities in different tumor types. Preliminary in-vivo evidences in multiforme glioblastoma (GBM) showed 64CuCl2 efficacy, although, the proper dose to reach the therapeutic effect is still under evaluation. For this reason, currently is important to pone attention and to consider the possibility of GBM cancer cells to develop radioresistance to this new radiopharmaceutical. The aim of the present study was to develop and characterize two GBM cell lines U87MG-RR and U373MG-RR radioresistant to 64CuCl2. Therefore, to understand the molecular network leading to radioresistance. In this context, microRNA alterations and their possible role were also evaluated.

Methodology
Radioresistant cell lines were generated by exposing U87MG, U373MG cell lines to increasing doses of radiation for 32 weeks. The development of radioresistance was evaluated through cell viability assay. IC50 has been evaluated in the parental cell lines to test their drug sensitivity and to find the best dose for cell treatment. To characterize radioresistant cell lines membrane permeability alterations and DNA damage, induced gamma-H2AX nuclear foci, have been assessed using a fluorescence microplate reader and a fluorescence microscope. We also investigated 64Cu cell incorporation and subcellular distribution at 1h, 3h, 24h, 48h, 72h post-treatment in all the cell lines measuring gamma-radiation emission. miRNA expression in parental and radioresistant cell lines were evaluated using TaqMan Array MicroRNA Cards Pool A and B, which allowed to analyze a total of 768 miRNAs.

Results
Cell viability assays confirmed radioresistance. Both the radioresistant cell lines exhibited reduction in membrane permeability and in DNA Double strand breaks indicating the capability to skip the drug killing effect. Cell uptake assays showed a 15% reduction in internalization of 64Cu at 24h and 48h post-treatment in the radioresistant cell lines comparing to the sensitive ones. Radioactivity measures in fractions showed a distribution mainly in the cytoplasm comparing to the nuclei in all the cell lines. The radioactivity slowly migrates into the nucleus in all the cell lines from a 5% at 24h to a 20% of internalization at 72h, indicating a 64Cu flux into the nucleus in both the sensitive cell lines and the resistant ones. In both the radioresistant cell lines, we observed a group of deregulated miRNAs compared to the parental ones.

Conclusion

This is the first study describing the development and characterization of two novel 64CuCl2 radioresistant cell lines and contributing to understand the potential role of 64CuCl2 as theragnostic agent. This in-vitro evaluation will be useful to implement the approach for dosimetric analysis considering that the proper dose reaching the nucleus is essential to have a therapeutic effect but is also important to identify the best dose scheme to avoid radioresistance. The actors responsible for modulating radioresistance could be miRNAs, therefore further studies are necessary to evaluate their role and identify potential treatment to restore 64CuCl2 responsiveness.

IAEA-CN-285/147

Role of PET-CT in Primary Staging of Colorectal Cancer - Institutional Experience

R. Milardovic

Clinical Center of Sarajevo University, Bosnia and Herzegovina

Corresponding Author: milardovic2001@yahoo.com

Background
Valid PET-CT guidelines have established the role of PET-CT in the imaging of colorectal cancer (CRC). The role of PET-CT in preoperative staging of primary CRC and its economic impact have been evaluated, but the results are somewhat controversial. The aim of the present study is to determine whether PET-CT demonstrated any added value to routinely performed radiological modalities in preoperative staging of CRC at our institution.

Methods
We retrospectively analyzed all patients we tracked in our PET-CT database who were imaged between 2014-2019 for the primary staging of CRC. All patients were diagnosed with colonoscopy and biopsy, and preoperative work-up was performed with CT. Patients were imaged according to the institutional low-dose PET-CT protocol and regardless of CEA level. The efficacy of PET-CT for detection of regional and distant metastases based on the results of CT findings was evaluated. TNM status and the treatment plans with and without PET-CT were compared, and any discordance was noted. Alterations in clinical management and their impact on patients were also noted.

Results
15 patients (8 male and 7 females, mean age 58.9+- 14.5) underwent PET-CT imaging for primary staging of CRC. All primary cancers, two colon and thirteen rectal, demonstrated increased FDG uptake with mean SUVmax 19.4+-8.4. Sensitivity and specificity of PET-CT for detection of primary CRC was 100%. PET-CT verified regional and/or distant metastases in 11 patients (73,3%) at the time of presentation.
In nodal staging, diagnostic accuracy of PET-CT was higher than that of CT. For liver metastases, sensitivity and specificity were 75% and 100%, respectively; and for lung metastasis 100% and 100%, respectively.
Preoperative management plan was changed in four patients (26,6%). After PET-CT, two patients (13,3%) were upstaged, and chemotherapy was added to the initially planned surgical resection. In another two patients (13,3%), a planned adjuvant chemotherapy was given up because patients were downstaged based on PET-CT findings.

Conclusion
In such a small group of patients, we demonstrated an added value of PET-CT to conventional imaging in preoperative staging of CRC. However, to further validate the results, we recommend more extensive studies to be undertaken. We recommend PET-CT to be included in staging of primary CRC in selected cases, primarily high-grade CRCs and with inconclusive radiological findings.

IAEA-CN-285/150

18F-PSMA 1007 PET-CT in Localizing Recurrence in Biochemistry Relapse in Prostate Cancer

M. Agolti, L. Solari

Clinic Modelo, Argentina

Corresponding Author: centrodemedicinanuclear@hotmail.com.ar

Background
30-50% of patients curative-intent treated for Prostate Cancer will relapse in the first ten years. Localizing the sites and restaging is very important for therapeutical indications. PSMA ligands have shown great efficiency in this area, however, 68Ga is not permitted to be used in our country, its cost is too high for developing countries, and its urinary excretion reduces the diagnosis of local recurrence.

Methodology
We made 18F-PSMA 1007 PET-CT in 16 patients with biochemical recurrence, considered rising PSA, above 0,2 ng/ml across two measures after radical prostatectomy or PSA level equal or greater than 0.2 ng/ml above the Nadir after radiotherapy. 14 studies were positives (87,5%).

Results
We found eight patients (50%) with local recurrence, in vesicourethral anastomosis (membranous urethra, bladder neck, and surrounding soft tissue), seminal vesicle bed, remnant ducti deferentia and rectroprostatic/Denonvilliers fascia. According to general literature our findings in local recurrence are higher, that could be explained for a better diagnostic accuracy with 18F-PSMA over 68G-PSMA, probably due to the non-urinary excretion of the first one. We found seven patients with exclusively relapse in pelvic lymph nodes (43,73%). We found increased uptake in lymph nodes of less than 10 mm except for one lymph node that was 12 mm. In five patients we found both local relapse and regional relapse (31,25 %). And we found distant metastasis (not regional lymph nodes, bones , lungs or liver) in seven patients (43,73%), five of them had PSA values over ten, only two of them had lower values: PSA of 0,5 with mixed bone mts (blastic and lytic) with low uptake and who started antiandrogen therapy in the last five months and another patient with PSA 2,57 with only one blastic bone metastasis

Conclusion
18F-PSMA 1007 is very useful in localizing relapse, especially we found high incidence in
local recurrence, probably for the non-urinary elimination. We found most regional relapse in normal size lymph nodes and we could identify nine oligometastasic (fewer than three or five lesions) patients (56,25%) which can be treated with metastasis directed therapy specially in local and regional oligometastasic recurrence.

IAEA-CN-285/151

Utility of PET-CT 68Ga-PSMA in the Response to Treatment of Patients who Received 177Lu-PSMA for Metastatic Castration-Resistant Prostate Cancer (MCRPC)

I. Soldevilla Gallardo, D. Cardosa Cisneros, F. O. García Pérez
S. López Buenrostro

The National Cancer Institute, Mexico

Corresponding Author: irmasoldevilla81@hotmail.com

Background
Prostate cancer is the most common cancer in men in the USA and Europe, as well as one of the most common malignancies worldwide and one of the leading causes of cancer mortality in men. A recent approach to the treatment and diagnosis of prostate cancer specifically targets prostate-specific membrane antigen (PSMA). PET-CT 68Ga or 18F-PSMA try to fill some critical gaps in the staging of prostate cancer and the evaluation of response to treatment, as well as in the selection of patients for treatment with peptide receptor radionuclide therapy 177Lu-PSMA(PRRT), however, there are no accepted response criteria with this radiopharmaceutical. The aim of this study was to assess the utility of the EORTC molecular score in the response to treatment with PET-CT 68Ga-PSMA, in patients with MCRPC treated with 177Lu-PSMA., to determine the correlation of response between the molecular score of PET-CT and the clinical response in patients treated with 177Lu-PSMA and to establish a correction for semiquantitative parameters (SUVmax), by means of the physiological concentration of the radiopharmaceutical in the liver.

Methodology
A descriptive, cross-sectional and retrospective study was carried out. Eighteen patients were selected who had a PET-CT 68Ga-PSMA study prior to treatment with peptide receptor radionuclide therapy 177Lu-PSMA(PRRT), as well as whose evaluation of response to treatment was within 6-8 weeks after treatment every two treatment cycles. Six of the eighteen selected patients were removed from the database because an incomplete clinical record. A descriptive analysis was performed for the variables of interest. Using the GraphPad Prism 8 program, a multivariate analysis was performed, as well as the Spearman correlation coefficient between the variables described.

Results
Through the multivariate analysis, the EORTC response criteria had a statistically significant correlation with the APE value (p 0.27), however, the rest of the variables (EORTC with correction for hepatic SUVmax and ECOG) did not have statistical significance. EORTC response criteria with correction for liver SUVmax had a statistically significant correlation with ECOG (p 0.18).

Conclusion
The evaluation of response to treatment in patients with MCRPC using clinical-biochemical and molecular imaging parameters is a challenge at the present time. The PET-CT 68Ga-PSMA or
18F-PSMA study is a promising tool for evaluating response to treatment in patients who receiving 177Lu-PSMA, due to the good correlation between biochemical parameters and the EORTCscore of molecular

response. However, a greater number of studies with homogeneous patient samples are required to assess the impact of PET-CT in this topic.

IAEA-CN-285/155

Head to Head Comparison of 68Ga-PSMA-11 vs 2-18F-FDG PET-CT in Non-Prostate Tumors

J. E. Vargas Ahumada, F. O. Garcia Perez, M. Acuña Hernandez, Q. G. Pitalúa Cortés, E. Ignacio Álvarez, F. Lemus Ramirez

The National Cancer Institute, Mexico

Corresponding Author: drjoelvargas7@gmail.com

Background
18F-FDG PET-CT has rapidly become a widely used imaging modality for evaluating a variety of malignancies. PET-CT with 68Ga-PSMA-11 (prostate-specific membrane antigen) is highly useful for disease staging and detection of recurrent prostate cancer. PSMA expression has been reported in a variety number of malignant tumors. Angioneogenesis is the mechanism attributed to increased uptake at these sites. Given the success and the increasing number of case reports on PSMA uptake, our objective was to evaluate the avidity of PSMA in non-prostatic malignancies and compare the diagnostic accuracy with 18F-FDG PET-CT. The aim of this work is to compare the metabolic parameters of 18F-FDG PET-CT and volumetric parameters obtained with 68Ga-PSMA-11 PET-CT in non-prostatic malignancies.

Methodology
A total of 50 patients with non-prostate tumors underwent 68Ga-PSMA-11 and 18F-FDG PET-CT within 21 days; gastrointestinal tract (n=3), breast (n=2), liver (n=13), thyroid (n=10), urological (n=16), skin and soft tissues (n=6) tumors were included. The main image criterion of positivity was the presence of focal uptake areas in one or more locations and/or higher than in the surrounding tissue background regardless of the presence or absence of lesion in the corresponding CT images. The quantification of SUVmax, MTV, TLG, PSMA-TV (PSMA-derived tumor volume) and TL-PSMA (total lesion PSMA) was evaluated in each of them with the corresponding radiotracer. All tumors were correlated with histopathology and immuno-histochemistry.

Results
Of the total patients, 50.9% were women and 49.1% men. The average age was 57.2 ± 14.8 years.
Regarding the histopathological diagnosis, the most frequent were: 25.4% clear cell renal carcinomas, 24.4% hepatocellular carcinomas well, moderately and poorly differentiated and 17.6% papillary thyroid carcinoma. To establish if there were statistically significant differences between the volumetric and metabolic parameters, a one-way analysis of variance (ANOVA) was calculated, statistically significant values were found in malignancies such as hepatocellular carcinoma and clear cell carcinoma, the results are recorded in table 1. On the other hand, Levene's test was performed in the group with a diagnosis of hepatocellular carcinoma to establish equality of variances, finding that the group with a moderately differentiated diagnosis of hepatocellular carcinoma was the group that presented statistically significant differences in SUVmax values (p 0.03).

Diagnosis	Parameter	Mean and standard deviation	*p*
Thyroid Cancer	SUVmáx PSMA	7.8 ± 6.1	0.8
	SUVmáx FDG	8.7 ± 5.1	
	PSMA-TV	4.6 ± 2.8	0.8
	MVT - FDG	4.3 ± 4.6	
	TL-PSMA	23.3 ± 19.2	0.5
	TLG-FDG	31.3 ± 33.8	
Breast Cancer	SUVmáx PSMA	6.8 ± 3.6	0.2
	SUVmáx FDG	3.5 ± 1.5	
	PSMA-TV	52.6 ± 36.2	0.5
	MVT - FDG	48.8 ± 41.9	
	TL-PSMA	195.8 ± 178.6	0.2
	TLG-FDG	118.3 ± 124.0	
Hepatocarcinoma	SUVmáx PSMA	19.6 ± 13.3	**0.02**
	SUVmáx FDG	7.3 ± 7.9	
	PSMA-TV	18.6 ± 31.3	0.2
	MVT - FDG	20.2 ± 31.0	
	TL-PSMA	178.8 ± 225.5	0.8
	TLG-FDG	163.6 ± 405.2	
Gastrointestinal Tract	SUVmáx PSMA	33.0 ± 6.8	0.3
	SUVmáx FDG	17.6 ± 17.2	
	PSMA-TV	41.9 ± 59.1	0.3
	MVT - FDG	61.3 ± 88.3	
	TL-PSMA	473.6 ± 746.8	0.4
	TLG-FDG	1295.7 ± 2168.7	
Clear cell carcinoma	SUVmáx PSMA	18.7 ± 13.5	**0.0003**
	SUVmáx FDG	5.9 ± 4.8	
	PSMA-TV	27.0 ± 68.0	0.2
	MVT - FDG	23.0 ± 56.5	
	TL-PSMA	58.4 ± 87.7	**0.04**
	TLG-FDG	15.7 ± 20.8	
Skin and soft tissues tumors	SUVmáx PSMA	12.8 ± 7.9	0.7
	SUVmáx FDG	11.1 ± 10.3	
	PSMA-TV	119.5 ± 153.3	
	MVT - FDG	120.1 ± 155.1	
	TL-PSMA	371.8 ± 303.9	0.2
	TLG-FDG	795.9 ± 893.7	

Conclusion

68Ga-PSMA PET-CT showed higher values statistically significant in volumetric and metabolic parameters when compared with 18F-FDG PET-CT in clear cell renal carcinomas and hepatocellular carcinomas specially in moderately differentiated group. With these findings, the expression of PSMA in a variety of non-prostatic malignancies, gives us the potential theragnostic application and as an alternative imaging modality for staging and restaging in tumor types where FDG PET-CT imaging has low diagnostic accuracy.

IAEA-CN-285/158

Treatment Planning in Peptide-ReceptorRadionuclide Therapy (PRRT) Using PET Data and Physiologically Based Pharmacokinetic Model: A Simulation Study

D. Hardiansyah[1], P. Kletting[2], G. Glatting[2]

[1] University of Indonesia
[2] Ulm University, Germany

Corresponding Author: denihardiansyah@ui.ac.id

Background
A standard injected activity is usually the method of choice for treatment in peptidereceptor radionuclide therapy (PRRT) due to the complexity and the workload of individual treatment planning. The advantages of individualized treatment over the standard activity approach are difficult to assess in clinical trials. Furthermore, PET data has not been used for individual treatment due to the short half-life of the radionuclide in PET, different compounds and amounts of the drugs. Therefore, we performed an in silico clinical study using a physiologically based pharmacokinetic (PBPK) model to investigate 1) the effect of individualization on the predicted time-integrated activity coefficients (TIACs) and 2) the possibility of using PET data for individual treatment planning in PRRT.

Methodology
Biokinetics data of 111In-DTPAOC from 15 patients with neuroendocrine tumours derived using planar imaging were used. Six virtual patients (VPs) with different individualization were defined to investigate the effect of individualization to the prediction of TIACs. VPtrue is the PBPK model with the estimated individual parameters from the biokinetics data. Alteration of the individualizations were defined as follows: VP1 was the PBPK model with the mean values of the estimated parameters (standard activity), VP2 was the VP1 plus the physical parameters, VP3 was the VP2 plus the tumour volume, VP4 was the VP3 plus glomerular filtration rate, VP5 was VP4 plus tumour perfusion and VP6 was VP5 plus a simulated PET data after injection of 68Ga-DOTATATE at 60 min p.i. without noise and using Bayesian parameters. The biodistribution during therapy was simulated using the VPs assuming an i.v. infusion of 90Y-DOTATATE of 3.3 GBq over 30 min. The relative deviations RDs of VP1-6 to VPtrue were analyzed. We also investigated the effect of different sampling schedules and noises of simulated PET measurement on the RDs. The investigated noise levels and sampling schedules were the fractional standard deviation (FSD) of 10%, 1%, 0.1% and 0.01% and seven combinations of PET measurements at 30 min, 1 h and 4 h p.i..

Results
The RDs of the TIACs were extremely high for VP1, i.e. RDtumour=(625±1266)% and RDkidneys=(11±38)%. The inclusion of patient-specific data do not suffice to have an accurate determination of the TIACs, i.e. VP5: RDtumour=(-2±27)% and RDkidneys=(16±43)%. Finally, we found that integrating all available information and PET at one time point without noise could possibly suffice to have an accurate individual treatment planning, because VP6: RDtumour=(- 2±22)% and RDkidneys=(-0.1±0.5)%. We also found that for noisy simulated PET data, a two-timepoint of PET measurement at 1 and

4 h p.i. might be sufficient to predict the TIACs with relatively accurate RDs, i.e. <10%, for an FSD up to 1% in our patient group.

Conclusion

In this in silico clinical study we showed the effect of individual treatment planning in PRRT. By using a PBPK model, individual parameters and simulated PET data, we demonstrated that a simple and accurate individual treatment planning may be possible. Therefore, further developments in this topic are recommended.

IAEA-CN-285/162

Usefulness of 64Cu-DOTA in Gastro-Pancreatic Neuroendocrine Tumors, Compared to 68Ga-DOTATATE

F. Lemus Ramírez, M. Acuña Hernandez, F. O. Garcia Perez, E. V. Gomez Argumosa, J. Vargas Ahumada

The National Cancer Institute, Mexico

Corresponding Author: filibertomed@gmail.com

Background
64Cu (t1 / 2 = 12.7 h, 17.6% β +), can be produced in a biomedical cyclotron and distributed over distances of the order of thousands of kilometers by land or air with the possibility of using the radiotracer the day after its production. This radio metal is strongly bound to the same bifunctional chelating ligands that are present in peptide-based radiopharmaceuticals such as DOTA. 64Cu-DOTA produces images of excellent quality and high-resolution space. The images were characterized by a good tumor-background ratio over an image time window of at least 3 h. The aim of this study is to demonstrate the diagnostic efficacy when evaluating neuroendocrine tumors using 64Cu DOTA and compare with 68Ga DOTA.

Methodology
From March 2019 to March 2020, 64Cu-DOTA PET-CT was performed in 14 patients, of which 13 with a diagnosis of NET, giving a biodistribution time of 2 hours, of the same 10 had a positive result, the SUVmax of the sites of normal biodistribution and the target lesion, as well as the target lesion, SRD (Somatostatin receptor density) and TLSRE (Total lesion somatostatin receptor expression) were evaluated. Likewise, it was correlated with complementary 68Ga-DOTA PET- CT in a period not exceeding 3 months, quantifying the lesions detected in both methods.

Results
The median uptake in SUVmax with 64Cu-DOTA was: Tumor 17.8 +/- 14.5; Pituitary 5.7 +/- 2.2; thyroid 3.4 +/- 1.3; liver 9.4 +/- 4.6; spleen 25.9 +/- 10.9; adrenal 13.05 +/- 7.06; kidney 14.7 +/- 6.1; bladder 9.1 +/- 28.1; gluteal fundus 1.26 +/- 0.2. 12 of the 14 patients underwent 68Ga-DOTA, finding that in both cases a total of 64 lesions were detected. In the case of 68Ga-DOTA the median SUVmax for tumors and background was 17.8 +/- 21.4 and 1.3 +/- 0.3, respectively. For 68Ga-DOTA the SRD and TLSRE values for target lesion were: 27.1 +/- 72.9 and 184.6 +/- 1.6, respectively. While for 64Cu-DOTA the SRD and TLSRE values for target injury were: 31.6 +/- 90.2 and 141.6 +/- 1.6, respectively.
Histograms were performed to evaluate the distribution of the data, finding that the data does not present a normal distribution.
To establish whether the values in the 68Ga and 64Cu studies were equivalent, the non-parametric Wilcoxon signed-rank test was used.
With the above, it was found that all the variables do not present statistically significant differences, which means that these parameters can be evaluated in an equivalent way in both studies.

Conclusion

No statistical differences were identified between the median and SD of the SUVmax, , SRD and TLSRE in the lesions in the study with 64Cu-DOTA at 2 hours of injection vs 68Ga-DOTA at the time of injection, also there are no statistical differences between them, therefore, both radiometals appear to be equally effective with the advantage of the 64Cu being flexible in logistics.

IAEA-CN-285/165

Evaluation of a Natural Flavonoid Labelled With 11C for Alzheimer's Disease

M. Zeni[1], M. D. Santi[1], F. Arredondo[1], D. Carvallo[5], M. Peralta [2,3] R. Dapueto[1], J. L. Cabrera[2], M. G. Ortega[2,3], D. Carvalho[5], J. Abin-Carriquiry[5], A. Rey[4], J. Giglio[1]

[1] Cudim y Facultad de Quimica, Uruguay
[2] Laboratorio de Farmacognosia, Departamento de Ciencias Farmacéuticas, Facultad de Ciencias Químicas, Universidad Nacional de Córdoba, Argentina
[3] Instituto Multidisciplinario de Biologia Vegetal (IMBIV – CONICET), Argentina
[4] Área de Radioquímica, Facultad de Química, Universidad de la República, Uruguay
[5] Instituto de Investigaciones Biológicas"Clemente Estable" (IIBCE)

Corresponding Author: maiazenirc@gmail.com

Background
Alzheimer's disease (AD) is the most common form of dementia. The phosphotransferase glyco- gen synthase kinase 3-beta (GSK-3beta) has gained attention due to its association with axonal dysfunction, neuronal death and as a mediator of pro-inflammatory responses. For this reason, GSK3 is an interesting target in Alzheimer's disease. Glabranin, a flavonone from Dalea elegans native to Córdoba (Argentina) is a potential inhibitor of GSK, as suggested by in silico studies.
The objective of this study is the physicochemical and biological evaluation of (2S)-5,7-dihydroxy-8-(3-methylbut-2-enyl)-2-phenyl-2,3-dihydrochromen-4-one (Glabranin), labelled with 11C (11C-FLA).

Methodology
Glabranin was isolated from aerial parts of Dalea elegans as previously reported. Briefly, the benzene extract was obtained by soxhlet and processed using chromatographic techniques. The obtained compound was identified using spectroscopic and spectrometric techniques.
The labelling was performed by methylation on a TracerLAB FXc-pro (GE) module located in a hot cell MIP-1 (Comecer).
The radiochemical purity (RCP) was determined by HPLC using a 18C column (5µm 4.6x150mm), flow=1 ml/min. and a gradient of 1% of acetic acid in Water (A) and Acetonitrile(B) (%B 0 to 100 from 0 to 10 min). Lipophilicity was determined by means of logP=[n-octanol]/phosphate buffer (0.1M, pH=7.4). Plasmatic protein binding (PPB) was determined by size exclusion chromatography. Stability in plasma and in labelling milieu was assessed by HPLC.
For in vitro studies a primary culture of neurons from cortex and hippocampus of 16-18-week-old fetuses of C57 mice was used. Cells were cultivated in Neurobasal medium supplemented with B27 at 37°C and 5% CO2.
Cells were incubated with 11C-FLA for 5, 10 and 20 minutes at 37°C and washed with PBS. The binding is expressed as the percentage of the total incubation activity.

Results

The labeled compound was obtained with a yield of 2,9±1,1% (n =3) (not decay corrected) and a radiochemical purity of 96.6±2,3% (n= 4).

11C-FLA was stable in the reaction milieu and in human plasma for at least 2 h. The lipophilicity, calculated as the partition coefficient between octanol/buffer, was Log(P) =1.22±0.05 (n = 4), and the binding to plasma proteins 72±3% (60 minutes).

The maximum cell uptake in in vitro studies was 13,6% at 20 minutes with 10,18 MBq.

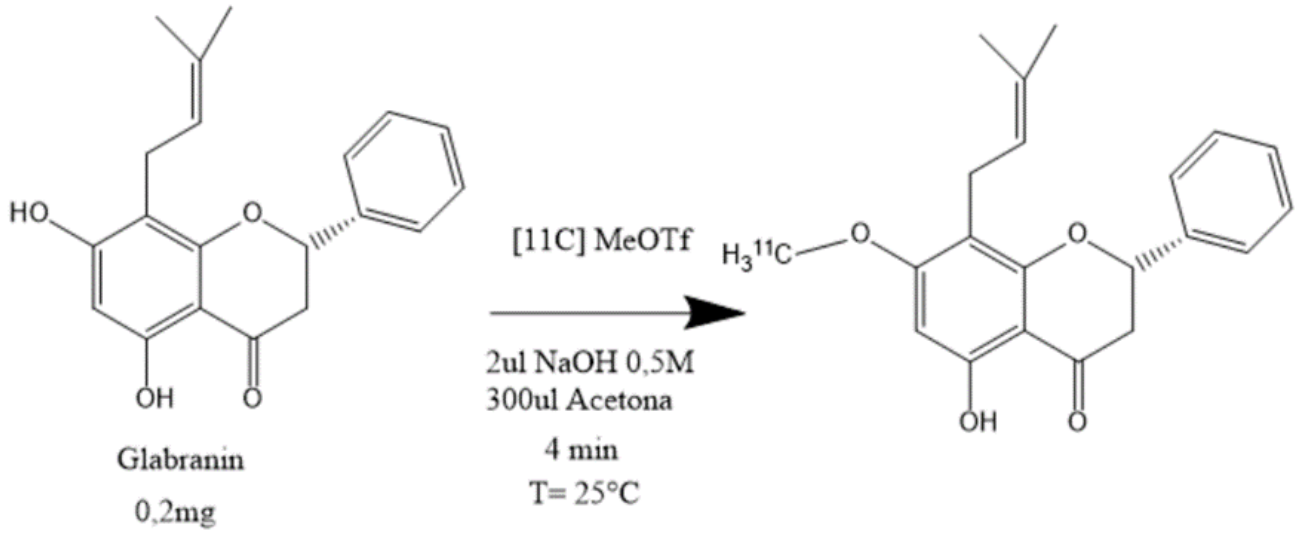

Conclusion

The 11C-FLA was obtained with adequate RCP and good stability. The physicochemical properties are adequate, and the radiotracer presented a good uptake in "in vitro". Consequently, 11C-FLA is a potential interesting radioligand to continue the studies of its potentiality as GSK-3β imaging agent in the AD.

Acknowledgements: ANII(POS_NAC_2018_1_151615).

IAEA-CN-285/171

Comparison PET-CT Analog BGO vs Digital LBS, and Impact on Phantom Image Quality. FSFB Experience

J. Daza, C. Blanco, P. Bernal

Santa Fe de Bogotá Foundation, Colombia

Corresponding Author: josea727@gmail.com

Background
This article presents a comparison between the physical characterization of two pieces of PET-CT equipment at the Hospital Universitario Fundación Santa Fe de Bogotá (FSFB), the first one a PET Discovery DSTE, analog equipment with photomultiplier tube technology associated with BGO crystals, and the second a PET Discovery MY digital equipment with Lutetium-based scintillator (LBS) time-of-flight correction (TOF) crystals and silicon photomultipliers. The performance of the equipment was evaluated following NEMA standards and phantom images to evaluate the image quality for different reconstruction filters.

Methodology
Tests of spatial resolution, sensitivity, dispersion fraction, loss of counts and precision of count rates were carried out under the standards recommended by the manufacturer, NEMA NU-2 2001 for analog equipment and NEMA NU-2 2012 in digital respectively. Image quality tests were also carried out with the Jaszczak phantom following the criteria of the American College of Radiology ACR, a dose of 10 mCi and three minutes of time per bed was considered, the images were reconstructed with iterative algorithms to maximize the expectation of ordered subset (OSEM) in the analog equipment and block sequential regularized expectation maximization (BSREM) in the digital equipment, and evaluated in the three criteria of resolution, uniformity and contrast.

Results
Spatial resolution measured as the maximum full mean width (FWHM) in mm for the 1 and 10cm CFO transaxial / axial measurements: 6.14 / 5.15 @ 1cm and 6.79 / 5.85 @ 10 cm for the analog equipment; radial / tangential / axial measurements of 3.83 / 3.77 / 4.02 @ 1cm, 4.75 / 3.87 / 5.03 @ 10 cm and 7.38 / 4.18 / 5.54 @ 20 cm in the digital equipment
Average sensitivity of the measurements at 0 and 10 cm in cps / kBq of 8.28 analog and 12.86 digital.
NECR peak of 50.44 kcps at 12.02 kBq / mL and 193.4 kcps at 21.9 kBq / mL respectively. Qualitative evaluation of phantom images, resolution (visualize smaller diameter cold bars with tolerance ≤ 11.1mm): 9.5 mm analog and 7.9 mm digital; uniformity: no artifacts on both teams; Contrast (display hot cylinder with smaller diameter and tolerance ≤ 16mm) 12 mm analog and 8 mm digital.

Conclusion
Comparison of the performance of Discovery systems under NEMA standards show similar spatial resolution, with increased sensitivity of digital equipment with a gain of 55% versus analog equipment, as well as better performance for NECR count rates.

The phantom image comparisons between PET-CT systems are satisfactory for the ACR accreditation criteria, but demonstrate better quality in the three qualitative criteria, being able to resolve smaller hot and cold bars and uniformity images with a higher degree of homogeneity, Results consistent with better sensitivity and optimization of BSREM reconstruction algorithms compared to OSEM.

These Results allow us to conclude that with the new system, images of better quality and greater definition are obtained, thus allowing a better diagnosis for our patients.

IAEA-CN-285/177

Accuracy of 11C-Methionine PET with Intravenous Contrast-Enhanced CT in Preoperative Localization of Parathyroid Adenomas

F. Bayembayev, A. Sadvakassova

Medical Centre Hospital, Kazakhstan

Corresponding author: farkhat.kz@gmail.com

Background
11C-methionine (MET) PET-CT is a promising imaging technique in the preoperative localization of parathyroid adenomas in patients with primary hyperparathyroidism (PHPT), providing both anatomical and metabolic information. In this retrospective study, we aimed to evaluate MET-PET in conjunction with CT performed with intravenous contrast-enhancement (CECT) in the preoperative localization of parathyroid adenomas (PTAs) in patients with biochemically confirmed PHPT.

Methodology
Between 2006 and 2016, 35 patients underwent MET-PET-CT with CECT and ultrasonography (US) and subsequent surgery. Review of MET-PET-CT was performed with the reader blinded for the clinical information. The results were compared with those of US and correlated to surgical findings and histopathology.

Results
31/35 (89%) patents had previously undergone surgery (6 - thyroid surgery, 25 - parathyroid surgery). Surgery after MET-PET-CT included minimal invasive localized procedure in 27 and wider exploration in 8 patients. In 6 patients, PTAs were located ectopically. Lateralization of the PTA by MET-PET-CT was incorrect in 5 patients with sensitivity 67%, specificity 50%, PPV 95% and NPV 91%. The sensitivity for US was 63%.

Conclusion
The sensitivity of MET-PET-CT correlates with that in previous reports on re-operative PHPT patients and somewhat higher than for US. Low sensitivity might be due to inverse contrast-enhancement of PTAs and false positive localization because of tracer accumulation in enlarged lymph nodes, owing to previous neck surgery. A larger study is warranted for further evaluation of MET-PET-CT with CECT, and also assessing the impact of different contrast-enhancement phases.

IAEA-CN-285/179

Characterization of Brain Perfusion Spect Abnormalities in Major Depressive Disorder Patients Free of Therapy with a Neurostat Data Base Program

G. Castro Muñoz[1], L. T. Massardo Vega[1], J. C. Quintana[2], J. Spuler[1], B. Riedel[1], D. Muñoz[1], D. Vicentini, R. Lastra, R. Alay, P. Padilla

[1] University Hospital, Chile
[2] Pontificia Catholic University, Chile

Corresponding Author: gabrielcastro.m89@gmail.com

Background
It is well known in major depressive disorder (MDD) there are diverse brain abnormalities with some controversial findings in regional blood flow distribution observed with SPECT and PET tracers with bilateral diminution at cortical frontal level or even diffuse and increased flow in some deep structures and mesial cortex.
The goal of this study was to present brain perfusion abnormalities in a group of MDD patients compared with a recognized adult normal data base, as an academic exercise for postgraduate students.

Methodology
We evaluated 36 MDD patients ranging from 25-52 y.o, with clinical score HAM-D17≥15 and Beck questionnaire ≥12. All were free of specific medication and other conditions that may affect brain perfusion. They were studied at rest after administration of 99mTc-ethylcysteinate dimer. SPECT was acquired 30 minutes later with two head SIEMENS e–Cam; quality control of the radiolabeling was adequate (mean:95%).
Neurostat 3D-SSP program (iSSP3.5) is a data base allowing comparison between a case against the normal group. It considers normal a Z score between -2 and +2, expressed in a color scale; we read them as an integer number in the most relevant areas affected in MDD. Each case was compared with gender and age range in the base. Figure 1.
Figure 1. Case 10, a 27 y.o. male. Left. Z scores of decreased perfusion regarding normal subjects are shown in a color bar with a negative number scale; showing a significant hypoperfusion mainly in prefrontal cortex. Right. Z scores of increased perfusion in the same patient, demonstrating mainly mesial abnormalities.

Results
Analysis by regions.
Enthorinal cortex presented increased perfusion in all cases (left mean Z: 4.3, right 5.7). The post-central gyrus (parietal lobe) was abnormal in 14/36 cases at left (8 increased and 6 decreased) and in 16/36 at right (2 increased and 14 decreased).
At prefrontal cortex, the dorsolateral region presented decreased perfusion in all cases at left(mean Z:-4.2) and all but 4 at right(mean Z:-3.4); the ventrolateral region was decreased at left in 21/36 cases(mean Z:-2.9) and at right, the last was abnormal in 26/36 cases, 25 decreased and 1 increased(mean Z:-2.8.).
Both temporal gyri presented decreased perfusion in 34/36 at left and 35/36 at right, more marked in the latter (mean Z:-3) being the worse the left medium and the right superior regions.

Parietal gyri presented decrease perfusion in a lesser number of patients (mean Z: -1.5 at left, -2.1 at right) without cases of increased perfusion.

Analysis by Brodmann areas (BA)

In our group of MDD patients, we observed decreased perfusion was present in the dorsolateral, premotor prefrontal cortex, pregenual anterior cingulate and mesial temporal. A higher number of regions with increased perfusion than expected were found, mainly at enthorinal and cingulate cortex.

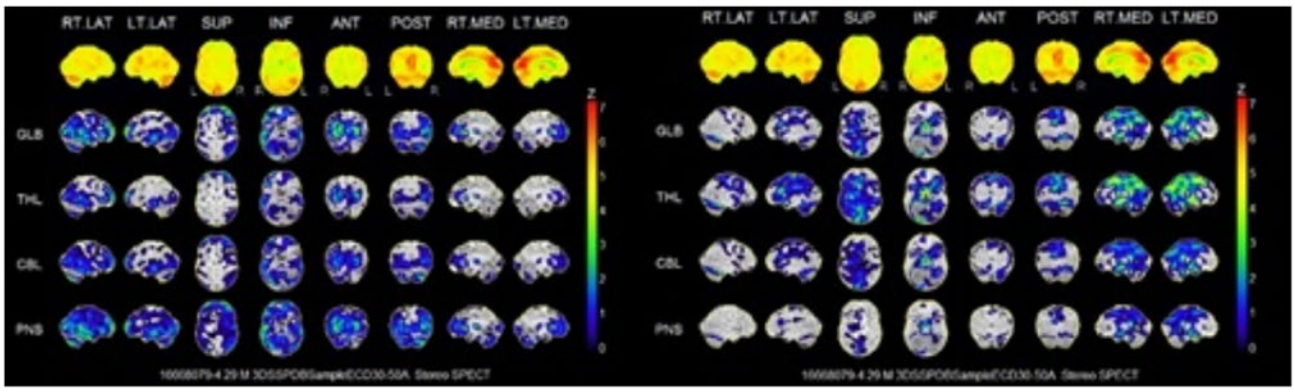

Conclusion

This interpreting exercise using a normal data base could improve post-graduate students training to obtain better reproducibility.

IAEA-CN-285/188

Malignant Pecoma: A Rare Tumor with High Avidity for 18F-FDG PET-CT: Case Report

A. M. Alvarez, M. Pabon Luiz, M. Renjifo, N. Martinez, E. Manzi

Valle de Lili Foundation, Colombia

CorrespondingAuthor: luz.pabon@fvl.org.co

Background
Primary Perivascular epithelioid cell tumor (PEComas) is a rare mesenchymal neoplasm. These cells exhibit both smooth muscle cell and melanocytic differentiation. It is usually benign but has the potential to malignize and metastasize. It has been known to occur in several sites, these include uterus, kidney retroperitoneum, lungs, and pancreas. Among the diagnostic images used are computed tomography (CT) and magnetic resonance imaging (MRI). Positron emission tomography (PET-CT) has few studies regarding the metabolic behavior of these tumor cells but can be a useful diagnostic imaging procedure for staging and follow-up in this disease. The aim of this paper is to present two cases of malignant PEComa, describe the difficulties in the clinical diagnosis and the role of 18F-FDG PET-CT as a diagnostic tool in this pathology.

Methodology
We report two cases of PEComas in two males between 70-90 years old. Both tumors had histological characteristics of PEComa. All had difficulty in clinical diagnosis and PET-CT was performed.

Results
PET-CT was useful in both cases as a diagnostic tool to evidence of primary tumor lesion, degree of malignancy and extension. All presented high avidity for 18F-FDG.
The first case is a 73-year-old man with a 6-month history of a petrous mass in his left parotid associated with otalgia. 18F-FDG PET-CT showed intense pathological hypermetabolism in left parotid mass with SUV max of 21.3g/ml associated with enlarged laterocervical conglomerate lymph nodes. The patient was taken to left parotidectomy and cervical lymph node resection. Pathology and immunohistochemical findings result in malignant PEComa. During follow-up, one year after surgery, he presented a lymph node relapsed requiring a new intervention.
The second case is an 83-year-old man with a diagnosis of intra-abdominal malignant PEComa who was taken to surgery for nephrectomy, adrenalectomy, splenectomy, distal pancreatectomy and lymphadenectomy. Fourteen months after surgery patient presented with abdominal pain. CT scan reported a mass with heterogeneous density and enhancement that surrounds the left adrenal gland. A 18F-FDG PET-CT was requested to confirm tumor relapse, showing intense hypermetabolic mass of heterogeneous density and activity in the left adrenal gland with its highest uptake towards the inferior and posterior border with SUV max of 15.6 g/ml, which comes into contact with the aorta and vertebral bodies. Patient died months later.

Conclusion

18F-FDG PET-CT has proved to be a valuable tool as a diagnostic imaging procedure in this rare neoplastic disease, presenting high metabolic activity in our patients. Since it is a rare tumor that can evolve to malignancy, we consider it can be a useful image for staging and follow-up in patients with these types of pathology.

IAEA-CN-285/189

Implications of Incidentalomas in 18F-FDG PET-CT Studies

A.M. Alvarez, S. Prada, L.M. Pabon, M. Renjifo, N. Martinez, E. Manzi

Valle de Lili Foundation, Colombia

Corresponding Author: luz.pabon@fvl.org.co

Background
An incidentaloma is an abnormality found unexpectedly in a diagnostic study. These findings have become increasingly common in all diagnostic studies including 18F-FDG PET-CT with hypermetabolic foci not related to the primary tumor being studied and that do not correspond to physiological uptake. In the medical literature it is described that up to 5% of incidentalomas correspond to second malignancies. Understanding the risk of malignancy is essential to guide the need for further evaluation of an incidentaloma. This retrospective study has the objective of determining the incidence of incidentalomas in 18F-FDG PET-CT in our population, evaluating its frequency, location and associations, risk of malignancy and economic impact of carrying out recommended complementary studies.

Methodology
Between 2012-2018, 4767 patients were referred to our institution for a 18F-FDG PET-CT. PET-CT was performed in a hybrid computer biograph mct128 PET-CT (Siemens, Germany) previous intravenous administration of 18F-FDG. For the statistical analysis, a descriptive analysis of variables was performed. We compared the SUVmax with the Mann-Whitney test or the student t-test. ROC curve analysis was performed to determine a clinically useful SUVmax cut-off point. For the subgroup analysis, we selected three locations of incidentalomas with high malignancy rates describe in literature (Thyroid, Breast and Prostate). The monetary evaluation was performed using ISS2001 manuals from Colombia + 50% adjustment, presented in US Dollars ($).

Results
From a total of 4767 patients referred to 18F-FDG PET-CT in our institution, 721 studies presented an incidentalomas (15.1%). The most frequent locations of incidentalomas were Head and Neck (32%), Thyroid (21.6%), Intestinal (15%), Gastric (7.7%), Breast (4.6%). Prevalence of incidentalomas was higher in those over 60 years old. For the subgroup analysis, we selected three locations (Thyroid, Breast and Prostate 18F-FDG PET-CT incidentaloma).
Focal thyroid incidentalomas correspond to 3.5% of the total (171 cases), with malignancy rate of 26.9%. When analyzed this subgroup by sex, it was evident that only men presented a significant area under the curve (AUC=0.8875) with SUVmax cut-off point of 9.9g/ml (S83.8%, E90.9%, LR+9.1, LR-0.18). SUVmax was not statistically significant for women (AUC=0.4931). The performance of recommended complementary studies generated an additional cost of 52.6 $ per patient. Breast incidentalomas correspond to 0.8%. Prostate incidentalomas correspond to 0.18% of the total (9 cases), with malignancy rate of 40%.

SUVmax was not statistically significant. The performance of recommended complementary studies generated an additional cost of 162.48 $ per patient.

Conclusion

The frequency of 18F-FDG PET-CT incidentalomas in our population is similar to the global reported. SUV max cut-off points in incidentalomas to differentiate Benig vs. Malignant is not useful (except in men with thyroid incidentalomas with SUVmax of 9.9g/ml). According to the subgroup analysis, the economic impact for the health system of carrying out recommended complementary studies to study incidentalomas found in PET was 68.64USD.

IAEA-CN-285/191

Role of 18F-FDG PET-CT in Stratification of Recurrent Ameloblastic Carcinoma: A Case Report

L. M. Pabon, A. M. Alvarez, M. Renjifo, F. Medina, N. Martinez, E. Manzi

Valle de Lili Foundation, Colombia

Corresponding Author: luz.pabon@fvl.org.co

Background
Ameloblastic carcinoma (AC), is a rare odontogenic neoplasm, with an incidence that ranges from 1-3%. The clinical course of AC is typically aggressive with an ulcerated mass with extensive local destruction. It has a distinct predilection for the mandible, associated with lymph node involvement and metastases to various sites, including lung metastases in up to 80% of cases and, less common, bone. Metastases can be independent of local relapse. AC can originate de novo or in an initially benign pre-existing lesion. The transformation from ameloblastoma to AC occurs in less than 3% of cases. The predilection age is 30 years but can be found in patients between 10-80 years. It is more frequent in men with a 2:1 ratio. AC requires extensive surgical resection; recurrence can be observed with more than 50% of cases within the first 5 years after primary surgery. To date, there are very few studies on the use of Positron Emission Tomography (18F-FDG PET-CT) in the diagnosis, stratification or follow-up of AC. We describe a case of an ameloblastoma with transformation to AC with emphasis on imaging features of 18F-FDG PET-CT. The aim of this paper is to present a case of ameloblastoma with transformation to ameloblastic carcinoma and the utility of 18F-FDG PET-CT for stratification and determination of metastatic involvement in this pathology.

Methodology
A 60-year-old female reported to the outpatient consult with a chief complaint of painful mass in her right mandible. A 18F-FDG PET-CT was requested during follow-up for re-staging.

Results
Resection biopsy of the mass in the right mandible demonstrated ameloblastoma and observation was recommended. Follow-up revealed an increase in mass size, after which extensive surgical resection was performed, 12 months after the initial diagnosis. Histologic examination of the tissue reported ameloblastic carcinoma ex plexiform ameloblastoma with positive margins. Five months after the second resection, a new mass had grown in the submandibular region with a left sub-mandibular adenomegaly and pulmonar nodules, demonstrated by a neck-thorax computed tomography (CT). Suspecting metastasis, a 18F-FDG PET-CT is requested to restage patient, with report of left submandibular hypermetabolic foci, metastatic lung involvement and bone lytic lesions in addition to hypermetabolic pancreatic lesions. In the latter, two possibilities were mentioned, metastatic involvement vs. second primary involvement, histopathological approach was suggested. In the literature search we did not find any reports of pancreatic metastases in patients with ameloblastic carcinoma.

Conclusion

In a low frequency entity, the 18F-FDG PET-CT may be useful as an adjuntive modality for staging ameloblastic carcinoma in search of distant lesions even in the absence of local relapse, however, given the low incidence of this pathology there are not enough studies to determine the performance of this test in this entity.

IAEA-CN-285/194

Optimization of the Reconstruction Parameters in the PET-CT Images: A Simulated Study in Phantom

M. A. Coca Perez[1], J. Garay Urrutia[1], C. BazaesVelasquez[1], C. Delgado Meza[2] J. Escobar Flores[2]

[1]Medscan Nuclear Medicine and PET-CT Center
[2]San Sebastian University of Concepción

Corresponding Author: macp970617@gmail.com

Background
The quantification of PET-CT images to study different tumors allows obtaining an accurate diagnosis. SUV is a useful parameter for the diagnosis and monitoring of treatments, because it allows quantifying metabolic activity. SUV and image quality are affected by the characteristics of PET-CT equipment, acquisition protocol and the reconstruction algorithms. The image quality evaluation and the SUV value need to be optimized to achieve a correct diagnosis. Various organizations such as the JSNM and the EANM have established standardization protocols. The aim of this study is to determine the optimal reconstruction parameters to maximize the SUV with adequate image quality through phantom study in our PET-CT Biograph Duo.

Methodology
A Jaszczak phantom was used to evaluate the optimal parameters for image quality and SUVmax level. The phantom included 4 cylindrical inserts (0.5, 1, 1.5 y 2ml) filled with 18F-FDG solution with a 20:1 ratio of activity compared to the Background. Data were acquired with a variation of 2, 3 and 4 minutes of the acquisition bedtime and reconstructed with OSEM with 2 iterations and 16 subsets similar to a clinical practice. The acquired images were reconstructed with a Gaussian smoothing filter with a range of FWHM (2 mm to 10 mm with 1mm intervals). VOIs for the four sources were created in each of the images reconstructed with the different FWHM of the Gaussian filter and the SUVmax was also recorded. A 2 cm Background ROI was added for each source to record the background SUVmax of each source. To evaluate the image quality, the background variability and estimation of a count profile for the different acquisition times were determined following the Methodology used by Yuji Tsutsui, 2018.

Results
The effect of nine variations in Gaussian Filter settings on image quality and SUVmax at different acquisition times on PET-CT images was determined. The effect on image quality and SUVmax differs depending on the variation of the FWHM in the smoothing filter and the acquisition time. As results, it was observed that SUVmax values decrease as FWHM increases and this behavior is repeated for the different acquisition times. The percentage of background variability decreases as the FWHM increases independent of the acquisition time. The variation in account profiles decrease as the FWHM increases, regardless of acquisition time, reaching peaks of 2,500 to 3,000 in gray levels for the 3-minute acquisition and 2,000 to 2,500 for the 4-minute acquisition.

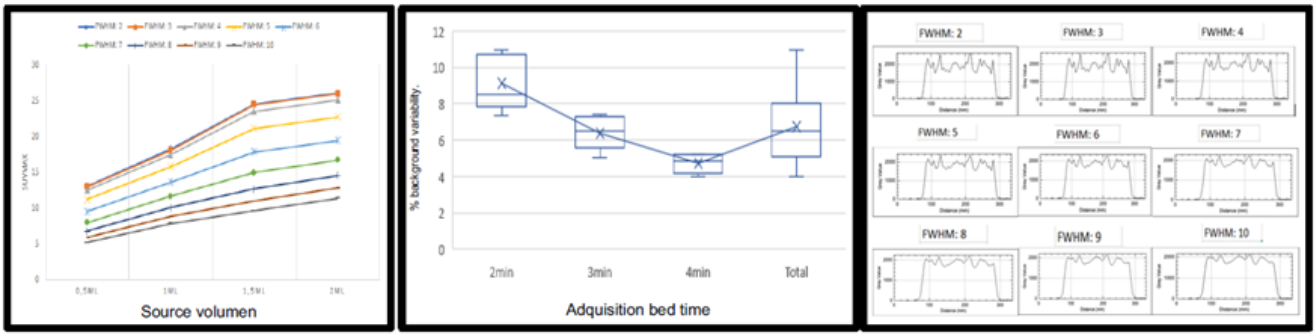

Figure 1. Left: SUVmax on acquisition at 3 minutes per bed time; Center: Percentage of background variability per bed time; Right: Counts profile obtained from ROIs at 3 min

Conclusion

Optimization of the acquisition and reconstruction parameters for PET-CT images was achieved, guaranteeing to maximize SUVmax values and adequate Image quality in a phantom with 4 sources of different volumes filled with 18F-FDG solution. As Results, we are proposing 3 minutes of acquisition bedtime as optimal time and the application of the Gaussian filter with FWHM values of 6 mm or 7 mm in image reconstruction.

IAEA-CN-285/197

Staging and Simulation for Radiation Therapy in only one PET-CT Scan on Nasopharyngeal Cancers: A Single Institutional Study

T. T. Ngo[1], H. B. Tran[2], T. K. Mai[2], D. T. Tran[3]

[1]Bach Mai Hospital, Viet Nam
[2]Hanoi Medical University, Viet Nam
[3]Military Medical University, Viet Nam

Corresponding Author: drngothuytrang@gmail.com

Background
18F-FDG PET-CT (PET-CT) has been a validated imaging method in nasopharyngeal cancer staging. However, there was no previous study about its efficacy in simulation for radiation therapy planning in Vietnam. We aimed to validate the application of the PET-CT in staging and radiation simulation in a single scan.

Methodology
Prospective study on 60 newly diagnosed nasopharyngeal carcinoma (NPC) at Bach Mai Hospital, from Feb 2010 to Feb 2015. All 60 patients underwent PET-CT scans for staging, and 30 patients among this group indicated curative radiation therapy after scanning. Comparison with existing CT/MRI images and changes in staging were collected for analysis with STATA 8.0. We collected information about side effects during treatment and follow-up visits. Tumor responses were evaluated at the follow-up visit three months after completing the treatment.

Results
The median age of patients was 49.0+15.1 years old with the majority being male. Male/Female ratio was 3:1. Common symptoms for initial visit were: tinnitus (50%), neck lymph nodes (48.3%), headache (28.3%), blocked nose (20%), epistaxis (18,3%). 28.4% of patients came to the hospital after three months since the first symptom. The first endoscopy could not detect the tumor in two patients (3.3%). Histopathological confirmed that 86.7% of patients were non-differentiated carcinoma, and 13.3% were squamous carcinoma. PET-CT was superior to routine CT/MRI in detecting involved lymph nodes ($\chi 2 = 21.0$; $p < 0.001$). T, N, M stages changed in 11/60, 26/60, and 3/60 patients, respectively. Overall stages changed in 38.3% of patients (23/60). SUVmax of the tumor had an increased value in patients with vs. without lymph nodes: 12,2 +/- 5.1 vs. 9.1 +/- 3.2 ($p < 0.01$) as well as with vs. without distant metastases: 14.9 +/- 3.2 vs. 111 +/- 4.9 ($p < 0,05$). There was a correlation between the size of tumors and lymph nodes and SUVmax: $r = 0.48$, and $r = 0.75$, respectively. There was a decrease in SUV uptake in lymph nodes in comparison with the primary tumor, and supraclavicular lymph nodes were the highest uptake group. Using PET-CT images for radiation simulation reduced the gross treatment volume in 73.3%, 26.7% of patients, respectively, in comparison with using conventional CT images. 100% of patients achieved a complete response after treatment. Early side effects were grade I mucositis (73.3%), dermatitis (26.7%) and dry mouth (10%). Late side effects were grade I-II xerostomia (63.3%), grade I trismus (23.3%), and neck stiffness (13.3%).

Conclusion

PET-CT is a superior validated method in staging and simulation for radiation therapy planning at our Hospital. Usages of PET-CT image is not only useful for initial diagnosis but also save waiting time for radiation therapy. The acute toxicities of treatments were mild and recoverable in the majority of cases. Exclusions from radiotherapy after PET-CT scan is not a favorable prognosis factor. Further study and follow-up are needed to confirm the efficacy in terms of disease-free survival and overall survival.

IAEA-CN-285/201

Optimization of 90Y-PET-CT Reconstruction Protocol for Volumetric Dosimetry Quantification in Selective Internal Radiation Therapy (SIRT) Procedures

A. Capotosti[1], R. Moretti[1], D. Cusumano[3], M. Capogni[4], M. D'arienzo[4], T. Scotognella[2], L. Azario[2], M. De Spirito[2], L. Indovina[2]

[1]Fondazione Policlinico Universitario A. Gemelli IR-CCS, Italy
[2] Catholic University Sacro Cuore
3 Policlinico Universitario "Agostino Gemelli
[4] ENEA, Istituto Nazionale di Metrologia delle Radiazioni Ionizzanti

Corresponding Author: amedeo.capotosti@policlinicogemelli.it

Background
Radioembolization with 90Y-microspheres is increasingly used in Hepatocellular carcinoma (HCC) treatments. The new generation of PET-CT scanner with Time-of-Flight (ToF) technology allows to implement volumetric 90Y-dosimetry techniques to investigate tumor dose-response directly based on 3D 90Y-activity distribution acquired from PET imaging. Many authors have tried to establish a routine protocol for 90Y PET-CT in terms of bed-time acquisition, matrix, number of Equivalent Iterations (E.I.) and magnitude of post reconstruction gaussian filter using common and original methods. The aim of this study is an up-to-date evaluation of the best 90Y PET-CT reconstruction parameters for a Siemens Biograph mCT PET-CT scanner.

Methodology
Three phantoms (a cylindrical uniform one [1], IEC NEMA Body [2] and IEC NEMA Torso [3]) were acquired using a therapeutic amount of 90Y. Activity measurements were performed using ENEA-INMRI portable triple-to-double coincidence ratio (TDCR) counter which provides a relative standard uncertainty below 1%. The impact of different types of matrix and number of E.I. was evaluated through the SUV analysis in phantom [1] and RC analysis in Phantom [1,2] respectively. Then, the magnitude of post-reconstruction gaussian filter was evaluated with a dosimetric approach through the analysis of the Dose Volume Histogram (DVH) using the Root Mean Square Error (RMSE) and the Full With at Half Maximum (FWHM) as metrics in integral DVH (iDVH) and differential DVH (dDVH) respectively with respect to mathematical phantoms.

Results
SUV and RC analysis for Phantoms [1] and [2] showed that SUV and RCs are independent from the choice of reconstruction matrix: Linear FITs showed angular coefficient of 1.25×10-3 for SUV and ranged from -7.3×10-2 to 1.5×10-3 for RCs. Considering that 90Y-PET spatial resolution for mCT scanner is about 3mm, it was fixed a 256 matrix (3.18 × 3.18 mm voxel). The RCs for phantoms [1,2] as a function of E.I. showed that already for 21 E.I. a convergence is achieved: Linear FITs showed angular coefficient ranged from -2.2×10-4 to 3.5×10-4. On the contrary, an increase in the number of E.I. only results in higher image noise; then 21 E.I. has been fixed. The results on phantom [3] showed that for larger volumes of interest (whole liver) RMSE is independent from the filter's magnitude (angular coefficient: 0.015) while FWHM decreases

with increasing filter (FWHM [Gy]: 41.4 – 30.9). For smaller volumes (37mm sphere diameter) RMSE increases with increasing filter (from 34% to 74% Gy) and the use of larger filter only result in an underestimation of the mean dose (from 172.21 to 133.79 Gy). A 6 mm filter provide an adequate level of dosimetric accuracy both for big and small volumes.

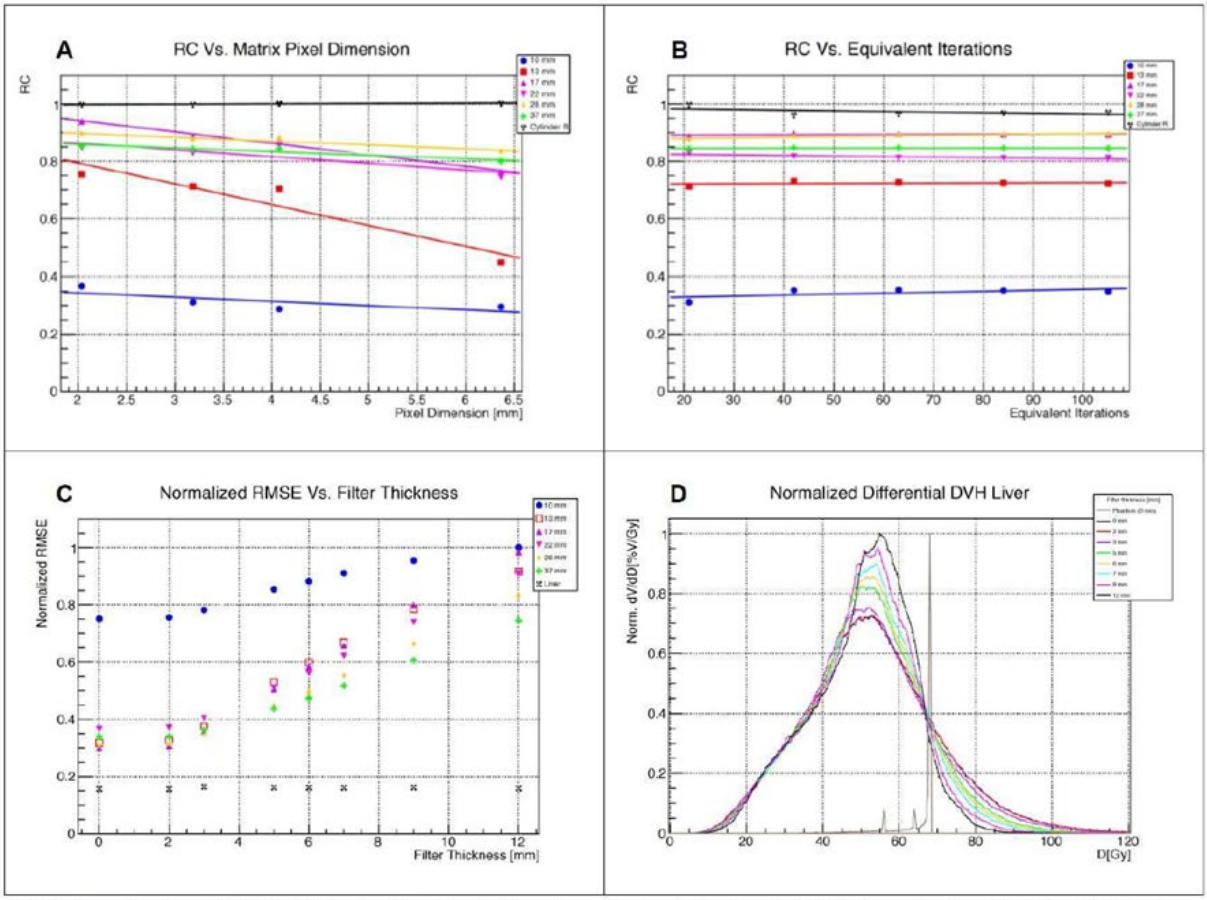

Fig1: A: RC values as function of Matrix Pixel Dimension shows there is independence from the choice of matrix; B: RC values as function of Equivalent Iterations shows, as A-case, that there is independence from the choice of number of equivalent iterations; C: Normalized RMSE as function of Filter Thickness shows flatness for larger volumes while an increasing trend for smaller ones; D: Normalized dDVH for Liver compartment shows a gaussian shape whose width decreases with the increase of the filter thickness.

Conclusion

In this work, it is emphasized that when 90Y is imaged, the optimization of reconstruction parameters, especially for choice of gaussian filter, depends on the nature of clinical case. The proposed method using old (RC convergence) and new metrics (RMSE and FWHM) Results in a more complete optimization for 90Y PET images reconstruction.

IAEA-CN-285/204

Diagnostic Performance of 68-Gallium Prostate-Specific Membrane Antigen Positron Emission Tomography-Computed Tomography in Intermediate and High-Risk Prostate Cancer

M. Haidar

American University of Beirut, Lebanon

CorrespondingAuthor: mh209@aub.edu.lb

Background
68-Gallium prostate-specific membrane antigen positron emission tomography-computed tomography (68Ga-PSMA PET-CT) is an imaging modality that promises improved sensitivity and specificity of detection of prostate cancer lesions based on their increased uptake of PSMA-based radiotracers. It remains an emerging modality that has not yet been endorsed in the guidelines for the management of prostate cancer pending more established evidence to prove its efficacy. The objective of the study is to assess the value of 68Ga-PSMA PET-CT in the detection and localization of patients diagnosed with intermediate or high-risk prostate cancer.

Methodology
Twenty-three patients with intermediate or high-risk prostate cancer had undergone 68Ga-PSMA PET-CT imaging prior to robotic assisted radical prostatectomy. Surgical specimens were then submitted for histological examinations. Lesions visualized on PET-CT and histology were independently mapped unto a 36-segment (Prostate Imaging Reporting and Data System version 2 [PI-RADSv.2]) map of the prostate. Concordance of visualization on PET-CT as compared to the histology as gold standard reference was then assessed.

Results
Sensitivity for all lesions identified on 68Ga-PSMA PET-CT was 42.37%; specificity was 88.61%. Both parameters were higher when considering only index lesions for which sensitivity was 68.42% and specificity was 98.23%. Sensitivity for the index lesions in intermediate risk group was 53.2% and was higher in the high-risk group reaching 83.33%.

Conclusion
68Ga-PSMA PET-CT provides accurate localization of tumor lesions in patients with intermediate and high-risk prostate cancer.

IAEA-CN-285/205

PET-CT for Radiotherapy Planning of Pediatric Central Nervous System (CNS) Tumors

E. Slobina, E. Abbasova, O. Zheludkova, A. Smyslov, A. Dykina, V. Vasilyev, F. Antonenko

Scientific Center of Roentgenoradiology, Russian Federation

Corresponding Author: e.slobina@gmail.com

Background
To present the possibilities of clinical application of modern neuroimaging (NI) such as 11C- methionine (MET) PET-CT and 18F-tyrosine (FET) PET-CT for radiotherapy planning of pediatric central nervous system (CNS) tumors.

Methodology
Since 2015, 12 patients, age median 8 years old (6-13), received a comprehensive treatment about pediatric central nervous system (CNS) tumors (4 –primary tumors, 8 – reccurent) according to SIOP protocols. In all cases, preliminary planning of radiation therapy was performed using MRI and MET and FET PET-CT and the 3D conformal radiation therapy technique included dose optimization (IMRT or VMAT).

Results
In the frame of the correct delineation of the glioma extent conventional MRI sequences are particularly limited in their ability to identify nonenhancing glioma subregions. Radiolabeled amino acids for PET imaging have the ability to cross the intact blood brain barrier, providing evidence that this technique identifies the glioma extent more reliably than standard MRI. When comparing the results of the preliminary planning by MRI and MET and FET PET-CT for IMRT and VMAT, the target treatment volumes were minimize up to 9 times, total treatment time was reduced from 10 to 15 minutes, with IMRT up to 2 - 4 min, with VMAT. The number of treatment monitor units decreased on average by 2.3 times when using VMAT, while the coverage of the planned treatment volume (PTV) of 95% of the treatment isodose did not significantly differ and amounted to 97.6% (IMRT) and 94.8% (VMAT) with a significant reduction in radiation exposure to dose-limiting organs. After analyzing the obtained dose-volume histograms, VMAT technology was applied in 5 patients at the local exposure stage. In 4 patients, treatment was carried out using 1-2 coplanar healing arches (arches), in 1 patient - using 2 non-coplanar healing arcs. Radiation therapy using IMRT or VMAT technologies after successful verification of treatment plans according to the quality assurance program adopted in the RRCD was performed using the Eclipse Planning System (ARIA) on a TrueBeam® linear accelerator. The early and late effects of radiation therapy were evaluated on an RTOG scale and were minimal.

Conclusion
The use of modern IMRT and VMAT technologies resulted in an optimal dose distribution in the individually planned treatment volume with MET and FET PET-CT, and when using VMAT, a lower dose level in dose-limiting organs was achieved, measured by dose-volume histograms, the number of treatment monitor units

was reduced, the total treatment session time was reduced. The use of combining modern methods of NI including MET and FET PET-CT and VMAT technology opens up new possibilities in the treatment of oncological diseases in children, since due to the above described properties, the time spent by the child on the treatment apparatus is significantly reduced, the risk of developing secondary tumors is reduced, which requires further study of the clinical application of the MET and FET PET-CT on a more significant number of clinical cases in larger clinical trials.

IAEA-CN-285/206

Bioinspired Green Polymeric Materials for Nanotheranostic Applications

S. N. Mohd Janib, R. Tajau, M. Hamzah, W. H. B. Wan Kamal, S. S. Abdul Hamid

Malaysian Nuclear Agency

Corresponding Author: najila@nm.gov.my

Background

Nanoscale therapeutic systems have emerged as novel therapeutic modalities for cancer treatment and are expected to lead to major advances in cancer detection, diagnosis and treatment. These nanoconstructs can be prepared from either natural or synthetic polymers. The use of natural or green polymeric nanocomposites are increasingly being preferred to replace non-degradable synthetic polymers. The growing concern of their bio-incompatibility, possible toxicity and carcinogenicity has propelled the re-visitation of natural polymers. Vegetable oil has attracted increasing attention as one of the most promising options because of its ready availability, relatively low cost, environmental sustainability, and low eco-toxicity. Palm-based vegetable oils are outstanding renewable raw material for developing new monomers and polymers. The aim of this study is to develop a new bio-based polymeric material from palm oil that can be endowed with functional moieties and be visualized using molecular imaging techniques to improve the treatment and detection of cancer.

Methodology

Various formulation of palm oil-based polyester nanoparticles have been developed for use as multifunctional agents for packaging, transport and delivery of imaging and therapeutic agents. Acrylated palm olein (APOO) and polyol derived using gamma radiation grafting technique and transesterification of palm oil are promising candidates for future development as nanotheranostic agents. Size characterization of the products were conducted using dynamic lights scattering (DLS) And transmission electron microscopy (TEM). Further confirmation and physical characterization of the nanoparticles were performed using NMR, FTIR, GPC, DSC and TGA. Biological assessment of the construct to determine cellular toxicity and uptake was done using MTT assay and confocal microscopy respectively. Tumour homing peptide (RGD) and bifunctional chelating agent (DOTA) was appended using standard bioconjugation protocol.

Results

Nanoparticles of varying sizes and physical characteristics (low molecular weight, functional Hydroxyl end groups, good thermal properties) were obtained. The nanoconstruct exhibited no effect on cell viability. facile conjugation with tumour specific peptides allows specific targeting and accumulation of the particles in cancer cells.

Conclusion

We have developed several palm oil-based polyester nanoconstruct that would be suitable to use for the targeted delivery of imaging and therapeutic agents. the resultant polymer with ideal physicochemical properties that are biocompatible, and biodegradable makes it ideal for biomedical applications. linking tumour homing peptides to the particle will increase the capacity of the construct to deliver drugs and imaging probe into tumours and thereby greatly improve therapeutic impact.

IAEA-CN-285/207

Optimization of Medical Exposures in Nuclear Medicine: A Simple Practical Approach in Pediatric Bone Studies

L. A. Torres Aroche[1], M. A. Coca Perez[2], C. Casaco Santana[1], Y. Peña Quian[1], E. Sanchez Mendoza[1], A. PratsCapote1, Y. Sánchez González1, G. L. Poli[3]

[1] Nuclear Medicine Service, CENTIS, Cuba
[2] MEDSCAN, Chile
[3] ASST Papa Giovanni XXIII, Italy

Corresponding Author: leonel.torres.cuba@gmail.com

Background

Optimization of medical exposures is an important component to ensure radiation protection of patients undergoing radiation medicine procedures, including conventional nuclear medicine (NM) studies. One key element is the assessment of the minimum levels of administered activity (AA) of radiopharmeceuticals to ensure an image quality which is adequate for a sound diagnosis. In this work we describe a simple practical approach that can be used for optimization of planar scintigraphies routinely performed in NM practice. Application of this Methodology to pediatric bone scan studies with 99mTc-MDP is also reported. These Results were obtained as part of the IAEA-CRP-E24020 activities.

Methodology

The proposed method is based on the simulation of different activity levels derived from a single activity administration. Static scintigraphies are replaced by dynamic studies with a properly chosen number of frames and frame duration. The frames can thus be summed to generate static images, with the number of summed images defining the value of the simulated AA. The simulated static images corresponding to different levels of AA are then presented to experienced NM physicians to assess the minimum levels of AA resulting in a sufficiently adequate image quality. The proposed method was implemented to optimize 99mTc-MDP planar bone scans in pediatric patients. In the study AA and corresponding effective doses were and compared to international recommendations from 35 patients in three age groups. Dynamic studies were acquired for 18 subjects, with 10 frames and total acquisition time equal to the original static acquisition. Three experienced observers assessed the image quality according to a predefined scale and identified the optimized activity levels. The effects of the intervention actions were evaluated on 21 pediatric patients. Finally, comparison of data with EANM and NACG recommendations was performed.

Results

Analysis of the data collection performed to assess the baseline situation for 99mTc-MDP bone studies highlighted AA levels for the three age groups of patients higher than 93% (0-5 y), 68% (5-10 y) and 43% (10-18 y) as compared to NACG recommendations The intervention study showed that the optimized AA was between 60% and 70% of the baseline value .The proposed intervention was therefore a reduction in AA of 30% as compared to initial values. Data collection was repeated for 21 pediatric patients after introduction of the intervention. Image quality was assessed to be adequate by experienced NM physicians, while the

mean relative difference between AA prior and post introduction of the intervention decreased by 22%, corresponding to a reduction of effective dose of approximately 20%.

Conclusion

A method to optimize the AA used in conventional NM planar studies was developed and implemented for 99mTc-MDP bone studies of pediatric patients. The same Methodology can be applied to other planar studies (e.g. renal, thyroid, etc.) commonly performed in NM practices. The results showed how this simple method can be used to effectively enhance radiation protection of patients in NM practices.

IAEA-CN-285/208

First Experience with Peptide Receptor Radionuclide Therapy in the Kwa-Zulu Natal State Healthcare Sector

N. Nyakale, L. Harry, P. Ramdass, F. Peer

Sefako Makgatho Health Sciences University, University of Kwa-Zulu Natal, South Africa

Corresponding Author: n.nyakale@yahoo.com

Background

In South Africa, peptide receptor radionuclide therapy (PRRT) for treatment of Neuroendocrine tumours (NETs) has only been accessible to private and self-funded patients. Kwa-Zulu Natal (KZN) is the first province in South Africa to avail this treatment to patients who access the state sector healthcare. The aim of this study is to report our initial Results and experience with Lutetium-177 DOTATATE PRRT in the KZN state sector and contribute to the overall South African experience.

Methodology

Medical records of eligible patients who underwent Lutetium-177 DOTATATE (LuTate) PRRT at our institution since inception in 2016 to February 2020 were reviewed. All patients referred for PRRT were deemed inoperable and unresponsive and/or intolerant to conventional therapy. All patients underwent somatostatin receptor (SSR) imaging at baseline, had 4 to 6 cycles of PPRT at an interval of approximately 8 weeks between cycles followed by SSR imaging 6 months after the last cycle of PRRT.

Results

The 17 patients treated during this period, 8 females and 9 males with mean age of 57 +/-12.6 years, underwent a total of 65 cycles of PRRT. The predominant primary site of NETs was the pancreas (5). Other sites included small bowel (3), bronchial (2), rectum (2), head and neck glomus tumours (2), cervix (1) and 2 were unknown. Sixteen (94%) of the patients had metastatic disease, 75% of which involved spread to 3 or more organ sites. Four patients did not complete the scheduled 4 cycles of treatment: 2 patients only received 1 cycle, due to death from unrelated causes and disease progression respectively; one patient had 2 cycles due to discordant findings between 68Ga DOTATATE and LuTate images; in one patient treatment was interrupted after 3 cycles due to high accumulated radiation dose to the kidneys.

We noted disease progression in 2/17 (1%) patients, stable disease in 6/17(35%) patients and partial response in 8/17 (47%) patients. Some patients complained of nausea during the administration of treatment which was likely related to the amino acid infusion administered for renal protection, but none of the patients experienced serious adverse events. One patient died due to unrelated causes and no further analysis could be done with regards to other adverse events of the treatment. One patient experienced grade 3 to 4 anaemia, while 4 patients experienced grade 1 to 2 anaemia. We noted transient grade 1 thrombocytopaenia in 7/16 (43%) and grade 1 to 2 leukopenia in 8/16 (50%) patients. Most of these findings occurred midcycle and the patients recovered by their 6 months follow up. Only 1 patient experienced mild renal impairment during therapy, but the patient was known with a history of renal dysfunction and successfully co-managed with the renal unit.

Conclusion

Despite the commonly late presentation of our patients, our findings are consistent with those reported in the literature proving PRRT to be a safe treatment for NETs with mild to moderate and mostly transient adverse effect.

IAEA-CN-285/215

18F-FDG PET-CT in the Diagnosis and Combined Treatment of Symptomatic Epilepsy in Adults

T. Dakukina, E. Slobina

National Center for Mental Health, Belarus

Corresponding Author: e.slobina@gmail.com

Background
To present and evaluate the possibilities of clinical application of modern neuroimaging (NI) such as 18F-FDG PET-CT on treatment of symptomatic pharmacoresistant epilepsy in adults.

Methodology
Since 2017, 20 patients, age median 24 years old (18-58), about generalized seizures continued to be held anticonvulsant therapy, which led to a decrease in seizure frequency on average from 13 to 8 in month. In all cases taking into account the progressive course of the disease, when any a combination of 2-3 essential anticonvulsants, including the latest, did not have a noticeable effect on the frequency and severity of attacks, patients were treated by combination therapy, including antiepileptic drugs and autologous bone marrow stem cells (AMSC CM).

Results
Electroencephalogram (EEG) showed epileptiform activity. PET-CT examination of the brain with 18F-FDG after the first course of the introduction of AMSC CM revealed a pattern of increased metabolic active-STI of the left hemisphere of the brain. Significant a new increase in fixation of the radiopharmaceutical in the left frontal, parietal, temporal and occipital lobes.
On an EEG, after the first course of stem cell administration, significantly decreased the amount of epileptic formal activity. The frequency of spikes in the left temporal region STI decreased from 30 to 2 per min, the frequency of bilateral synchronization discharges of acute alpha waves remained at the level of 1-2 in minutes. At a frequency of alpha rhythm of 10.5 Hz, normalization occurred of its frequency-spatial structure, but the structure maximum mean coherence values are still was presented in the form of a triangle, which indicated the presence of an active epileptic process.
On the EEG, after the second course of stem cell administration, paroxysmal activity was not registered. A reduction in the pathological structure of the maximum values of mean coherence in the form of a triangle was noted. In order to assess the functional state of the brain according to metabolic activity were carried out repeated PET-CT with FDG after 5 months after the second course of the introduction of AMSK KM. The obtained data on the metabolism of the radiopharmaceutical in dynamics and when compared with relative reference regions testify in favor of stabilization (striving for reference values) of metabolic activity in the interested areas: in the left parietal, temporal and occipital lobes. Control PET-CT study was performed under identical conditions, which is a prerequisite for assessing dynamics (the study was conducted on the same scanner, with the same entered activity, subject to variables of the research protocol).

Conclusion

Combining modern methods of NI including 18F-FDG PET-CT are very useful tools in the evaluation of effectiveness of complex treatment for symptomatic pharmacoresistant epilepsy. The encouraging results of the evaluation of effectiveness of the proposed method of treatment of pharmacoresistant epilepsy have been obtained, which requires further study of the clinical application of the 18F-FDG PET-CT on a more significant number of clinical cases in larger clinical trials.

IAEA-CN-285/216

Visual and Quantitative Assessment of Residual Aggressive Lymphoma with the Lesion Synthesis Toolbox

C. Wiefels[1], A. Miglietta[2], H. Gabrani-Jumaa[2], R. Klein[2], W. Zeng[2]

[1] Fluminense Federal University, Brazil
[2] University of Ottawa Heart Institute, Canada

Corresponding Author: cwiefels@ottawaheart.ca

Background
Deauville scales have been widely used to assess treatment response in aggressive lymphoma with 18F-FDG PET. A Deauville score of 3 and 4 (3= uptake above mediastinal blood pool and below liver, 4=uptake above liver) separates resolved from residual disease. Although visual assessment has been recommended, a semiquantitative assessment with the value of SUVmax of the lesion, liver and mediastinal blood pool is commonly used for Deauville score.
The Lesion Synthesis Toolbox was developed at our group to generate well characterized synthetic lesions in real patient data. The model has been validated in a human perception experiment. The objective of the study is to compare the visual and semiquantitative assessment of artificially introduced well-characterized lesions in real patient FDG PET.

Methodology
The Lesion Synthesis Toolbox software was used to generate synthetic lesions of varying size (1.5-2.5 cm) and contrast (varying from 80-150% of the liver uptake) in manually defined locations in the patient's thoraco-abdominal region to mimic lymphoma lesions. Visual assessment was performed by two nuclear medicine physicians experienced on FDG PET independently and blinded to other results. The lesions were classified as Deauville score 3 or 4. The inter-observer agreement was assessed with Cohen's Kappa.

Results
A total of 115 lesions from 15 18F-FDG PET studies were evaluated. Deauville score 3 and 4 was observed in 58 and 57 lesions by Reader 1, compared to 70 and 45 by Reader 2, with a good agreement at 83% and a kappa of 0.65 (95%CI:0.51,0.79). The agreement between semiquantitative measurement with SUVmax and visual assessment was 84%, with a kappa of 0.69 (95%CI: 0.55,0.82) for Reader 1 and 81%, with a kappa of 0.62 (95%CI:0.48,0.76).

Conclusion
Our preliminary Results show good agreement between semiquantitative and visual assessment and inter-reader agreement of simulated lymphoma lesions in real FDG PET patients, which enables further characterization of lesion size, shape, location and contrast as contributing factors in the assessment of lymphoma.

IAEA-CN-285/218

Hybrid Imaging Sensitivity Features on a Gamma MRI Device

A. Abril, L. Agulles Pedros

National University, Colombia

Corresponding Author: lagullespedros@gmail.com

Background
Medical images aim to give more information available in the lowest spatial resolution. This can be achieved by a combination of anatomical images and functional information. The most common are SPECT-CT and PET-CT. To overcome the use of two ionizing imaging techniques, PET-MRI has been growing in the last decade. Although MRI offers better contrast features, it still lacks two very important features versus CT: time and money. Time; MRI usually needs more acquisition time than CT scanners. Money; MRI devices usually are more expensive than CT ones, especially if NM-devices have to fit on it. Then, a new hybrid gamma MRI device has been developed, based on dosimetric gel. The idea was to develop a detector without an electronic readout system, cheaper, easy to implement in an MRI device, and that simplifies the fusion of anatomical and functional images by using only MRI acquisitions. The solution is to use a gel that presents physical and chemical changes that can be measured by T2 MRI. Planar images may be obtained from a patient injected with radiopharmaceuticals, if a collimator is located between the patient and the gel within the MRI magnet bore. This work describes the main sensibility factors for this novel hybrid MRI gamma imaging device

Methodology
To evaluate MRI sensitivity, a set of T2 maps were performed based on MonteCarlo simulations of a 99Tc point source. The source was located at 15 cm under the center point of the gel detector, which consists of 20 times 20 times 6 cm3 water surrounded by air. A collimator was located between the gel and the source. Cell septa were set as 1 mm width with 4 mm inner space, being each cell 5 mm width. The overall dimensions of the collimator were the same as the gel. On the other hand, it was performed another set of in silico experiment with two-point sources of 511 and 140 keV dose deposition to determine the intensity decay as a function of the slice location; both sources at 1 MBq. The mass attenuation coefficient in the gel is fitted in order to distinguish the source energy detected in each pixel. This step is done as follows; the dose is detected in each pixel of the 10 slices (see Fig). Applying known dose T2 calibrations, the analysis of the decay of the signal as a function of the layers depth in each pixel gives the linear attenuation coefficients mu per pixel. Since the source energy E is known, a mu(E) can be determined and selected from the fitted values in each pixel.

Results
Simulation of MRI shows that SNR above 60 can be achieved, experiments even improved the SNR.CNR larger than 5 can be achieved simulation common nuclear medicine conditions. Photons energy discrimination can be implemented.

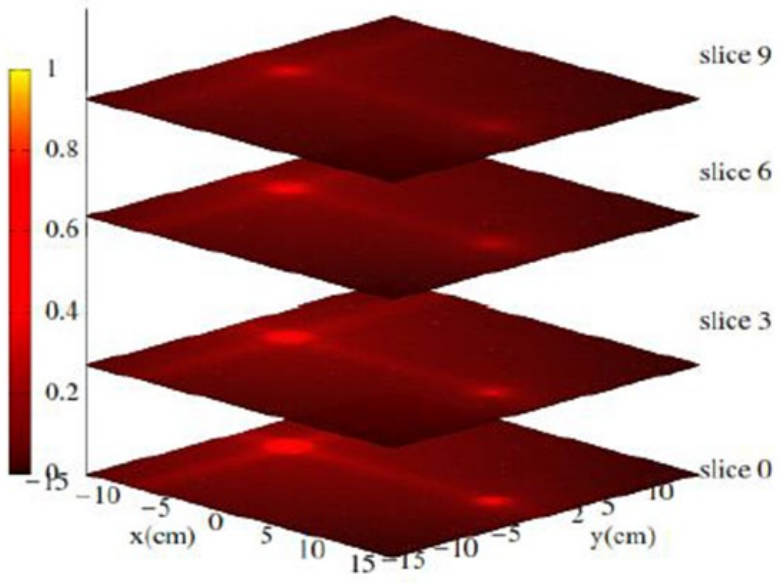

R_2 normalised intensity maps image. 10 slices were acquired. The first, second, third, sixth and last slice are shown.

Conclusion

Simulations show that the device can achieve CNR and SNR similar to common nuclear medicine techniques. A new technique to distinguish scattered from direct photons or different radiopharmaceutical energies can be applied to this new device.

IAEA-CN-285/219

QUANUM Audits in Latin America: 10 Years of Contribution to Quality Improvements of Nuclear Medicine Practices

D. Paez[1], E. Estrada[1], M. Dondi[1], L. A. Torres Aroche[2], T. Massardo[3], M. Marengo[4]

[1] Nuclear Medicine and Diagnosic Imaging Section, IAEA, Austria
[2] Nuclear Medicine Service, CENTIS, Cuba
[3] University Hospital, Chile
[4] S. Orsola-Malpighi Polyclinic, Italy

Corresponding Author: leonel.torres.cuba@gmail.com

Background
The QUANUM (Quality Management Audits in Nuclear Medicine Practices) programme was developed and introduced by the IAEA in 2007 and has been periodically updated, thus reflecting the evolving nature of nuclear medicine. The QUANUM programme has significantly contributed to enhancing the quality and safety of clinical nuclear medicine services (NMS) in IAEA Member States (MS). It has promoted the establishment of quality management systems (QMS), the adoption of quality culture and the implementation of systematic reviews of all processes, with the goal of improving the overall quality of the clinical services provided by the NMS. As part of the support provided to MS, the IAEA has conducted 76 QUANUM audits worldwide. The objective of this study was to evaluate the impact of the 22 external audits carried out by the IAEA in seven LA countries and the changes implemented as a result of the audits.

Methodology
In the past ten years, a total of 22 external audits were performed in nuclear medicine services of seven Latin American countries. A follow-up audit was also carried out in two of the centers. QUANUM external audits are requested by institutions on voluntary basis and are not intended to provide acreditation or certification of NM facilities, but rather identify areas of improvement and advise on how to achieve the changes needed. Audit teams are multidisciplinary and typically comprise of a nuclear medicine physician, a radiopharmacist, a medical physicist, a technologist and a staff member of the Nuclear Medicine and Diagnostic Imaging Section of the IAEA, all of them with competences as quality auditors. With few exceptions, all auditors come from the LA region. All audited NMS provided basic data in advance, including the results of their self-assessments using the QUANUM checklists, as well as an updated nuclear medicine database (NUMDAB) form and some additional information.
The auditors rigorously adhere to the QUANUM methodology in which 14 checklists are used to identify non-conformities (NC), following a score ranging from 0 to 4. To stratify the prioritization of non-conformities, these are categorized as minor, major and critical. Auditors and auditees perform an analysis of the NC detected, and possible solutions are evaluated, always taking national and international standards as a reference. At the end of the audit process, an action plan is proposed to face the NC.

Results

Figure 1 includes the audits performed in LA. The audited services have differences in their infrastructure, scope of service, development of human resources and level of implementation of QM. However, the QUANUM programme has proven to be applicable to many NMS across a variety of economic circumstances. The global compliance level of the audited centers was 71.0 ± 14.9% (Figure 2) raning from 57.4 to 83.2%; The areas with the highest levels of compliance with international standards were radionuclide therapies (76.8%), radiation safety (78.16%), human resources 75.2%, and general clinical services (73.9%). Radiopharmacy levels 1 and 2 have the lowest compliance levels around 57.4% and 62.5%, respectively.

Common NC were related to a lack of written or non implemented standard operation procedures, inadequate processes in the area of radiopharmacy area and insufficient or inadequate radiation protection procedures. The common strengths were related to the availability of well-trained human resources and a high commitment to quality.

Another result of QUANUM in LA was the adoption of QMS and local audit processes in some countries such as Brazil and Cuba. It has also encouraged general managers to provide alternative solutions to address the NC and implement corrective measures.

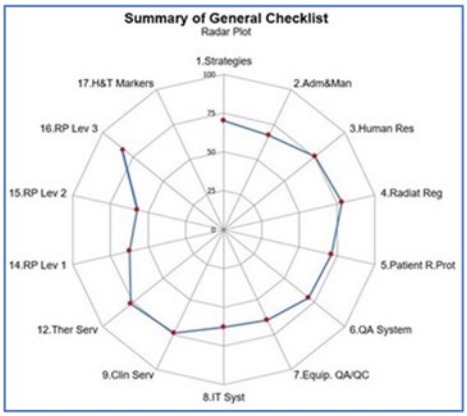

Conclusion

The QUANUM audits in LA showed an acceptable level of compliance with quality requirements in the evaluated centers (> 70%). They also contributed to identifying common areas for improvement in the region. On the other hand, the QUANUM programme has contributed to the adoption of a quality culture and to promote the implementation of the QMS in NM services.

IAEA-CN-285/221

90Y-Microspheres Radioembolization for Liver Treatment in NGHA, Statistics and Dosimetry

N. Senhou

National Guard Health Affair, Saudi Arabia

Corresponding Author: naima.senhou@gmail.com

Background
Hepatocellular carcinoma (HCC) is a major cause of cancer related death worldwide. In recent Saudi Cancer Registry of year 2015. Liver cancer ranked sixth among Saudi males and twelfth among Saudi females. There were 376 liver cancer cases accounted to 3.1% of all cancer cases diagnosed among Saudi nationals in 2015.In order to estimate the survival, the distribution among female and male also the response after radioembolization treatment with 90Y microspheres in national guard health affairs hospital, the patients data were collected and analyzed.

Methodology
In this work the patient data was collected from 2015 to 2019, a total of 140 liver cancer cases were treated by Y-90. There were 90 cases treated one time, 22 cases treated twice, and 2 cases treated for three times. Because of the missing information regarding the first diagnostic and death for some patients, only a total of 34 patients' data had been treated and analyzed. The survival functions were estimated using the Kaplan-Meier estimator from the date of liver cancer diagnosis to the date of last follow up (events). Patients who met the following criteria were eligible for inclusion in the study of HCC cancer. Tumor dose up to 160 Gy was delivered for the treatment of only one liver lobe. Patients with dose more than 160 Gy, and patients treated for the whole liver were excluded from the study and considered as censored. The calculated survival duration has been calculated as number of weeks based on SEER*Stat statistical software.

Results
In our results the proportion of five types of liver cancer were analyzed, we found out that some types of cancer have a major contribution compare it to the total patients treated in National Guard Health Affairs hospital, we have a total of 140 cases all of them underwent a treatment with Yttrium 90. Overall, most of patients had hepatocellular carcinoma with a total of
87%. Other type of liver cancer included the following: colorectal metastases with contribution of 6%, cholangiocarcinoma contributed by only 4%, neuroendocrine tumour by 2%; and finally, 1% for gallbladder metastatic cancer. Our results showed that the survival after radioembolization with 90Y microspheres can increase by 12% for two fraction treatment, the increase can reach 37% in case of three fractions. Fractioning the dose has clear effect on the survival from 51 to 88 weeks for patients received 3 fractions of radioembolisation treatment.

Conclusion
The obtained results showed that the number of male patients is almost twice the number of female; also the multi-fraction treatment can increase the survival by 12 to 37% for more than a single fraction.

IAEA-CN-285/222

Equivalent Uniform Dose in Dosimetry Voxel: Applicability Study of the Concept in Radionuclide Therapy

U. De Souza Fonda

Nuclear Medicine Center, Brazil

Corresponding Author: uyshaf@gmail.com

Background
Equivalent uniform dose (EUD) is used in radiotherapy to predict the cellular response in situations of heterogeneous aborbed dose distribution. There are proposals to use the same concept in radionuclide therapy. However, nuclear medicine imaging systems (SPECT and PET) provide a limited representation of radiopharmaceutical distribution, and consequently of dose distribution in the patient's body. Emission tomography images are subject to statistical fluctuation, and therefore heterogeneity, that does not correspond to the real distribution. This study aims to evaluate the influence of total counts and reconstruction parameters in the uncertainty of radiopharmaceutical distribution and their impact on voxel dosimetry, with emphasis on dose heterogeneity and the equivalent uniform dose.

Methodology
18F-PET images were acquired in Jaszczak, NEMA IQ and cylinder phantoms. Images were acquired with total counts varying from 1% to 100% of that recommended in the standard procedure (100% = 27.16 MBq and 159 million counts). OSEM iterative reconstruction was performed using 24, 16, or 4 subsets, and 10, 4, or 2 iterations. A dosimetry software (Imalytics, Philips) was used to generate parametric images of dose. Dose heterogeneity was measured after dosimetry based on single images and based on cumulated activity images, obtained after manually assigning times for two sequences of images (high count sequence- HCS:100% 40% 25% 10%; low count sequence- LCS:10% 4% 2.5% 1%).

Results
No significant changes were observed in the heterogeneity values in the dose images, when the number of subsets and iterations varied. Dose heterogeneity based on single images increased with the reduction in total counts. The influence of counts in dose distribution is visually detectable (figure 1). Dose heterogeneity based on cumulated activity was greater on LCS as compared to HCS (Figura 1 – table 2), but only minor changes in heterogeneity were noticed when different times were assigned inside the same sequence

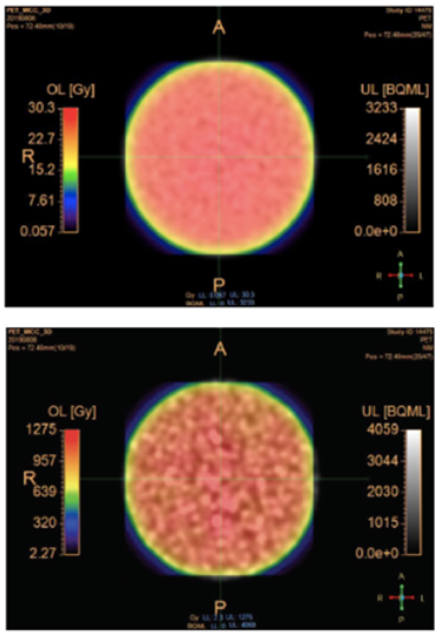

Table 1. Results of single image.

Activity concentration [%]	Radioactivity decay [MBq]	Integral uniformity [%CFOV] (mean ± SD)	Single image (mean ± SD)	Percentage uncertainty [%]
100	27.16	2.43 ± 0.56	29.76 ± 0.13	0.43
40	10.86	3.55 ± 0.16	48.19 ± 0.19	0.39
25	6.79	3.53 ± 0.19	59.55 ± 0.34	0.57
10	2.72	3.98 ± 0.21	83.81 ± 0.36	0.43
4	1.09	4.88 ± 0.58	87.04 ± 0.35	0.40
2.5	0.68	5.55 ± 0.73	102.26 ± 0.61	0.59
1	0.27	6.52 ± 1.08	120.94 ± 0.79	0.65

Legend: MBq, Mega Becquerel; CFOV, central field of view; SD, standard deviation.

Table 2. Results of the sequence of image.

	Time interval [h]	Activity concentration [%]	Integral uniformity [%CFOV]	Sequence of image [mean ± SD]	Percentage uncertainty [%]	Cumulative activity [kBq]
Series 1	**24; 96; 168; 336**	100 40 25 10	2.78	985.75 ± 13.13	1.33	19.06
		10 4 2.5 1	3.86	97.48 ± 2.35	2.41	1.87
Series 2	**4; 24; 96; 168**	40 100 25. 10	2.72	636.28 ± 8.51	1.34	14.97
		4 10 2.5. 1	3.79	62.99 ± 1.47	2.33	1.47
Series 3	**24; 120; 240; 360**	100 40 25. 10	2.78	1171.76 ± 15.59	1.33	23.51
		10 4 2.5 1	3.77	115.92 ± 2.77	2.39	2.31

Legend: h, hours; CFOV, central field of view; SD, standard deviation; kBq; kilo Becquerel.

Figure 1. Uniformity in PET images acquired with 100%-1 of the recommended activity and counts. Less counts leads also to a proportionally increased heterogeneity in voxel dosimetry.

IPET - 2020 *goes virtual*

BEYOND THE VISIBLE

IAEA
International Atomic Energy Agency
Atoms for Peace and Development